UNIVERSIDADE FEDERAL DO RIO GRANDE DO SUL

PROGRAMA DE PÓS-GRADUAÇÃO EM ADMINISTRAÇÃO

Lucas Mussoi Almeida

ESSAYS IN CRYPTOFINANCE

Porto Alegre

2025

ESSAYS IN CRYPTOFINANCE

Lucas Mussoi Almeida

Thesis submitted as a requirement for the Doctoral degree in Administration, with an emphasis in Finance, at the Business School of the Federal University of Rio Grande do Sul.

Advisors:

Marcelo Scherer Perlin, Ph.D. UFRGS	Fernanda Maria Müller, Ph.D. UFRGS

Examiners:

Jéfferson Augusto Colombo, Ph.D. FGV EESP	Leandro dos Santos Maciel, Ph.D. FEA USP
Guilherme Pumi, Ph.D. UFRGS	Henrique Pinto Ramos, Ph.D. UFRGS

Porto Alegre
Setembro de 2025

ESSAYS IN CRYPTOFINANCE

Lucas Mussoi Almeida

Advisors: Marcelo Scherer Perlin
Fernanda Maria Müller

Examineers: Prof. Jéfferson Augusto Colombo
Prof. Leandro dos Santos Maciel
Prof. Nome do Terceiro Examinador Sobrenome
Prof. Henrique Pinto Ramos

PORTO ALEGRE, RS – BRASIL
SETEMBRO DE 2025

CIP - Catalogação na Publicação

Almeida, Lucas Mussoi
Essays in Cryptofinance / Lucas Mussoi Almeida. -- 2025.
90 f.
Orientador: Marcelo Scherer Perlin.

Coorientadora: Fernanda Maria Müller.

Tese (Doutorado) -- Universidade Federal do Rio Grande do Sul, Escola de Administração, Programa de Pós-Graduação em Administração, Porto Alegre, BR-RS, 2025.

1. Cryptofinance. 2. Bitcoin. 3. Decentralized Finance. 4. Risk. 5. Smart contracts. I. Perlin, Marcelo Scherer, orient. II. Müller, Fernanda Maria, coorient. III. Título.

Elaborada pelo Sistema de Geração Automática de Ficha Catalográfica da UFRGS com os dados fornecidos pelo(a) autor(a).

Abstract

This dissertation presents an empirical analysis of decentralized finance through three distinct studies. By harnessing the power of on-chain data, this research delves into the mechanics of DeFi, exploring how we assess financial risk and measure market efficiency. Furthermore, it directly addresses the significant economic externalities of the sector by measuring the annualized energy draw of Bitcoin's global mining industry. The first article, *Risk forecasting comparisons in decentralized finance: An approach in constant product market makers* (this research was presented at the Annual Conference of the Banco Central do Brasil (2024) and subsequently published in the Journal of Economics and Business, Volume 133, 2025; 2024 JCR Impact Factor: 3.4), pioneers by comparing risk measures between centralized and decentralized exchanges. By employing a vast dataset from Uniswap V2 Liquidity Pool (LP) and conducting a meticulous comparative analysis of Value-at-Risk (VaR) and Expected Shortfall (ES) forecasts, using both parametric Generalized Autoregressive Conditional Heteroskedasticity (GARCH) models and the non parametric DeepAR neural network, it demonstrates that liquidity provision generally presents a statistically significant lower risk profile than an equivalent buy and hold strategy. A critical exception exists for stablecoin pairs, where protocol fees become the primary risk driver. This research provides a crucial empirical foundation for developing sophisticated, model informed risk management tools in Decentralized Finance (DeFi).

The second article, *Pricing efficiency in cryptocurrencies: the case of centralized and decentralized markets* (published in the Journal of Economics and Business, Volume 133, 2025; 2024 JCR Impact Factor: 3.4), offers a comparative analysis of market efficiency between liquidity pool mechanisms and traditional order book systems. Utilizing Asymmetric Multifractal Detrended Fluctuation Analysis (asymmetric MF-DFA) and the Thermal Optimal Path (TOP) method on data from Binance and Uniswap V2, it reveals that algorithmic LP can achieve superior weak form market efficiency compared to Centralized Exchanges (CEX) order books. The study conclusively identifies the Decentralized Exchanges (DEX) as the lead market in price discovery, transmitting signals to its centralized counterpart with an average lag of under 24 hours. This efficiency premium, driven by radical transparency and

high velocity arbitrage, intensified significantly following the Ethereum 2.0 upgrade.

The third article, *Bitcoins halving events and the fractal nature of mining energy consumption*, investigates the long term impact of Bitcoins programmed monetary policy on its mining energy consumption behavior. Applying asymmetric MF-DFA to data from the Cambridge Centre for Alternative Finance, it uncovers the complex, multifractal nature of Bitcoins energy dynamics, showing an evolution from persistent, heterogeneous behavior before halving events toward more efficient and random consumption characteristics after each subsequent halving. The analysis provides the first documented evidence of a significant cross-chain effect, showing that Ethereum's transition to Proof of Stake (PoS) consensus triggered an immediate and sustained decrease in the persistence of Bitcoin's energy consumption patterns. This finding reveals previously unrecognized interconnectivity between seemingly independent networks and creates new pathways for assessing the environmental relationships within blockchain ecosystems.

Resumo

Esta dissertação apresenta uma análise empírica de finanças descentralizadas por meio de três estudos distintos. Utilizando dados *on chain*, a pesquisa examina avaliação de risco financeiro, eficiência de mercado e consumo energético anualizado da mineração de Bitcoin. O primeiro artigo, *Risk forecasting comparisons in decentralized finance an approach in constant product market makers* (*Computational Economics*, 2025), desenvolve uma metodologia comparativa para medidas de risco entre CEX e DEX. Empregou-se dados de LP da DEX Uniswap V2, conduzindo uma análise comparativa de previsões de *Value at Risk* e *Expected Shortfall*. Para isso, fez-se uso tanto de modelos paramétricos GARCH quanto do modelo de rede neural não paramétrica DeepAR, os resultados demonstraram que a provisão de liquidez geralmente apresenta perfil de risco estatisticamente inferior à estratégia tradicional de *buy and hold*. Uma exceção crítica ocorre em pares de *stablecoins*, onde as taxas do protocolo tornam-se o principal fator de risco. Esta pesquisa fornece base empírica crucial para desenvolver ferramentas sofisticadas de gestão de risco informadas por modelos em DeFi.

O segundo artigo, *Pricing efficiency in cryptocurrencies the case of centralized and decentralized markets* (*Journal of Economics and Business*, 2025), oferece uma análise comparativa da eficiência de mercado entre os mecanismos de *liquidity pools* e o tradicional sistema de *order books*. Utilizando *Asymmetric Multifractal Detrended Fluctuation Analysis* e o método *Thermal Optimal Path* em dados da corretora Binance e do Uniswap V2, revelamos que os algorítmos contidos nos *smart contracts*, que regem as *liquidity pools*, são mais eficientes na *weak form* de eficiência de mercado quando comparados aos *order books* centralizados. O estudo também identifica o mecanismo decentralizado como líder na descoberta de preços, transmitindo sinais para sua contraparte centralizada com defasagem média inferior a 24 horas. Este prêmio de eficiência, impulsionado pela radical transparência e arbitragem, mostrou-se intensificar após a atualização 2.0 do Ethereum.

O terceiro artigo, *Bitcoins halving events and the fractal nature of mining energy consumption*, investiga o impacto de longo prazo da política monetária programada do Bitcoin em seu comportamento de consumo energético de mineração. Aplicando *Asymmetric Multifractal Detrended Fluctuation Analysis* à dados do *Cambridge*

Centre for Alternative Finance, desvenda-se a natureza multifractal complexa da dinâmica energética do Bitcoin. O estudo revela uma evolução nos padrões de consumo energético, transicionando de um comportamento heterogêneo no período pré-halving para características de consumo mais eficientes e estocasticamente aleatórias após cada evento de halving subsequente. A análise apresenta a primeira evidência documentada de um efeito *cross-chain* significativo, demonstrando que a transição do Ethereum para o *Proof of Stake* provocou uma redução imediata e persistente na regularidade dos padrões de consumo energético da mineração de Bitcoin. Essa constatação revela uma interconexão até então não reconhecida entre *blockchains* aparentemente independentes.

Contents

List of Figures **x**

List of Tables **xii**

Introduction **1**

I Risk forecasting comparisons in decentralized finance: An approach in constant product market makers **5**

1 Introduction . . . 6
2 Data and methodology . . . 10
2.1 Data acquisition . . . 10
2.2 Risk measures . . . 11
2.3 Risk forecast models . . . 13
2.4 Methodological procedures . . . 15
3 Results . . . 17
4 Conclusion . . . 25

II Pricing efficiency in cryptocurrencies: the case of centralized and decentralized markets **29**

1 Abstract . . . 29
2 Introduction . . . 30
3 Data and Methodology . . . 33
3.1 Data . . . 33
3.2 Methodology . . . 34
3.3 Asymmetric Multifractal Detrended Fluctuation Analysis . . . 36
3.4 Thermal Optimal Path . . . 39
4 Results . . . 41
5 Conclusion . . . 46

III Bitcoin's halving events and the fractal nature of mining energy consumption **48**

1 Introduction . . . 48

2 Data and Methodology 51
2.1 Data 51
2.2 Methodology 53
3 Results 57
4 Conclusions 68

References **69**

List of Figures

I.1 Forecasted evolution of VaR and ES risks, using the best GARCH models from Table I.5 to I.8, at 1% and 5% significance levels, observed for the returns of the ETH-BTC liquidity and the portfolio. The time frame for this analysis spans from September 24, 2021, to February 22, 2022. 19

I.2 Forecasted evolution of VaR and ES risks, using the *DeepAR* models, at 1% and 5% significance levels, for the returns of the ETH-BTC liquidity and the portfolio. The time frame for this analysis spans from September 24, 2021, to February 22, 2022. 19

III.1 Visualization of the Bitcoin network's energy consumption dynamics. Panel A displays the historical annualised electricity consumption in terawatt-hours (TWh), derived from the Cambridge Bitcoin Electricity Consumption Index (CBECI). Panel B presents the transformed series using the first difference of natural logarithms (Δlog). 52

III.2 Time-varying asymmetric multifractality in Bitcoin mining energy consumption. The rolling upward (H_+), downward (H_-), and overall Hurst exponent (H), along with the delta alpha ($\Delta\alpha$) are shown, calculated from the logarithmic returns using asymmetric MFDFA with a window size of 256 observations. To clarify the short-term trend without losing critical information, the results are smoothed using a 90 days moving average. Horizontal shaded band indicates values over 0.5. 64

III.3 Time-varying asymmetric multifractality in Bitcoin mining energy consumption. The rolling upward (H_+), downward (H_-), and overall Hurst exponent (H), along with the delta alpha ($\Delta\alpha$) are shown, calculated from the logarithmic returns using asymmetric MFDFA with a window size of 384 observations. To clarify the short-term trend without losing critical information, the results are smoothed using a 90 days moving average. Horizontal shaded band indicates values over 0.5. 65

III.4 Time-varying asymmetric multifractality in Bitcoin mining energy consumption. The rolling upward (H_+), downward (H_-), and overall Hurst exponent (H), along with the delta alpha ($\Delta\alpha$) are shown, calculated from the logarithmic returns using asymmetric MFDFA with a window size of 512 observations. To clarify the short-term trend without losing critical information, the results are smoothed using a 90 days moving average. Horizontal shaded band indicates values over 0.5. 66

List of Tables

I.1 Descriptive statistics of the Liquidity Pool's token returns. The sample period runs from November 14, 2020, until February 02, 2022. . . 12

I.2 Hyperparameters used for the tunning of the *DeepAR* model. 17

I.3 Mean forecasted risks values of the GARCH model which performed the better in VaR and ES considering two significance levels - 1% and 5%. The risk models are assessed by employing the apoppriate score function (loss function). Samples range from 2020/11/14 to 2022/02/22. 21

I.4 Mean forecasted risks values of the probabilistic DeepAR model which performed the better in VaR and ES considering two significance levels - 1% and 5%. The risk models are assessed by employing the appropriate score function (loss function). Samples range from 2020/11/14 to 2022/02/22. 23

I.5 Selected GARCH and DeepAR models through mean score value criteria for Value-at-Risk and Expected Shortfall at $\alpha = 0.01$ considering Liquidity Pool tokens time series valuation. 26

I.6 Selected GARCH and DeepAR models through mean score value criteria for Value-at-Risk and Expected Shortfall at $\alpha = 0.05$ considering Liquidity Pool tokens time series valuation. 26

I.7 Selected GARCH and DeepAR models through mean score value criteria for Value-at-Risk and Expected Shortfall at $\alpha = 0.01$ considering the pair Portfolio time series valuation. 27

I.8 Selected GARCH and DeepAR models through mean score value criteria for Value-at-Risk and Expected Shortfall at $\alpha = 0.05$ considering the pair Portfolio time series valuation. 27

II.1 Results of market efficiency analysis using the A-MFDFA method for various cryptocurrency pairs (ETH/BTC, ETH/DAI, ETH/USDT) on decentralized (UNISWAP-V2) and centralized (Binance) exchanges for three distinct rolling window sizes. Daily observations ranges 08-11-2020 to 05-21-2023. 44

II.2 Results of market efficiency analysis using the A-MFDFA method for various cryptocurrency pairs (ETH/BTC, ETH/DAI, ETH/USDT) on decentralized (Uniswap-V2) and centralized (Binance) exchanges for three distinct rolling window sizes. Daily observations ranges 08-11-2020 to 09-15-2022 (before the Merge) and 09-16-2022 to 05-21-2023 (after the Merge). 45
II.3 This table presents the TOP method results across time lags from -3 to +1 days, highlighting temporal relationships between decentralized and centralized exchange pairs. It includes the percentage of lags under 1 day, indicating instances where decentralized pairs lead, and the average lags/leads per day, offering insights into temporal dynamics and synchronization patterns. 46

III.1 Descriptive statistics for the annualized electricity consumption time series. Statistics are shown for the raw data in levels (Annualised Consumption, TWh) and its first log-difference ($\Delta \log(y_t) = \log(y_t) - \log(y_{t-1})$). 53
III.2 Mean values of asymmetric MFDFA metrics for the logarithmic returns of Bitcoin mining energy consumption across different halving eras. Metrics include the upward (H_+), downward (H_-), and overall (H) Hurst exponents, the multifractal strength (ΔH), its shuffled counterpart (ΔH_{shuff}), and the fractal spectrum width ($\Delta\alpha$). Results were calculated using rolling window lengths of 256, 384, and 512 observations. The table also includes the mean (μ) and standard deviation (σ) of the raw energy consumption (TWh) for each period. 60
III.3 Timeline of exogenous shocks and protocol-defined events considered in this study for their potential influence on the multifractal properties of Bitcoin's energy consumption. 62
III.4 F-statistics from Chow tests assessing structural breaks in the Hurst exponent time series computed from Cambridge Bitcoin Electricity Consumption Index (CEBCI) data. Breakpoints represent major on-chain events and off-chain shocks, Table III.3, impacting Bitcoin mining energy patterns. The test employed a 90-day window before and after each shock to detect structural changes. 63

Acronyms

AMM Automated Market Makers

ARNN Autoregressive Recurrent Neural Networks

ASIC Application-Specific Integrated Circuit

asymmetric MF-DFA Asymmetric Multifractal Detrended Fluctuation Analysis

BTC Bitcoin

CBECI Cambridge Bitcoin Electricity Consumption Index

CEX Centralized Exchanges

CFMM Constant-Function Market Maker

DApps Decentralized Applications

DeFi Decentralized Finance

DEX Decentralized Exchanges

DFA Detrended Fluctuation Analysis

DiD Difference-in-Differences

EMH Efficient Market Hypothesis

ES Expected Shortfall

ETH Ethereum

ETH-BTC Ethereum-Bitcoin

ETH-DAI Ethereum-DAI

ETH-USDC Ethereum-USDC

ETH-USDT Ethereum-Tether

GARCH Generalized Autoregressive Conditional Heteroskedasticity

GAS Generalized Autoregressive Score

HS historical simulation

IL Impermanent Loss

LP Liquidity Pool

MDM Market Deficiency Measure

MF-DFA Multifractal Detrended Fluctuation Analysis

PoS Proof of Stake

PoW Proof of Work

PUE Power Usage Effectiveness

RVaR Range Value-at-Risk

TOP Thermal Optimal Path

USA United States of America

VaR Value-at-Risk

WBAVR Wild Bootstrap Automatic Variance Ration

Introduction

The conceptual foundation of blockchain technology, a cryptographically secured and distributed ledger, predates its most famous application. However, it was the 2008 whitepaper (NAKAMOTO, 2008) by the pseudonymous Satoshi Nakamoto that presented Bitcoin (O'DWYER e MALONE, 2014) as a practical implementation of this concept, engineered explicitly in response to the erosion of confidence in the traditional financial sector exposed by the 2007/2008 crisis (EARLE, 2009). Bitcoin introduced a novel consensus mechanism, Proof of Work (PoW), to secure a decentralized network without a central authority (GERVAIS *et al.*, 2016b). In its early years, Bitcoin's pricing mechanisms were rudimentary, evolving from simple peer-to-peer trades on internet forums where enthusiasts, not yet foreseeing its investment potential, negotiated prices and transferred coins directly between wallets. The subsequent proposal of Ethereum aimed to address perceived limitations in Bitcoin's programmability and scalability, introducing a generalized blockchain with a built-in scripting language for smart contracts (BUTERIN *et al.*, 2014). This critical innovation unlocked a new design space for decentralized applications, enabling the creation of sophisticated on-chain pricing mechanisms. This led to the development of Constant Function Market Makers (CFMMs) (ANGERIS e CHITRA, 2020; HANSON, 2003), algorithmic protocols that fundamentally differ from traditional order books by using liquidity pools and deterministic functions to price assets automatically.

The complex ecosystem of DeFi has emerged directly from the evolution of blockchain technology from a simple digital currency into a programmable, global computing platform. The rapid proliferation of these new financial structural components presents a critical set of interconnected challenges that form the core of this thesis. First, there is the challenge of managing novel financial risks in permissionless systems, where immutable smart contracts introduce unique vulnerabilities. These include both technical exploits, such as smart contract frauds and price manipulation attacks, and financial risks inherent to protocol design, such as impermanent loss for liquidity providers. Mitigating these vulnerabilities requires new frameworks for quantifying risk, a core contribution of this thesis. Second is the assessment of market efficiency within these new pricing mechanisms, whether Constant-Function

Market Maker (CFMM) based DEX achieve efficiency comparable to or different from the CEX order books they aim to disrupt. The third challenge involves understanding the behavioral dynamics of the significant environmental footprint associated with the cryptographic security of PoW. This remains a major point of external criticism and internal debate, and this thesis contributes by analyzing the multifractal nature of Bitcoin's energy consumption patterns and their response to programmed halving events and regulatory shocks.

This thesis is structured upon the premise that these three challenges - financial risk, market efficiency, and environmental sustainability - are not isolated concerns but are deeply intertwined facets of the blockchain ecosystem's maturation. To fully grasp the implications of decentralized systems, one must examine them through these complementary lenses. To address this, the thesis comprises three empirical articles, each serving as a foundational element that is independently substantial yet integral to the cumulative argument. A core methodological innovation unifying these studies is their reliance on novel, on-chain data sources, moving beyond the limitations of conventional centralized exchange data (AL-YAHYAEE *et al.*, 2020; CHENG *et al.*, 2019) to analyze the native activity of blockchain environments. This approach provides a more authentic and granular understanding of economic behaviors, from liquidity provisioning and price discovery to energy expenditure, thereby offering a truer representation of the DeFi economy's underlying dynamics.

A foundational component of this research is Article I, which conducts a pioneering exploration of DEX, focusing on the unique financial risks inherent in platforms like Uniswap-V2, which utilizes CFMM pricing mechanisms and LP to facilitate trustless trading (ANGERIS e CHITRA, 2020; HANSON, 2003; KRISHNAMACHARI *et al.*, 2021). A significant contribution is its use of a large dataset of LP, sourced from The Graph protocol, to address a critical gap in the literature by providing a comprehensive analysis of financial risk. It meticulously comparesVaR and ES forecasts using both parametric GARCH models and a novel non-parametric *DeepAR* neural network approach (SALINAS *et al.*, 2020), directly contributing to the improvement of DeFi risk tools. The results yield crucial policy implications, underscoring the need for enhanced user safeguards in this rapidly evolving financial landscape (BASEL COMMITTEE ON BANKING SUPERVISION, 2013; MÜLLER *et al.*, 2022).

In this application, the empirical analysis of financial risk in Uniswap-V2 demonstrates that liquidity provision, a core mechanism of DeFi, typically constitutes a lower risk financial strategy than maintaining a buy and hold portfolio. A notable exception exists for stablecoin pairs where protocol fees become the primary risk driver. The comparative forecasting exercise yields a critical methodological insight by demonstrating the superior efficacy of GARCH models for VaR estimation which

is complemented by the pronounced ability of the advanced DeepAR neural network to accurately capture tail risk events as quantified by ES. These results provide an empirical foundation for the development of next-generation risk management tools and carry implications for regulatory policy, highlighting the urgent need for sophisticated, model-informed safeguards to protect users in the dynamically evolving DeFi landscape.

Building upon the analysis of decentralized market microstructure, in Article II it shifts the focus to market efficiency. It conducts a pioneering comparative analysis of the weak form of the Efficient Market Hypothesis (EMH) across centralized (Binance) and decentralized (Uniswap-V2) pricing mechanisms for key Ethereum pairs (NADARAJAH e CHU, 2017; URQUHART, 2016). Using multifractal detrended fluctuation analysis (MF-DFA) and its asymmetric extension (A-MFDFA) (CAO *et al.*, 2013; NAEEM *et al.*, 2021; SHAHZAD *et al.*, 2020), this research tests the hypothesis that decentralized liquidity pools exhibit different efficiency properties than centralized order books. Furthermore, it utilizes the TOP method (SORNETTE e ZHOU, 2005; ZHOU e SORNETTE, 2006) to establish lead-lag relationships between these markets, offering insights into price discovery processes and the impact of significant blockchain events like the Ethereum 2.0 hard fork.

Empirical evidence decisively challenges the traditional hierarchy of market structures, revealing that the algorithmic liquidity pools of Uniswap-V2 can surpass the efficiency of centralized order books. The application of asymmetric MF-DFA demonstrates that the Ethereum-Bitcoin (ETH-BTC) pair achieves a greater degree of weak-form efficiency on the decentralized exchange. This superiority intensified significantly after the Ethereum 2.0 upgrade. This efficiency premium is driven by the foundational pillars of DeFi, namely radical transparency and a high velocity of arbitrage activity, which collectively act as a potent corrective force against market inefficiencies. The DEX leading role in price discovery is conclusively established by the TOP method, which identifies Uniswap-V2 as the lead market, transmitting pricing signals to Binance with an average lag of under 24 hours. These findings collectively portray the DEX not as a nascent alternative but as increasingly dominant venue for efficient price formation in the digital asset ecosystem.

Article III addresses one of the most pressing critiques of the blockchain space, the energy consumption of Bitcoin's PoW consensus mechanism (KÜFEOĞLU e ÖZKURAN, 2019; O'DWYER e MALONE, 2014; VRANKEN, 2017). It investigates the long-term impact of Bitcoin's programmed halving events on the network's energy consumption patterns - a relationship that remains insufficiently understood (LI *et al.*, 2019, 2023). Using data from the Cambridge Centre for Alternative Finance (CCAF) (CAMBRIDGE CENTRE FOR ALTERNATIVE FINANCE, 2022), it analyzes whether these deliberate supply shocks cause measurable regime shifts in

energy use, further contextualized by external regulatory shocks like China's mining ban. The application of asymmetric MF-DFA reveals the complex, multifractal nature of Bitcoin's energy dynamics (ALMEIDA *et al.*, 2025; CAO *et al.*, 2013).

The multifractal analysis reveals Bitcoin mining energy consumption evolved from persistent, heterogeneous patterns toward efficient randomness across halving epochs. Early periods showed strong multifractality during consumption declines, reflecting unconstrained expansion. Operational maturity increased post-China ban, with converging scaling behaviors. A paradigm shift occurred post-fourth halving where long-range correlations dominated fat-tailed distributions, indicating structural dependencies now suppress volatile expansions. The results indicate that miner responsiveness is scale-dependent. Furthermore, Ethereum's transition to PoS induced significant cross-chain effects, most notably a sharp decline in the persistence of Bitcoin's energy consumption dynamics - evidenced by a statistically significant reduction in both upward and downward Hurst exponents, as confirmed by Chow test results.

Together, these three articles form a comprehensive examination of the fundamental challenges and dynamics within the blockchain ecosystem, encompassing Bitcoin, DeFi, and their underlying architectures. Through the innovative application of on-chain data analysis and multifractal econometrics, this work contributes for financial research, yielding market-relevant findings on DEX efficiency, pioneering research on risk models for liquidity provision, and producing a novel characterization of the energy dynamics that underpin blockchain security.

This thesis is structured into five sections, beginning with an Introduction that frames the research agenda in Cryptofinance. Chapter I contains the article *Risk forecasting comparisons in decentralized finance: An approach in constant product market makers*, published in Computational Economics (2025, JCR IF: 2.2; Qualis A1), which quantifies and compares risk levels in CEX and DEX trading environments. Chapter II presents *Pricing efficiency in cryptocurrencies: the case of centralized and decentralized markets*, presented at the Annual Conference of the Banco Central do Brasil (2024) and published in the Journal of Economics and Business (2025, JCR IF: 3.4), which compares market efficiency between centralized and decentralized exchanges. Chapter III includes the article *Bitcoin's halving events and the fractal nature of mining energy consumption*, a study on the long-term evolution and efficiency of Bitcoin's energy use following halving events and external shocks. The thesis concludes by synthesizing these findings into a cohesive framework linking DeFi risk, market efficiency, and Bitcoin's energy dynamics.

Chapter I

Risk forecasting comparisons in decentralized finance: An approach in constant product market makers

This study leverages decentralized liquidity pool data sourced from UNISWAP-V2 to forecast Value-at-Risk (VaR) and Expected Shortfall (ES) employing the Generalized Autoregressive Conditional Heteroskedasticity (GARCH) model with varied error distributions and the deep learning probabilistic forecasting algorithm known as *DeepAR*. Performance evaluations of these distinct forecasting methodologies are conducted using an appropriate loss function. Results indicate that the GARCH model with a normal distribution consistently outperforms other models, particularly when forecasting VaR. Conversely, the *DeepAR* model exhibits limited effectiveness in VaR forecasting across all scenarios, except for liquidity pools involving at least one stablecoin. However, it demonstrates greater reliability in predicting most ES risk measures and associated data. Our findings underscore that in a subset of the data, providing liquidity to pairs involving at least one *stablecoin* entails statistically significant lower risk compared to holding an equivalent amount of crypto assets. Furthermore, this research contributes to the advancement of novel risk management tools and strategies tailored for liquidity providers.

Keywords:

Notes: This research was presented at the XXIII Encontro Brasileiro de Finanças (2023) and published in Computational Economics, Volume 65, 2025 (2025 JCR Impact Factor: 2.2; Qualis A1).

1 Introduction

Blockchain technology emerged in response to eroding trust in the traditional financial sector, notably following the 2007/2008 Subprime Mortgage crisis (EARLE, 2009). Initially rooted in information systems research (LABAZOVA, 2019), the body of literature concerning blockchain acknowledges critical limitations, such as recording delays, and delves into assessing the performance metrics of diverse blockchain designs (WALSH *et al.*, 2016; XU *et al.*, 2017b).

Characterized as *Public permissionless*, fully decentralized blockchains enable universal access for reading, writing, and validating information (BECK e MÜLLER-BLOCH, 2017; BECK *et al.*, 2018). They prove beneficial for applications engaging numerous untrusted participants, often employing *proof-of-work* (GERVAIS *et al.*, 2016a) or *proof-of-stake* (SALEH, 2021a) consensus mechanisms to facilitate agreement on system updates.

Blockchains extend their utility across diverse industry domains (CHAUHAN *et al.*, 2018; DÜDDER e ROSS, 2017), including the execution and compilation of financial contracts, as exemplified by Bitcoin Bitcoin (BTC). The bulk of blockchain research primarily centers on providing insights into cryptocurrencies, notably BTC, and their functionalities (BÖHME *et al.*, 2015; NARAYANAN *et al.*, 2016). Significant focuses within this literature encompass user privacy and the identification of fraudulent activities (ALQASSEM *et al.*, 2018; KOSBA *et al.*, 2016; MAESA *et al.*, 2019; REYES-MACEDO *et al.*, 2019; TOYODA *et al.*, 2019; WANG *et al.*, 2020; XIA *et al.*, 2021).

Over nearly a decade, a sophisticated financial ecosystem, termed DeFi, has gradually taken form within existing blockchain platforms. DeFi embodies a collection of smart contracts executing business logic, such as lending, trading, and derivatives, on *public permissionless* blockchains. Within DEX, addressing currency exchange challenges involves deploying a CFMM pricing mechanism (HANSON, 2003; KRISHNAMACHARI *et al.*, 2021) - a focal area of DeFi research since the seminal work by SZABO (1996). A CFMM essentially comprises liquidity pools (LPs) [1], facilitating asset pricing through a scoring rule mapping current pool sizes to marginal prices (AIGNER e DHALIWAL, 2021; ANGERIS e CHITRA, 2020; LOESCH *et al.*, 2021). Liquidity providers, akin to investors in DEXs, earn a fixed percentage (e.g., 0.05%, 0.3% or1%) of transaction fees distributed among participants proportional to their stakes in the pool.

When a liquidity provider deposits two distinct assets into a UNISWAP-V2 pool, they are issued liquidity tokens representing their stake in the pool. These tokens offer flexibility, allowing their holders to redeem them at any time for the original coins

[1] Traditional finance has a similar mechanism: Exchange Traded Funds (ETF).

or trade and transfer them to other users. However, upon dissolution, the resulting amount and total value may deviate from the initially supplied values owing to the inherent volatility of cryptocurrencies and the lucrative arbitrage opportunities for traders. These pools serve as facilitators for direct cryptocurrency trading from user wallets, eliminating the necessity to match buy and sell orders. This mechanism ensures efficient and continuous trading operations while providing participants the opportunity to earn fees and rewards for their contribution to liquidity provision.

Within a decentralized exchange environment, liquidity providers may encounter an issue known as Impermanent Loss (IL) (ADAMS *et al.*, 2020; AIGNER e DHALIWAL, 2021; LOESCH *et al.*, 2021). This phenomenon arises due to the price volatility of the contributed assets, potentially resulting in a reduction of overall returns for providers (UNISWAP, 2023).

UNISWAP-V2, operating as a Decentralized Exchange (DEX) and employing a constant-product function, has emerged as a prominent on-chain authority for determining the relative price of asset pairs (ANGERIS e CHITRA, 2020; CALDARELLI e ELLUL, 2021). Consequently, it becomes imperative to assess the risks associated with instruments establishing cryptoasset prices, ensuring synchronization between off-chain and on-chain data sources. Another aspect demanding attention is the escalating number of active users utilizing non-custodial Metamask wallets (CONSENSYS, 2021), exhibiting a staggering 1.800% increase in monthly active users within a year, coupled with integration into established governmental payment methods (CONSENSYS, 2022). However, it is noteworthy that each active wallet may not represent a distinct individual or entity (TASCA *et al.*, 2018). Nevertheless, this surge underscores mounting interest in decentralized environments, aligning with the pursuit of *well-diversified* portfolios (KAJTAZI e MORO, 2019) in the context of *web3.0*.

Existing research utilizing decentralized data from DEXs remains limited, often constrained to a select few liquidity pools (LPs). For instance, LO e MEDDA (2022) examine the effectiveness of the UNISWAP-V2 financial market through the Ethereum-Tether (ETH-USDT) liquidity pool. Additionally, regulatory inconsistencies and systemic stability risks associated with stablecoins are explored by ADACHI *et al.* (2020), while KLAGES-MUNDT *et al.* (2020) delve into economic modeling frameworks for stablecoin designers. Studies by HEIMBACH *et al.* (2021) and BERG *et al.* (2022) respectively scrutinize flow dynamics between UNISWAP-V2 liquidity pools and inefficiencies between UNISWAP-V2 and SushiSwap DEX, addressing sub-optimal trade routing. WANG *et al.* (2022b) exploit cyclical arbitrage using decentralized data. The utilization of the GARCH model in decentralized data analysis remains limited, as observed in HANSEN *et al.* (2022) investigating the volatility of the Ethereum-USDC (ETH-USDC) pair in UNISWAP-V2 through

GARCH(1,1).

Effective risk management within asset liquidity pools holds paramount importance due to the potential for substantial losses. MÜLLER *et al.* (2022) emphasize the significance of accurate risk measure forecasting as a crucial facet of comprehensive risk management. VaR and ES are widely acknowledged risk measures in both academic literature and regulatory capital determination practices (BASEL COMMITTEE ON BANKING SUPERVISION, 2013). Accurate estimation of VaR and ES is essential for informed investor decision-making. Previous studies have compared diverse VaR and ES forecasting methodologies ((ACEREDA *et al.*, 2020; LIKITRATCHAROEN *et al.*, 2018; LIU *et al.*, 2020; TROSTER *et al.*, 2019; TRUCÍOS e TAYLOR, 2022; TRUCÍOS, 2019)), with MÜLLER *et al.* (2022) contributing further by forecasting Range Value-at-Risk (RVaR). Primarily, these investigations rely on econometric models like GARCH and Generalized Autoregressive Score (GAS). While few studies consider Machine Learning models for risk prediction (GÖRGEN *et al.*, 2022), rare works conduct comparative analyses between statistical and machine learning techniques (SHEN *et al.*, 2021). Notably, the data used in these research studies are sourced from exchanges or cryptoasset price-tracking websites, aggregating prices via volume-weighted averages from different exchanges. In the landscape of DeFi, bold investment alternatives like providing liquidity to LPs are increasingly common in investor portfolios, albeit approached cautiously (YOUSAF e YAROVAYA, 2022).

This article presents a comprehensive analysis of VaR and ES risk measures in the domain of decentralized data. The dataset derives from individual liquidity pools within the UNISWAP-V2 decentralized exchange, with daily prices sourced from *The Graph*, a decentralized protocol enabling indexing and querying of Ethereum blockchain data. Spanning from May 5th, 2020, to February 22nd, 2022, this dataset comprises 62,808 distinct liquidity pool addresses following a meticulous cleaning process. Additionally, a simple $1/N$ portfolio strategy (with $N = 2$) emulates a buy-and-hold tactic for the two crypto assets constituting each liquidity pool. A wide range of decentralized data can be gathered from the *web 3.0*.

Central to our dataset is the focus on the CFMM as a decentralized price formation mechanism, allowing asset trades without a fixed unit of exchange (ANGERIS *et al.*, 2022a,b; DAIAN *et al.*, 2019; FRONGILLO *et al.*, 2023; GOYAL *et al.*, 2022; HANSON, 2003). This concept markedly diverges from the conventional order book system in traditional finance. Moreover, parallels between Automated Market Makers (AMM) and prediction markets in traditional finance underscore their development (FRONGILLO *et al.*, 2023; OTHMAN e SANDHOLM, 2010; SLAMKA *et al.*, 2012). We estimate the risk using the GARCH model and *DeepAR* approach. *DeepAR* (SALINAS *et al.*, 2020) utilizes Autoregressive Recurrent Neural Networks

(ARNN) to probabilistically forecast time series future distributions by learning from the entire dataset, in contrast to separate models for each time series

Our research distinctly relies solely on data from the UNISWAP-V2 decentralized exchange, a unique utilization within this context. To date, limited research has incorporated risk measures with decentralized data from liquidity pools, such as HEIMBACH *et al.* (2022a), estimating ES for 9 LPs from UNISWAP-V2 using historical simulation (HS). However, studies have illustrated HS's inferior predictive performance compared to parametric methods like GARCH models (MÜLLER e RIGHI, 2022). Our contribution lies in conducting a meticulous comparative analysis of VaR and ES forecasting models. This involves employing appropriate loss functions, encompassing parametric modeling with GARCH using various distributions and lag parameters, alongside the introduction of a non-parametric ARNN approach - *DeepAR*. This unconventional comparison between statistical GARCH and machine learning ARNN models in forecasting VaR and ES constitutes a unique aspect of our research. Moreover, *DeepAR* remains relatively unexplored for ES predictions, with promising outcomes noted in VaR prediction as seen in FATOUROS *et al.* (2022).

The policy implications of our research highlight the need for educational initiatives to apprise users of the risks and benefits of Decentralized Exchanges (DEXs) and the broader blockchain ecosystem. Policymakers are urged to erect structural barriers, considering the rising popularity of DEXs due to reduced cryptocurrency risks proposed in our research, to curb potential channels for risk transmission to traditional financial markets. Recognizing the pivotal role of liquidity provision in DEX success, policymakers may consider incentivizing liquidity providers and implementing programs to ensure adequate liquidity in these markets.

This article is organized into distinct sections, each contributing essential insights into our analysis of risk measures using GARCH and *DeepAR* models within decentralized data. The 2 section provides comprehensive background information concerning the data and methodology employed in this study. It outlines various risk measures, such as GARCH, while introducing *DeepAR* as a forecasting method utilized within this context. This section delves into the specifics of decentralized data, encompassing score functions and the intricate process of hyperparameter tuning for the *DeepAR* model. The 3 section presents the outcomes derived from our analysis, offering valuable insights into the efficacy of different risk measures and evaluating the performance of the *DeepAR* model within a decentralized framework. These findings illuminate the effectiveness and suitability of these models in handling decentralized data for risk estimation purposes. Lastly, the 4 encapsulates the study by emphasizing the key findings and implications gleaned from the research. It elucidates critical takeaways and outlines potential avenues for future exploration

and development within this field, ultimately concluding the article with a nuanced perspective on the significance of the findings and their impact on future research trajectories.

2 Data and methodology

This section presents the dataset obtained from The Graph decentralized protocol and introduces the calculation methods for Value-at-Risk (VaR) and Expected Shortfall (ES), along with their respective scoring functions. Additionally, it delineates the methodologies utilized to compute these risk measures, focusing primarily on the GARCH and *DeepAR* approaches, emphasizing the crucial tuning process for *DeepAR's* hyperparameters. Finally, this section expounds on the methodological procedures integral to the outcomes presented in this research.

2.1 Data acquisition

The data utilized in this study is sourced from *The Graph* (https://thegraph.com/). Specifically, we queried the UNISWAP-V2 subgraph available at https://api.thegraph.com/subgraphs v2. Employing a *Python* script, we indiscriminately gathered information on all liquidity pools created within UNISWAP-V2 until February 22, 2022. For each liquidity pool (LP), we executed appropriate queries to acquire individualized data, encompassing key parameters such as: `dailyVolumeToken0` and `dailyVolumeToken1`: Representing trade volumes for tokens 0 and 1 within the liquidity pool, respectively; `reserve0` and `reserve1`: Denoting the quantities of tokens 0 and 1 constituting the liquidity pool at specific timestamps; `dailyVolumeUSD`: Accumulated trade volume in USD at each trade instance; `reserveUSD`: Reflecting the liquidity derived from live conversions to USD; and `totalSupply`: Varied values contingent on transactional activities involving burns and mints, affecting the total supply within the liquidity pool.

Our dataset was purposefully structured with daily observations, a frequency commonly used in related works (FATOUROS *et al.*, 2022; HEIMBACH *et al.*, 2021; MÜLLER *et al.*, 2022), aiming to streamline computational processing for risk models while aligning with prevalent research practices. The dataset, formatted in JSON, encapsulates various key parameters: `dailyVolumeToken0` and `dailyVolumeToken1`, representing trade volumes for tokens 0 and 1 within the liquidity pool at specific timestamps, while `reserve0` and `reserve1` denote the quantities of tokens 0 and 1 composing the pool. Additionally, `dailyVolumeUSD` signifies accumulated trade volume in USD, and `reserveUSD` reflects liquidity converted to USD. The variable `totalSupply` denotes the quantity of LP tokens, subject to fluc-

tuations due to transactions, burns, and mints.

As of February 22, 2022, 12:00 AM (GMT), liquidity pools with at least one transaction contained a total of $USD 5,462,905,325.26$. Notably, the longest-standing liquidity pool, ETH-USDC, spanned 657 days from May 5, 2020, to February 22, 2022. The creation of liquidity pools surged following the inception of UNISWAP-V2 in the decentralized environment. From 4th May 2020 to 15th February, 2022, an average of 35.31 new pools emerged daily, peaking at 115 pools on September 21th, 2020. From the initial set of 62,808 liquidity pools, 3,896 involved at least one stablecoin, with 87 forming strictly stable liquidity pools. These were filtered based on their daily mean transaction volume, selecting the top 29 pairs with consistent data lengths and temporal synchronicity. The selection criteria aimed to include pairs commonly favored by DeFi investors while excluding those associated with irregular trading patterns or limited transaction records. This comprehensive selection of liquidity pools surpasses the scope of prior research, where selections were often limited to 12 LPs or restricted to BTC or Ethereum paired with a stablecoin (HANSEN *et al.*, 2022; HEIMBACH *et al.*, 2021; KILIMCI *et al.*, 2021; SIHANANTO *et al.*, 2022).

The analyzed timeframe spanned 465 days, initiating on November 14, 2020, and concluding on February 22, 2022. This period encapsulated tumultuous events, including the peaks of the SARS-CoV-2 pandemic, a significant United States of America (USA) presidential inauguration, global disruptions in supply chains, and the unprecedented peak in BTC pricing. It differed from the original data by 193 days, stemming from the individual launch dates of each liquidity pool. The selection of pools based on their daily mean transaction volume suggests inherent value perceived by users (investors), guiding our choices. The shortened period aims for consistency in observing patterns and facilitating categorical model comparisons. This timeframe also encompasses the lifecycle of liquidity pools, exemplified by specific instances such as the ETH-TEND pair in I.1, which experienced a staggering loss of more than 99% of its value. Additionally, it reflects the transition of an unconventional investment approach to a widely debated option, evident in the substantial increase in BTC and ETH prices by 130.24% and 456.38% respectively during this period.

2.2 Risk measures

The random variable X represents the outcome associated with any asset, where $X \geq 0$ signifies a gain and $X < 0$ indicates a loss. This variable is defined within the probability space $\mathcal{X} := \mathcal{X}(\Omega, \mathcal{F}, \mathcal{P})$. The functions F_X and F_X^{-1} correspond to the cumulative distribution function and the inverse function of X, respectively.

Table I.1: Descriptive statistics of the Liquidity Pool's token returns. The sample period runs from November 14, 2020, until February 02, 2022.

Pair address	Coin names	Returns mean	Standard Deviation	Kurtosis	Skewness
0x08650bb9dc722c9c8c62e79c2bafa2d3fc5b3293	ETH-AMP	0.004835	0.059131	6.651434	-0.028724
0xc5be99a02c6857f9eac67bbce58df5572498f40c	ETH-AMPL	0.001130	0.061905	4.481216	-0.049043
0xc730ef0f4973da9cc0ab8ab291890d3e77f58f79	ETH-AUDIO	0.004493	0.064844	6.890275	-0.107408
0xbb2b8038a1640196fbe3e38816f3e67cba72d940	ETH-BTC	0.003007	0.045070	5.552948	-0.561386
0xa5e79baee540f000ef6f23d067cd3ac22c7d9fe6	ETH-CEL	0.002978	0.045140	5.512953	-0.304625
0xcffdded873554f362ac02f8fb1f02e5ada10516f	ETH-COMP	0.002246	0.057448	5.229382	-0.513556
0x32ce7e48debdccbfe0cd037cc89526e4382cb81b	ETH-CORE	0.002677	0.054735	5.733394	0.280460
0x3da1313ae46132a397d90d95b1424a9a7e3e0fce	ETH-CRV	0.004290	0.065133	7.055627	-0.780321
0xa478c2975ab1ea89e8196811f51a7b7ade33eb11	ETH-DAI	0.002536	0.026871	6.715019	-0.364145
0x4d5ef58aac27d99935e5b6b4a6778ff292059991	ETH-DPI	0.002552	0.055695	7.927443	-0.736460
0x7ba9b94127d434182287de708643932ec036d365	ETH-eRSDL	0.002866	0.080840	4.692515	0.214629
0x55d5c232d921b9eaa6b37b5845e439acd04b4dba	ETH-HEX	0.006898	0.058947	5.664145	0.010645
0xa2107fa5b38d9bbd2c461d6edf11b11a50f6b974	ETH-LINK	0.002358	0.058911	7.828114	-0.763793
0x819f3450da6f110ba6ea52195b3beafa246062de	ETH-MATIC	0.008094	0.066239	6.945842	0.220924
0xc2adda861f89bbb333c90c492cb837741916a225	ETH-MKR	0.003442	0.056651	7.716332	0.139178
0xffa98a091331df4600f87c9164cd27e8a5cd2405	ETH-POLS	0.004425	0.065330	5.904610	-0.279659
0x27fd0857f0ef224097001e87e61026e39e1b04d1	ETH-RLY	0.003739	0.062976	6.980647	0.229156
0x70ec2fa6eccf4010eaf572d1c1a7bcbc72dec983	ETH-ROOK	0.003751	0.075049	6.037947	0.482729
0x3dd49f67e9d5bc4c5e6634b3f70bfd9dc1b6bd74	ETH-SAND	0.007203	0.065980	6.220518	-0.108613
0x43ae24960e5534731fc831386c07755a2dc33d47	ETH-SNC	0.002329	0.058087	6.561864	-0.712413
0x3b3d4eefdc603b232907a7f3d0ed1eea5c62b5f7	ETH-STAKE	0.002715	0.064945	4.618415	-0.045599
0xc0bf97bffa94a50502265c579a3b7086d081664b	ETH-STRONG	0.005317	0.058099	5.026098	0.329018
0xd90a1ba0cbaaaabfdc6c814cdf1611306a26e1f8	ETH-SWAP	0.003139	0.068717	6.330821	0.027309
0xcfb8cf118b4f0abb2e8ce6dbeb90d6bc0a62693d	ETH-TEND	−0.017247	0.160188	11.063330	-0.479094
0xd3d2e2692501a5c9ca623199d38826e513033a17	ETH-UNI	0.003045	0.058999	7.517687	-0.370381
0xb4e16d0168e52d35cacd2c6185b44281ec28c9dc	ETH-USDC	0.002735	0.026923	6.631192	-0.355365
0x0d4a11d5eeaac28ec3f61d100daf4d40471f1852	ETH-USDT	0.002822	0.026937	6.551293	-0.361439
0x2fdbadf3c4d5a8666bc06645b8358ab803996e28	ETH-YFI	0.002570	0.057785	7.899990	-0.473001
0x3041cbd36888becc7bbcbc0045e3b1f144466f5f	USDC-USDT	0.000213	0.000543	5.923943	0.142786

The Value at Risk (VaR) and Expected Shortfall (ES) of X are defined as follows:

$$VaR^{\alpha}(X) = -F_X^{-1}(\alpha) = -\inf\{x : F_X(x) \geq \alpha\} \tag{I.1}$$

$$ES^{\alpha}(X) = \frac{1}{\alpha}\int_0^{\alpha} VaR^{u}(X)du, \tag{I.2}$$

where $X \in \mathcal{X}$ and $\alpha \in (0,1)$, with α denoting the significance level. VaR^{α} quantifies the maximum loss for a given significance level (α) within a specific period.

VaR, however, disregards losses beyond the α-quantile of interest and lacks coherence, failing to fulfill the sub-additivity axiom. Consequently, it does not adhere to the principle of diversification; the VaR of a portfolio may surpass the aggregated risk of individual assets.

Addressing VaR's limitations, Expected Shortfall (ES) emerges as an alternative, quantifying the expected value of losses beyond the α-quantile (VaR). Notably, ES maintains coherence, providing a more robust measure.

Despite the notable advantages of Expected Shortfall (ES), it lacks a crucial statistical property possessed by Value at Risk (VaR) known as elicitability. Elicitability in a risk measure denotes its status as the minimizer of an expectation derived from a specific score function (GNEITING, 2011; ZIEGEL, 2016). This property holds significant practical importance, facilitating the comparison of competitive models using the scoring rule.

Typically, VaR demonstrates elicitability under a specific score function (GNEIT-

ING, 2011)

$$S^{VaR^\alpha}(x,y) = \alpha(x-y)^+ + (1-\alpha)(x-y)^- = \alpha\max\{x-y,0\} + (1-\alpha)\min\{x-y,0\}, \tag{I.3}$$

where y_i are the observed return history and x_i are the forecasted VaR values.

While ES doesn't satisfy elicitability independently, it is jointly elicitable with VaR. Therefore, the mapping $\rho(X) = (VaR^\alpha(X), ES^\alpha(X))$ retains elicitability. The score function for ES is given by (FISSLER e ZIEGEL, 2016; GERLACH *et al.*, 2017):

$$\begin{aligned} S_t^{ES^\alpha}(y, VaR_t^\alpha, ES_t^\alpha) =& VaR^\alpha(I_{(y<VaR_t^\alpha)}) - \alpha) - yI_{(y<VaR_t^\alpha)} \\ &+ e^{ES_t^\alpha}\left(ES_t^\alpha - VaR_t^\alpha + \frac{I_{(y<VaR_t^\alpha)}}{\alpha}(VaR_t^\alpha - y)\right) \\ &- e^{ES_t^\alpha} + 1 - \log(1-\alpha), \end{aligned} \tag{I.4}$$

where $I(\cdot)$ is an indicator function that takes 1 when the argument is true and 0 otherwise, VaR_t^α and ES_t^α are the forecasted risk measures at a significance level α and y follow exactly as in Equation I.3.

2.3 Risk forecast models

To grasp the concepts better, we introduce two models: the GARCH model and *DeepAR*.

GARCH model

Our approach involves a parametric representation of the random variable X_t: $X_t = \mu_t + \sigma_t z_t$. Here, μ_t and σ_t are the mean and standard deviation of the asset, conditioned on the available information at time t. Meanwhile, z_t represents a white noise process, capable of adopting various probability distributions. An influential model used for forecasting the risk of an asset's daily return (X_t) is the AR-GARCH model.

In general terms, the AR(p)-GARCH(q,s) model is described as follows:

$$\begin{aligned} X_t &= \phi_0 + \sum_{i=1}^{p}\phi_i X_{t-i} + \epsilon_t = \mu_t + \epsilon_t, \\ \epsilon_t &= \sigma_t z_t, \qquad z_t \sim i.i.d.\, F(\boldsymbol{\theta}), \\ \sigma_t^2 &= a_0 + \sum_{j=1}^{q} a_j \epsilon_{t-j}^2 + \sum_{k=1}^{s} b_k \sigma_{t-k}^2, \end{aligned} \tag{I.5}$$

where p is the order of the autoregressive component, ϕ_i (for $i = 1, \cdots, p$) are the parameters of the autoregressive model, ϵ_t is the error term, z_t is a white noise process with distribution $F(\boldsymbol{\theta})$, where $\boldsymbol{\theta}$ is a vector of parameters of the distribution, including zero mean and unit variance in addition to additional parameters that vary as the distribution. μ_t and σ_t^2 are the mean and variance conditional on past information, q and s are the orders of the GARCH model, and a_j and b_k, for $j = 1, \cdots, q$ and $k = 1, \cdots, s$ are the parameters of the GARCH model ($a_0 > 0$, $a_j \geq 0$, $b_k \geq 0$).

Building upon the Equation (I.5) model, estimation of VaR and ES is approached as follows:

$$\begin{aligned} \text{VaR}_{t+1}^{\alpha} &= -\mu_{t+1} + \sigma_{t+1}\text{VaR}^{\alpha}(z_{t+1}), \\ \text{ES}_{t+1}^{\alpha} &= -\mu_{t+1} + \sigma_{t+1}\text{ES}^{\alpha}(z_{t+1}), \end{aligned} \tag{I.6}$$

where μ_{t+1} and σ_{t+1} are, respectively, the forecast mean and conditional standard deviation obtained by the AR-GARCH model.

DeepAR

The application of *deep learning* architecture in time series forecasting involves predicting the state $h^{(t)}$—the hidden units within the network—at time t. Following the framework proposed by Goodfellow et al. (2016), a dynamic system takes the form:

$$\mathbf{h}^{(t)} = f(\mathbf{h}^{(t-1)}, \mathbf{x}^{(t)}, \theta) \tag{I.7}$$

Here, $\mathbf{h}^{(t-1)}$ represents the system's state at step $t-1$, $x^{(t)}$ denotes an external signal, and θ encompasses metadata related to layer weights and biases. Our problem necessitates a multivariate approach, and Equation I.7 can be extended without loss of generality (LI *et al.*, 2017; SALINAS *et al.*, 2020; SEN *et al.*, 2019). Specifically, we draw upon the work of Salinas et al. (2020), which models the conditional distribution $P(\mathbf{z}_{i,t_0:T}|\mathbf{z}_{i,1:t_0-1}, \mathbf{x}_{i,1:T})$ of each time series $\mathbf{z}_i$ from times t_0 to T, given time series z_i.

The *DeepAR* model assumes a distribution as a product of multiple likelihood factors:

$$Q_\Theta(\mathbf{z}_{i,t_0:T}|\mathbf{z}_{i,1:t_0-1}, \mathbf{x}_{i,1:T}) = \prod_{t=t_0}^{T} Q_\Theta(z_{i,t}|\mathbf{z}_{i,1:t-1}, \mathbf{x}_{i,1:T})$$
$$= \prod_{t=t_0}^{T} p(z_{i,t}|\theta(\mathbf{h}_{i,t}, \Theta), \tag{I.8}$$

parameterized by the output $\mathbf{h}_{i,t}$ of an autoregressive recurrent network:

$$\mathbf{h}_{i,t} = h(\mathbf{h}_{i,t-1}, z_{i,t-1}, \mathbf{x}_{i,t}, \Theta),$$

where h represents a function governed by a multi-layer recurrent neural network, parameterized by Θ with *long short-term memory* (LSTM) cells. For a fixed z, $p(z_{i,t}|\theta(\mathbf{h}_{i,t}, \Theta)$ is a distribution with the function $\theta(\mathbf{h}_{i,t}, \Theta)$ (where $\mathbf{h}_{i,t-1}$ is the network output) as its input.

The *DeepAR* algorithm can learn future distribution parameters of a time series and can process multiple time series simultaneously, facilitating cross-learning. This algorithm's advantages span across numerous research fields (KHAN *et al.*, 2020; SHAN *et al.*, 2022).

2.4 Methodological procedures

The evaluation of financial risk associated with liquidity pools (LP) and their constituent portfolios involves examining LP returns and individual token returns (ADAMS *et al.*, 2020, 2021):

The LP return at time t, rLP_t, and the returns for tokens $rtoken0_t$ and $rtoken1_t$ are computed using logarithmic transformations:

$$rLP_t = \ln\left(\frac{reserveUSD_{t-1} \times totalSupply_t}{reserveUSD_t \times totalSupply_{t-1}}\right), \tag{I.9}$$

$$rtoken0_t = \ln\left(\frac{reserveUSD_t \times reserve0_{t-1}}{reserveUSD_{t-1} \times reserve0_t}\right). \tag{I.10}$$

where rLP_t is the liquidity pool return at time t; $rtoken0$ and $rtoken1$ are the returns of each of the tokens belonging to the liquidity pool. Whenever an investor provides liquidity to a UNISWAP-V2 pair, an equivalent amount of liquidity pool tokens is minted, reflecting the staked value. This token's price is determined by dividing the total amount $reserveUSD_t$ by $totalSupply_t$. A similar approach yields the return for the second token. The stationarity of both liquidity pool and token portfolio time series is confirmed using the Augmented Dickey-Fuller (ADF) test (DICKEY e FULLER, 1979a) and the Phillips-Perron (PP) test (PHILLIPS e PERRON, 1988).

Following these tests, our methodological approach unfolds in two phases: (i) model implementations and (ii) model score ranking. In (i) a combination of 5 lags for the GARCH(p,q) model, a common practice in cryptocurrency risk forecasting (JIMÉNEZ *et al.*, 2020; TROSTER *et al.*, 2019), results in 25 distinct models. Normal, Student-t, and asymmetric Student-t distributions are employed for each pair of lags, consistent with prior risk forecasting studies (DIAZ *et al.*, 2017; GUO, 2022; RIGHI e CERETTA, 2015). Furthermore, the *DeepAR* approach, as elucidated by SALINAS *et al.* (2020) and FATOUROS *et al.* (2022), predicts future distributions based on past behaviors. GARCH and *DeepAR* models are applied to forecast Value at Risk (VaR) and Expected Shortfall (ES) at significance levels $\alpha = 0.01$ and $\alpha = 0.05$, aligning with established standards in the literature (ARDIA *et al.*, 2019; MÜLLER e RIGHI, 2018; MÜLLER *et al.*, 2022; TRUCÍOS, 2019).

Finally, (ii) consists in obtaining VaR and ES score function values, which are implemented to compare the predicted risk models by computing the mean score function (NOLDE e ZIEGEL, 2017), which takes the following form for VaR and ES, respectively:

$$\bar{S} = \frac{1}{T} \sum_{i=1}^{T} S_i^{\rho}, \tag{I.11}$$

where S_i^{ρ} denotes the negatively oriented loss functions of the forecasted VaR or ES, derived from Equations I.1 and I.2. Lower values indicate superior model performance.

For the rolling window estimation with 250 observations (reflecting a period of rapid market capitalization growth), the minimum required by the Basel Committee (COMMITTEE *et al.*, 2013) for market risk forecasting is adhered to. While the parametric approach is straightforward, the non-parametric (*DeepAR*) method involves dividing the time series data into non-overlapping training and testing sets. The training set serves as input for the machine learning model, while the testing set is employed to compute the Continuous Ranked Probability Score (CRPS) (GNEITING e RAFTERY, 2007; HERSBACH, 2000), quantifying the distance between forecasted and actual values:

$$CRPS(F, x) = -\int_{-\infty}^{\infty} (F(y) - I(y \geq x))^2 dy, \tag{I.12}$$

Here, F represents the cumulative distribution function linked to the empirical probabilistic forecast, while $I(\cdot)$ symbolizes the Heaviside step function. This function takes on the value 1 for positive arguments and 0 otherwise. The variable x signifies the true value. CRPS, in essence, assesses the proximity between the predicted and real values. Similar to Equation I.11, a methodology for identifying

the most suitable model involves selecting the one with the minimized score mean function (DE LIMA SILVA *et al.*, 2019; GASTHAUS *et al.*, 2019).

Regarding the tuning of *DeepAR* hyperparameters, a grid search approach is employed (DE LIMA SILVA *et al.*, 2019; MATHONSI e VAN ZYL, 2021; WANG *et al.*, 2022a). At each forecasted step, the parameters are evaluated using CRPS, as mentioned earlier. This iterative tuning process continues until the conclusion of the rolling window procedure—spanning the entirety of the time series observations. Table I.2 displays the values of the two hyperparameters utilized to fine-tune the *DeepAR* model. The number of LSTM cells is determined by an intersection of the findings in probabilistic forecasting literature (MATHONSI e VAN ZYL, 2021) and the standard values recommended in the *DeepAR* guide[2]. Similarly, the determination of the number of hidden layers follows a comparable approach.

Table I.2: Hyperparameters used for the tunning of the *DeepAR* model.

LSTM cells	$\{10n \mid n \in \mathbb{N}, 4 \leq n \leq 10\}$
Hidden layers	1,2,3
Epochs	10
Learning rate	10^{-3}

We forecast the risk associated with 29 liquidity pools and their respective token portfolios, all initiated at the same point in time. The daily price of liquidity pool tokens is determined by dividing `reserveUSD` by `totalSupply`—refer to Section 2.1 for more details.

Leveraging *DeepAR* to predict the future probability density function of time series allows us to compute Value at Risk (VaR) by examining the 1% and 5% quantiles (adjusted with a negative sign). Conversely, Expected Shortfall (ES) is derived by averaging the return values that surpass the significance levels of 1% and 5% (also adjusted with a negative sign). This analysis employs liquidity pool returns alongside a buy-and-hold portfolio strategy involving both crypto assets in each liquidity pool. It's crucial to note the subtlety inherent in the distinction between providing liquidity and holding the same assets necessary to merge a predetermined amount of liquidity pool tokens following fluctuations in the price of one or both assets—referred to as Impermanent Loss (IL).

3 Results

To facilitate a comprehensive understanding of our findings, the results section is organized into two parts. The initial segment delves into a discussion centered around descriptive statistics pertaining to the risk observed. The subsequent section

[2] `https://docs.aws.amazon.com/sagemaker/latest/dg/deepar_hyperparameters.html`

showcases four tables, presenting an in-depth analysis of risk forecasting for both liquidity pools and portfolios. Here, GARCH and *DeepAR* models are employed to forecast Value at Risk (VaR) and Expected Shortfall (ES).

These tables meticulously exhibit risk forecast data for the top 29 liquidity pools within UNISWAP-V2, chosen based on their notably high average trading volume over a specified period. Each table illustrates the most accurate forecasted GARCH models, meticulously selected from a pool of 25 different lag pairs across three distributions—normal, Student-t, and asymmetric Student-t—pertaining to each liquidity pool and risk measure. Additionally, the tables present results derived from the *DeepAR* model.

Tables I.5 and I.6 showcase the outcomes for liquidity pools, focusing on α values of 1% and 5%, respectively. In parallel, Tables I.7 and I.8 showcase risk forecasts for portfolios employing a buy-and-hold strategy. This comprehensive breakdown provides a detailed analysis of risk across various liquidity pools and portfolios, shedding light on their forecasted VaR and ES through the lens of diverse modeling approaches.

Figures I.1 and I.2 offer concise visual summaries portraying the historical evolution of VaR, ES, and returns concerning the ETH-BTC pair. These visuals represent forecasts derived from the most accurate GARCH model (Tables I.5 through I.8) and the probabilistic forecasting *DeepAR* model, respectively. In Figure I.1, segments 1.A and 1.C illustrate VaR at 1% and 5% significance levels, while 1.B and 1.D showcase ES for these corresponding levels. Similarly, Figure I.2 presents VaR and ES illustrations from the *DeepAR* model, mirroring the same significance levels. Additionally, we present forecasts for the ETH-BTC portfolio, using models from Tables I.7 and I.8 over the same period.

Our dataset covers a period marked by significant events—on October 20, 2021, BTC reached an all-time high but declined by half its value by January 22, 2022. This downward trend may have been influenced by the Federal Reserve's inclination towards higher rates and the development of regulatory guidance for cryptocurrencies. Notably, in Figure I.2, the *DeepAR* forecasts exhibit higher risk peaks around the time when BTC plummeted to half its all-time high value, compared to the TableDeepAR forecasting in Figure I.1. Both Figures I.1 and I.2 adjust their forecasted values accordingly. As expected, VaR and ES values at 1% exhibit higher values compared to those at 5%. Remarkably, the forecasts generated by the *DeepAR* model appear to offer a more precise reflection of the time series evolution.

Table I.3 presents the mean forecasted risks derived from the encompassed GARCH models, spanning Tables I.5 to I.8. These results aim to delineate the risk disparity between providing liquidity (termed as *Liquidity Pool*) and adopting a buy-and-hold strategy for the assets (referred to as *Portfolio*). For instance, focusing on a specific

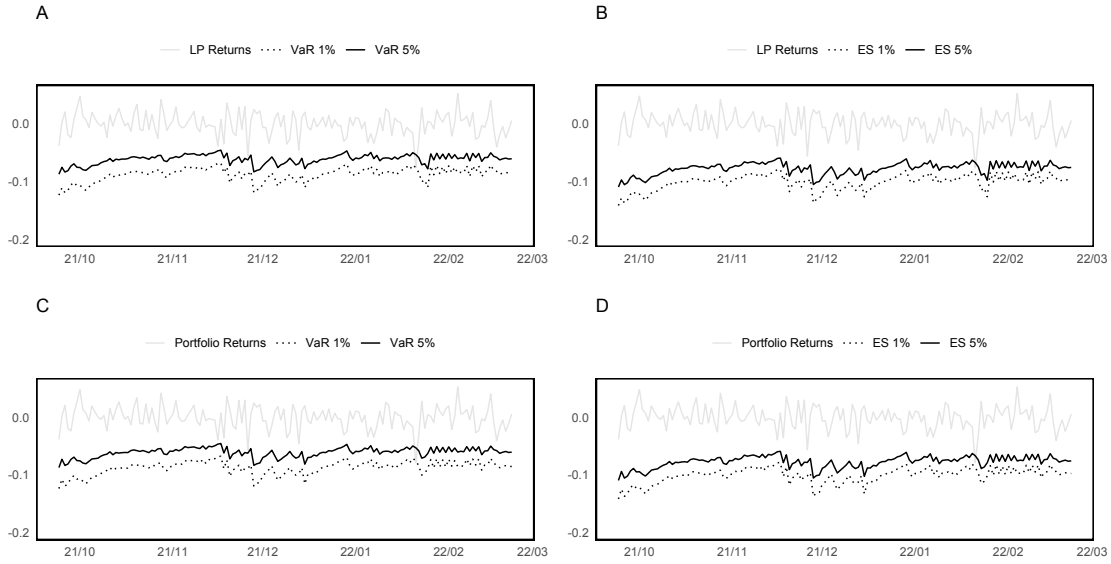

Figure I.1: Forecasted evolution of VaR and ES risks, using the best GARCH models from Table I.5 to I.8, at 1% and 5% significance levels, observed for the returns of the ETH-BTC liquidity and the portfolio. The time frame for this analysis spans from September 24, 2021, to February 22, 2022.

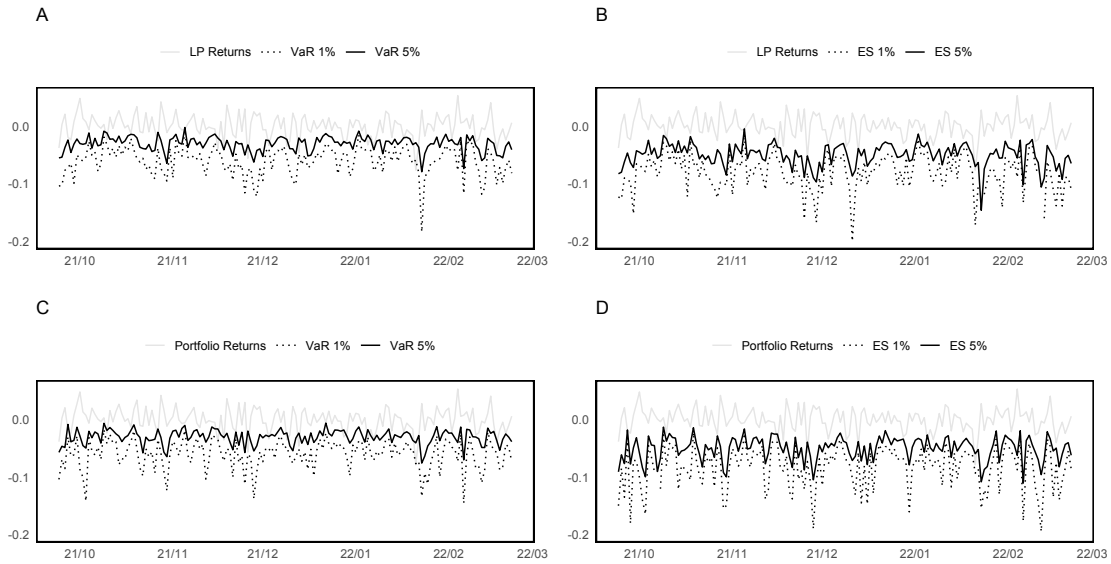

Figure I.2: Forecasted evolution of VaR and ES risks, using the *DeepAR* models, at 1% and 5% significance levels, for the returns of the ETH-BTC liquidity and the portfolio. The time frame for this analysis spans from September 24, 2021, to February 22, 2022.

risk model and significance level—let's consider $VaR^{0.01}$ for the ETH-BTC liquidity pool—the mean risk of the portfolio is approximately 0.19% higher. Notably, across the board, all portfolios consistently exhibit a tendency towards higher mean risk values compared to liquidity pools. To assess the statistical significance of this difference, we employ the unpaired Wilcoxon signed-rank test. This statistical test operates under the null hypothesis that the forecasted risks of both liquidity pools and portfolios share equal medians.

Table I.3: Mean forecasted risks values of the GARCH model which performed the better in VaR and ES considering two significance levels - 1% and 5%. The risk models are assessed by employing the apoppriate score function (loss function). Samples range from 2020/11/14 to 2022/02/22.

	Liquidity Pool ($VaR^{0.01}$)	Portfolio ($VaR^{0.01}$)	Liquidity Pool ($VaR^{0.05}$)	Portfolio ($VaR^{0.05}$)	Liquidity Pool($ES^{0.01}$)	Portfolio ($ES^{0.01}$)	Liquidity Pool ($ES^{0.05}$)	Portfolio Pool ($ES^{0.05}$)
ETH-AMP	0.111742	0.112247	0.077940	0.078715	0.128549	0.128919	0.098666	0.099312
ETH-AMPL	0.133051	0.132425	**0.089875*****	**0.093221*****	0.152405	0.151918	0.125348	0.117259
ETH-AUDIO	0.128521	0.130053	0.089913	0.091194	0.147717	0.149375	0.113585	0.115021
ETH-BTC	0.087370	0.087541	0.060995	0.061089	0.100483	0.100694	0.077223	0.077308
ETH-CEL	0.082378	0.082965	0.057804	0.058363	0.094597	0.095198	0.072872	0.073582
ETH-COMP	0.110131	0.110149	0.076960	0.077242	0.126413	0.126511	0.097213	0.097419
ETH-CORE	0.112922	0.112928	0.078702	0.078729	0.129937	0.129933	0.099684	0.099698
ETH-CRV	0.129577	0.129945	0.090808	0.090843	0.148871	0.149387	0.115025	0.114818
ETH-DAI	**0.049484****	**0.050433****	**0.034272****	**0.035058****	**0.057048****	**0.058077****	**0.043599****	**0.044485****
ETH-DPI	0.106587	0.106836	0.074519	0.074713	0.122458	0.122716	0.094257	0.094452
ETH-eRSDL	0.134626	0.136339	0.088523	0.090194	0.161172	0.162783	0.11715	0.118838
ETH-HEX	0.112086	0.114129	**0.076489***	**0.078597***	0.129786	0.131797	0.098316	0.100384
ETH-LINK	0.109937	0.110328	0.076672	0.077100	0.126477	0.126899	0.09707	0.0975203
ETH-MATIC	0.118313	0.118932	0.081745	0.082480	0.136496	0.1370573	0.10417	0.1048307
ETH-MKR	0.104268	0.104404	0.073103	0.073246	0.119763	0.119897	0.092212	0.092351
ETH-POLS	0.118004	0.118132	0.082893	0.083072	0.135462	0.135565	0.104431	0.104569
ETH-RLY	0.104084	0.104160	0.072694	0.072795	0.119692	0.119755	0.091941	0.092026
ETH-ROOK	0.132694	0.132952	0.093344	0.093680	0.152260	0.152479	0.11747	0.117760
ETH-SAND	0.136136	0.135867	0.094390	0.094482	0.156894	0.156445	0.119987	0.119857
ETH-SNC	0.113239	0.113579	0.079920	0.080293	0.129807	0.130128	0.100332	0.100707
ETH-STAKE	0.114633	0.115283	0.080391	0.080992	0.131659	0.132333	0.101399	0.102018
ETH-STRONG	0.092025	0.092761	0.057797	0.059198	0.113801	0.107051	0.079560	0.080920
ETH-SWAP	0.1275952	0.127905	0.089057	0.089409	0.146757	0.147046	0.124079	0.125094
ETH-TEND	0.388704	0.372610	0.278191	0.263004	0.961197	0.922924	0.575348	0.537748
ETH-UNI	0.112060	0.112939	0.078253	0.078956	0.128869	0.129450	0.098982	0.099793
ETH-USDC	**0.049224****	**0.050325****	**0.034035*****	**0.034995*****	**0.056777****	**0.057947****	**0.043349****	**0.044395****
ETH-USDT	**0.048887****	**0.050066****	**0.033776*****	**0.034820*****	**0.056401****	**0.057646****	0.043042**	**0.044168****
ETH-YFI	0.105258	0.105576	0.0739482	0.0740697	0.120786	0.121241	0.093329	0.093387
USDC-USDT	**0.000550*****	**0.000722*****	**0.0003513*****	**0.000512*****	**0.000649*****	**0.000827*****	**0.000473*****	**0.000641*****

Notes: * $p < 0.1$, **$p < 0.05$, *** $p < 0.01$. Statistical significance obtained by the Unpaired Wilcoxon signed-rank test.

When examining the outcomes of the Wilcoxon signed-rank test, it becomes evident that the liquidity pools in focus predominantly involve pairs that include at least one stablecoin. The noteworthy significance observed in the USDC-USDT pool arises from the nature of both being stablecoins. Investors in this pool earn income exclusively through the AMM contract fee - a 0.3% charge applied by the UNISWAP-V2 protocol on every transaction within a liquidity pool, distributed among the liquidity providers.

Similar significance levels were also identified in pairs such as ETH-USDT, ETH-DAI, and ETH-USDC. Additionally, statistical relevance was observed in the context of ETH-HEX and ETH-AMPL for the 5% Value-at-Risk measure. However, insights from Table I.4, containing results from the *DeepAR* models, indicate that providing liquidity for most pairs poses a higher risk compared to holding the assets across all risk measures and significance levels—except in the case of the USDC-USDT pair. This anticipated outcome aligns with the stable nature of pairs involving stablecoins, where impermanent loss has minimal impact due to the stablecoin's peg to the US dollar. Consequently, the liquidity token price remains relatively stable, with the protocol fees being the primary influencing factor.

Table I.4: Mean forecasted risks values of the probabilistic DeepAR model which performed the better in VaR and ES considering two significance levels - 1% and 5%. The risk models are assessed by employing the appropriate score function (loss function). Samples range from 2020/11/14 to 2022/02/22.

	Liquidity Pool ($VaR^{0.01}$)	Portfolio ($VaR^{0.01}$)	Liquidity Pool ($VaR^{0.05}$)	Portfolio ($VaR^{0.05}$)	Liquidity Pool($ES^{0.01}$)	Portfolio ($ES^{0.01}$)	Liquidity Pool ($ES^{0.05}$)	Portfolio Pool ($ES^{0.05}$)
ETH-AMP	0.137591	0.133804	0.067497	0.065060	0.195542	0.199094	0.113424	0.112537
ETH-AMPL	0.110978	0.107049	0.056202	0.056039	0.158536	0.150108	0.092208	0.089498
ETH-AUDIO	0.155094	0.144127	0.077023	0.074433	0.220406	0.202866	0.128510	0.120425
ETH-BTC	0.060311	0.060293	0.030392	0.030398	0.082153	0.084264	0.049667	0.050121
ETH-CEL	0.059334	0.061134	0.030675	0.030848	0.086447	0.088707	0.050443	0.051302
ETH-COMP	0.500123	0.502687	0.261711	0.262716	0.774459	0.754614	0.436420	0.435929
ETH-CORE	0.140305	0.133780	0.071922	0.067839	0.212767	0.186867	0.121199	0.111427
ETH-CRV	0.143977	0.140711	0.073736	0.070950	0.208615	0.197839	0.122517	0.117210
ETH-DAI	0.124605	0.118675	0.062982	0.061811	0.181674	0.170781	0.104894	0.100588
ETH-DPI	0.120076	0.116018	0.061621	0.059347	0.167894	0.159149	0.100165	0.095891
ETH-eRSDL	0.138509	0.132517	0.071808	0.070045	0.206226	0.180513	0.118490	0.110656
ETH-HEX	0.129042	0.132491	0.067126	0.066098	0.190817	0.180304	0.110958	0.107932
ETH-LINK	0.140352	0.139708	0.070967	0.070403	0.204287	0.209794	0.117699	0.119028
ETH-MATIC	0.149541	0.143402	0.076754	0.073283	0.207585	0.203213	0.124661	0.119016
ETH-MKR	0.105242	0.111713	0.054782	0.055828	0.149841	0.157859	0.089090	0.092389
ETH-POLS	0.139688	0.138638	0.070780	0.071646	0.202562	0.199762	0.117194	0.116428
ETH-RLY	0.116685	0.113552	0.059679	0.058421	0.165249	0.166483	0.097127	0.096650
ETH-ROOK	0.103389	0.101327	0.051947	0.050065	0.155249	0.145540	0.087917	0.083721
ETH-SAND	0.159325	0.151596	0.079585	0.076299	0.243275	0.221736	0.136644	0.128249
ETH-SNC	0.128272	0.123595	0.065592	0.064465	0.179050	0.174883	0.106456	0.104757
ETH-STAKE	0.122707	0.128761	0.065082	0.065953	0.184150	0.183216	0.107355	0.107752
ETH-STRONG	0.098224	0.094958	0.048956	0.048720	0.143451	0.131304	0.082021	0.078823
ETH-SWAP	0.125330	0.122440	0.064083	0.064674	0.176889	0.168782	0.104898	0.102564
ETH-TEND	0.140271	0.137038	0.071523	0.070414	0.207488	0.194554	0.118735	0.114571
ETH-UNI	0.120504	0.118272	0.062125	0.060923	0.169627	0.165705	0.100969	0.099181
ETH-USDC	0.093732	0.093479	0.047746	0.048321	0.130474	0.129014	0.078170	0.077598
ETH-USDT	0.060211	0.057705	0.030409	0.030647	0.086641	0.081373	0.050761	0.049040
ETH-YFI	0.118328	0.115555	0.060310	0.058940	0.170175	0.166359	0.099514	0.097338
USDC-USDT	**0.001248***	**0.001304****	0.000617	0.000661	0.001884	0.001875	0.001066	0.001093

Notes: * $p < 0.1$, **$p < 0.05$, *** $p < 0.01$. Statistical significance obtained by the Unpaired Wilcoxon signed-rank test.

In the subsequent section of the results, we delve into scrutinizing the most effective distributions for forecasting VaR and ES risks using the GARCH methodology. Tables I.5 and I.6 illustrate a predominant use of the normal distribution across both risk measures for liquidity pools (LP). Similarly, for the pair portfolio, as depicted in Tables I.7 and I.8, the normal distribution is prevalent at both 1% and 5

Consistency in the normal distribution's performance can be ascribed to the observation of lower losses when the distribution of the stochastic error term, z_{t+1}, features lighter tails compared to other distributions in Equations I.6. This points to conditional volatility, rather than z_{t+1}, serving as the primary driver of VaR in cryptocurrency contexts. Further reinforcing this notion is the dependence of unconditional variance on lags and parameters, where higher lags lead to increased unconditional variance, emphasizing the significance of the γ_{t+1} factor in both liquidity pool and portfolio risk. Similar findings were reported by MÜLLER e RIGHI (2022) in their study on predicting RVaR across various cryptocurrencies. Their research highlighted the effective performance of both normal and skewed normal distributions in forecasting RVaR.

Furthermore, the lag structures of the most competitive GARCH models differ from the commonly used GARCH(1,1) model prevalent in the literature. While HANSEN *et al.* (2022) employed GARCH(1,1) to assess ETH periodicity across various cryptocurrency exchanges, including UNISWAP-V2, TROSTER *et al.* (2019) compared AR(1)-GARCH(1,1) models with 5 different distributions against the GAS model for BTC VaR and ES forecasts. Incorporating the Median Shortfall, JIMÉNEZ *et al.* (2020) introduced further variations. Similarly, studies by RIGHI e CERETTA (2015), DIAZ *et al.* (2017), and GUO (2022) utilized the GARCH(1,1) model for Value-at-Risk and Expected Shortfall forecasts.

Particularly noteworthy, MÜLLER *et al.* (2022) expanded the scope by forecasting Range Value-at-Risk, ES, and VaR using AR(1)-GARCH(1,1) with seven different distributions. Their methodology involved leveraging the properties of an appropriate score function to identify the most suitable model. *Our* findings underscore the importance of exploring lag structures beyond GARCH(1,1) for more accurate predictions of cryptocurrency risk, suggesting a potential avenue for future research.

Existing literature strongly supports the efficacy of GARCH models as reliable predictors of both VaR and ES, often demonstrating consistent performance across different significance levels (MENG e TAYLOR, 2020; RIGHI e MÜLLER, 2022). This trend is notably evident across most entries in Tables I.6, I.7, and I.8, particularly evident in all liquidity pool returns at a significance level of $\alpha = 1\%$ (refer to Table I.5). A noteworthy observation is the exceptional performance of the GARCH model for both VaR and ES across various significance levels in portfolio pairs in-

volving ETH paired with stablecoins pegged to the US dollar, such as ETH-USDT, ETH-DAI, and ETH-USDC (essentially representing ETH's approximate value in US dollars). Literature consistently supports GARCH as the most effective model for these pairings, outperforming a majority of other models in terms of VaR and ES at a 5% significance level (TRUCÍOS e TAYLOR, 2022).

Moving to the *DeepAR* probabilistic forecasting model analysis, Tables I.5 and I.6 illustrate that, concerning Liquidity Pool tokens, the *DeepAR* model often outperforms the best GARCH model in the majority of ES risk forecasts, as indicated by the score function proposed in FISSLER *et al.* (2016). In Tables I.7 and I.8, a comparison between GARCH and *DeepAR* methods for the tokens Portfolio is presented, highlighting the best-performing method in bold. While GARCH models generally excel in predicting VaR for both Liquidity Pools and the Portfolio, there are instances where *DeepAR* models deliver superior forecasts for both VaR and ES concurrently. This trend is notably observed in the ETH-ROOK, ETH-CEL, ETH-BTC, ETH-AMPL, ETH-TEND, and ETH-SWAP portfolios. These findings resonate with previous research by SHEN *et al.* (2021) and REBANE *et al.* (2018), emphasizing GARCH's efficacy in ensuring VaR forecast reliability, while *DeepAR* stands out in predicting extreme values beyond the 1% and 5% quantiles. The effectiveness of *DeepAR* in forecasting VaR and ES for these specific Portfolios can be attributed to the unique characteristics inherent in cryptocurrency asset time series.

4 Conclusion

This study delves into risk prediction for investment products in Decentralized Finance (DeFi) by employing VaR and ES. Our analysis involves predicting risks associated with liquidity pools and holding assets, utilizing GARCH models and the *DeepAR* probabilistic forecasting algorithm. To evaluate the accuracy of these risk forecasts, we employ score functions referenced in GNEITING e RAFTERY (2007) and FISSLER *et al.* (2016) for VaR and ES, respectively.

An evident trend in mean forecasted values indicates that investments in liquidity pools, encompassing liquidity provision, are generally less risky than merely holding the assets. Specifically, our analysis using GARCH models strongly suggests that providing liquidity entails lower risk compared to the buy-and-hold strategy for a portfolio comprising two assets. However, according to the *DeepAR* model, this trend is less prevalent across different pairs.

To substantiate our findings, we employed the unpaired Wilcoxon signed-rank test, which supports statistical significance for pairs containing at least one stablecoin pegged to the US dollar. GARCH modeling reveals statistical significance in risk measures and significance levels for pairs involving at least one stablecoin

Table I.5: Selected GARCH and DeepAR models through mean score value criteria for Value-at-Risk and Expected Shortfall at $\alpha = 0.01$ considering Liquidity Pool tokens time series valuation.

	GARCH(p,q)								DeepAR	
	$VaR^{0.01}$				$ES^{0.01}$				$VaR^{0.01}$	$ES^{0.01}$
Coin names	dist	lags (p,q)	best score	GARCH(1,1)	dist	lags (p,q)	best score	GARCH(1,1)		
ETH-AMP	norm	(2,5)	0.110537	0.114278	norm	(2,5)	11.206530	11.559350	0.136869	**10.642572**
ETH-AMPL	norm	(1,3)	0.132906	0.135895	norm	(1,3)	13.161910	13.411050	0.155162	**11.853173**
ETH-AUDIO	norm	(5,5)	0.125389	0.128556	norm	(5,5)	12.523460	12.818210	0.137766	**10.612447**
ETH-BTC	norm	(1,4)	0.086817	0.087618	norm	(1,4)	9.042431	9.117085	0.098572	**8.096807**
ETH-CEL	norm	(1,4)	0.081586	0.084194	norm	(1,4)	8.515402	8.768158	0.093546	**7.803606**
ETH-COMP	norm	(4,4)	0.106495	0.107730	norm	(4,4)	10.842430	10.959960	0.116903	**9.409408**
ETH-CORE	norm	(5,2)	0.111400	0.117814	norm	(5,2)	11.156740	11.860630	0.139260	**10.425817**
ETH-CRV	norm	(1,4)	0.129673	0.129832	norm	(1,4)	12.918340	12.947120	0.144094	**11.156872**
ETH-DAI	norm	(1,5)	0.049450	0.050041	norm	(1,5)	5.368848	5.429327	0.059238	**5.305143**
ETH-DPI	norm	(4,4)	0.104298	0.105059	norm	(4,4)	10.651150	10.732060	0.118290	**9.634707**
ETH-eRSDL	norm	(5,5)	0.126908	0.141434	norm	(5,5)	12.942690	13.241020	0.143528	**10.850488**
ETH-HEX	norm	(5,4)	0.109941	0.112234	norm	(5,4)	11.250530	11.457060	0.128046	**10.138075**
ETH-LINK	norm	(5,1)	0.108203	0.110196	norm	(5,1)	10.991560	11.179260	0.123366	**9.920849**
ETH-MATIC	norm	(2,5)	0.119197	0.128442	norm	(2,5)	12.038710	12.851440	0.141206	**10.981544**
ETH-MKR	norm	(1,5)	0.102762	0.104096	norm	(1,5)	10.528660	10.651820	0.110360	**9.070702**
ETH-POLS	norm	(3,2)	0.117789	0.121636	norm	(3,)	11.860530	12.204230	0.126297	**10.206392**
ETH-RLY	norm	(4,5)	0.101179	0.105610	norm	(4,5)	10.349480	10.771330	0.114005	**9.180456**
ETH-ROOK	norm	(2,5)	0.131014	0.135082	norm	(2,5)	13.000210	13.358290	0.137403	**10.578605**
ETH-SAND	norm	(5,3)	0.141204	0.146510	norm	(5,3)	13.888200	14.361030	0.164820	**12.055655**
ETH-SNC	norm	(2,5)	0.109797	0.113221	norm	(2,5)	11.140790	11.445910	0.125771	**10.104911**
ETH-STAKE	norm	(5,4)	0.114424	0.121097	norm	(5,4)	11.549600	12.156720	0.123707	**9.917462**
ETH-STRONG	norm	(5,5)	0.091743	0.099667	norm	(5,5)	9.550507	10.296130	0.104592	**8.666080**
ETH-SWAP	norm	(1,5)	0.126153	0.127037	norm	(1,5)	12.597910	12.677190	0.139067	**10.785721**
ETH-TEND	norm	(5,3)	0.372560	0.376868	norm	(5,3)	26.179870	26.807430	0.492812	**17.530884**
ETH-UNI	norm	(5,3)	0.109022	0.112764	norm	(5,3)	11.068180	11.419980	0.123090	**9.923797**
ETH-USDC	norm	(1,5)	0.049371	0.049915	norm	(1,5)	5.361510	5.416968	0.060314	5.443156
ETH-USDT	norm	(1,5)	0.049155	0.049717	norm	(1,5)	5.339179	5.396811	0.060339	5.398263
ETH-YFI	norm	(5,1)	0.105053	0.106315	norm	(5,1)	10.669440	10.816520	0.118437	**9.512318**
USDC-USDT	norm	(2,5)	0.000678	0.000732	norm	(2,5)	0.087096	0.092726	0.001372	0.145823

Note: *DeepAR* that overperfom GARCH are in **bold**, otherwise GARCH perform better.

Table I.6: Selected GARCH and DeepAR models through mean score value criteria for Value-at-Risk and Expected Shortfall at $\alpha = 0.05$ considering Liquidity Pool tokens time series valuation.

	GARCH(p,q)								DeepAR	
	$VaR^{0.05}$				$ES^{0.05}$				$VaR^{0.05}$	$ES^{0.05}$
Coin names	dist	lags (p,q)	best score	GARCH(1,1)	dist	lags (p,q)	best score	GARCH(1,1)		
ETH-AMP	norm	(2,5)	0.077272	0.079895	norm	(2,5)	1.754686	1.811341	0.136730	**1.194265**
ETH-AMPL	sstd	(4,1)	0.090953	0.097585	norm	(1,3)	2.088956	2.126360	0.155011	**1.378297**
ETH-AUDIO	norm	(5,5)	0.088257	0.090110	norm	(5,5)	1.964091	2.006747	0.137624	**1.239211**
ETH-BTC	norm	(2,2)	0.061348	0.061898	norm	(1,4)	1.424740	1.435443	0.098501	**0.939946**
ETH-CEL	norm	(1,4)	0.058033	0.059892	norm	(1,4)	1.350160	1.388652	0.093448	**0.919983**
ETH-COMP	norm	(4,4)	0.075006	0.076127	norm	(4,4)	1.701026	1.719047	0.116510	**1.102668**
ETH-CORE	norm	(5,2)	0.078443	0.082745	norm	(5,2)	1.762701	1.861694	0.138965	**1.259035**
ETH-CRV	norm	(3,2)	0.091636	0.091794	norm	(1,3)	2.041059	2.042482	0.143908	**1.321751**
ETH-DAI	norm	(1,5)	0.034723	0.035115	norm	(1,5)	0.853966	0.863178	0.059171	**0.624399**
ETH-DPI	norm	(3,5)	0.073193	0.073832	norm	(3,5)	1.667771	1.679895	0.118169	**1.118866**
ETH-eRSDL	sstd	(55,)	0.083428	0.089924	sstd	(5,5)	1.931518	2.122399	0.143390	**1.280987**
ETH-HEX	norm	(5,4)	0.075408	0.077007	norm	(5,4)	1.741347	1.774161	0.127891	**1.190156**
ETH-LINK	norm	(4,2)	0.076198	0.077773	norm	(4,2)	1.726452	1.757468	0.123279	**1.149690**
ETH-MATIC	norm	(1,5)	0.083712	0.090106	norm	(1,5)	1.890270	2.017160	0.140925	**1.283172**
ETH-MKR	norm	(1,5)	0.072394	0.073229	norm	(1,5)	1.654147	1.672088	0.110237	**1.051723**
ETH-POLS	norm	(3,2)	0.083222	0.085770	norm	(3,5)	1.869857	1.922296	0.126135	**1.209683**
ETH-RLY	norm	(4,5)	0.071035	0.074048	norm	(4,5)	1.620945	1.682890	0.114227	**1.050466**
ETH-ROOK	norm	(2,5)	0.092241	0.094993	norm	(2,5)	2.046744	2.101794	0.137186	**1.266456**
ETH-SAND	norm	(5,3)	0.099642	0.103503	norm	(5,3)	2.202969	2.279403	0.164725	**1.467087**
ETH-SNC	norm	(2,5)	0.077330	0.079819	norm	(2,5)	1.747462	1.795168	0.125441	**1.156473**
ETH-STAKE	norm	(5,4)	0.081466	0.085984	norm	(5,4)	1.831322	1.922889	0.123426	**1.204123**
ETH-STRONG	sstd	(4,5)	0.058677	0.066140	sstd	(4,5)	1.474985	1.651552	0.104639	**1.017600**
ETH-SWAP	norm	(1,5)	0.088281	0.088940	norm	(1,5)	1.976625	1.989445	0.138879	**1.243612**
ETH-TEND	norm	(5,3)	0.268424	0.270284	norm	(5,3)	4.494257	4.583930	0.491966	**2.671407**
ETH-UNI	norm	(4,3)	0.076672	0.079130	norm	(4,3)	1.735136	1.787555	0.122950	**1.145125**
ETH-USDC	norm	(1,5)	0.034635	0.035024	norm	(1,5)	0.852467	0.860939	0.060223	**0.621842**
ETH-USDT	norm	(1,5)	0.034527	0.034902	norm	(1,5)	0.849329	0.858107	0.060325	**0.620118**
ETH-YFI	norm	(3,4)	0.074708	0.075357	norm	(3,4)	1.692886	1.707029	0.118563	**1.120290**
USDC-USDT	norm	(2,5)	0.000486	0.000531	norm	(2,5)	0.062957	0.063930	0.001367	0.065771

Note: *DeepAR* that overperfom GARCH are in **bold**, otherwise GARCH perform better.

Table I.7: Selected GARCH and DeepAR models through mean score value criteria for Value-at-Risk and Expected Shortfall at $\alpha = 0.01$ considering the pair Portfolio time series valuation.

	GARCH(p,q)								DeepAR	
	$VaR^{0.01}$				$ES^{0.01}$					
Coin names	dist	lags (p,q)	best score	GARCH(1,1)	dist	lags (p,q)	best score	GARCH(1,1)	$VaR^{0.01}$	$ES^{0.01}$
ETH-AMP	norm	(5,5)	0.110547	0.114377	norm	(5,5)	11.197760	11.556490	0.132428	**10.176505**
ETH-AMPL	norm	(1,4)	0.132319	0.135034	norm	(1,4)	13.130930	13.362140	**0.106813**	**8.889347**
ETH-AUDIO	norm	(5,5)	0.126570	0.128637	norm	(5,5)	12.602570	12.816310	0.145406	**11.207232**
ETH-BTC	norm	(2,2)	0.086911	0.087743	norm	(2,2)	9.048198	9.127403	**0.059734**	**5.377882**
ETH-CEL	norm	(1,5)	0.081751	0.084795	norm	(1,5)	8.527430	8.817545	**0.060732**	**5.393880**
ETH-COMP	norm	(5,4)	0.106415	0.107900	norm	(5,4)	10.825720	10.970070	0.507971	18.104094
ETH-CORE	norm	(5,2)	0.111263	0.117931	norm	(5,2)	11.145170	11.871800	0.132955	**10.158141**
ETH-CRV	norm	(3,2)	0.129180	0.130142	norm	(3,2)	12.883940	12.950870	0.139921	**10.919891**
ETH-DAI	norm	(1,5)	0.050056	0.050547	norm	(1,5)	5.427474	5.476727	0.117668	9.486044
ETH-DPI	norm	(4,4)	0.104372	0.105114	norm	(4,4)	10.655440	10.734860	0.114297	**9.332866**
ETH-eRSDL	sstd	(5,5)	0.128133	0.141891	norm	(5,5)	12.954620	13.245790	0.131557	**10.462088**
ETH-HEX	norm	(5,4)	0.110272	0.112503	norm	(5,4)	11.250820	11.451610	0.129616	**10.337795**
ETH-LINK	norm	(4,2)	0.108364	0.110392	norm	(5,1)	11.003770	11.193310	0.139902	**10.894965**
ETH-MATIC	norm	(1,5)	0.119131	0.128305	norm	(2,5)	12.018800	12.825310	0.137530	**10.560426**
ETH-MKR	norm	(1,5)	0.102764	0.104131	norm	(1,5)	10.526430	10.652720	0.109914	**8.974013**
ETH-POLS	norm	(2,2)	0.117705	0.121575	norm	(2,2)	11.848580	12.194570	0.137179	**10.755402**
ETH-RLY	norm	(4,5)	0.101164	0.105574	norm	(4,5)	10.346310	10.766430	0.110648	**8.933284**
ETH-ROOK	norm	(3,5)	0.130922	0.134945	norm	(3,5)	12.985780	13.339490	**0.098988**	**8.136261**
ETH-SAND	norm	(5,4)	0.140224	0.145747	norm	(5,4)	13.816200	14.292900	0.155981	**11.820627**
ETH-SNC	norm	(2,4)	0.109858	0.113271	norm	(2,4)	11.138660	11.444320	0.120490	**9.733591**
ETH-STAKE	norm	(5,4)	0.114691	0.120838	norm	(5,4)	11.567430	12.126020	0.129150	**10.286160**
ETH-STRONG	norm	(5,5)	0.091038	0.099237	norm	(5,5)	9.464559	10.239380	0.094797	**8.002285**
ETH-SWAP	norm	(1,5)	0.126091	0.126995	norm	(1,5)	12.585850	12.666760	**0.119599**	**9.719383**
ETH-TEND	norm	(5,3)	0.370137	0.375209	norm	(5,3)	26.176700	26.976020	**0.133977**	**10.418136**
ETH-UNI	norm	(4,3)	0.109757	0.112787	norm	(5,3)	11.070960	11.419500	0.114631	**9.250653**
ETH-USDC	norm	(1,5)	0.049974	0.050454	norm	(1,5)	5.417637	5.466093	0.092870	7.762717
ETH-USDT	norm	(1,5)	0.049766	0.050245	norm	(1,5)	5.395777	5.444305	0.057375	**5.153269**
ETH-YFI	norm	(2,4)	0.104980	0.106253	norm	(5,1)	10.666160	10.808610	0.116301	**9.365135**
USDC-USDT	norm	(4,5)	0.000728	0.000754	norm	(4,5)	0.092240	0.095211	0.001308	0.139327

Note: *DeepAR* that overperfom GARCH are in **bold**, otherwise GARCH perform better.

Table I.8: Selected GARCH and DeepAR models through mean score value criteria for Value-at-Risk and Expected Shortfall at $\alpha = 0.05$ considering the pair Portfolio time series valuation.

	GARCH(p,q)								DeepAR	
	$VaR^{0.05}$				$ES^{0.05}$					
Coin names	dist	lags (p,q)	best score	GARCH(1,1)	dist	lags (p,q)	best score	GARCH(1,1)	$VaR^{0.05}$	$ES^{0.05}$
ETH-AMP	norm	(5,5)	0.077539	0.080123	norm	(5,5)	1.755745	1.812320	0.132464	**1.143914**
ETH-AMPL	norm	(1,4)	0.094449	0.096039	norm	(1,4)	2.082562	2.116159	0.106713	**1.049893**
ETH-AUDIO	norm	(5,5)	0.089205	0.090266	norm	(5,5)	1.978063	2.007305	0.145346	**1.371571**
ETH-BTC	norm	(2,2)	0.061348	0.062005	norm	(2,2)	1.424167	1.437188	**0.059631**	**0.614887**
ETH-CEL	norm	(1,5)	0.058217	0.060378	norm	(1,5)	1.351619	1.396331	0.060659	**0.623518**
ETH-COMP	norm	(5,4)	0.075041	0.076288	norm	(5,4)	1.699577	1.720762	0.506464	2.806211
ETH-CORE	norm	(5,2)	0.078337	0.082823	norm	(5,2)	1.760470	1.863206	0.132697	**1.201590**
ETH-CRV	norm	(3,2)	0.091084	0.092154	norm	(3,2)	2.027524	2.044916	0.139759	**1.283176**
ETH-DAI	norm	(1,5)	0.035155	0.035524	norm	(1,5)	0.862327	0.870012	0.117650	1.141510
ETH-DPI	norm	(3,5)	0.073255	0.073891	norm	(3,5)	1.667620	1.680215	0.114104	**1.084935**
ETH-eRSDL	sstd	(5,5)	0.084576	0.090731	sstd	(5,5)	1.949702	2.128478	0.131282	**1.265228**
ETH-HEX	norm	(5,4)	0.075870	0.077410	norm	(5,4)	1.742142	1.773666	0.129371	**1.157031**
ETH-LINK	norm	(4,3)	0.076285	0.077920	norm	(4,2)	1.726948	1.759497	0.139531	**1.278608**
ETH-MATIC	norm	(1,5)	0.083823	0.090184	norm	(1,5)	1.887834	2.015276	0.137376	**1.241573**
ETH-MKR	norm	(1,5)	0.072417	0.073265	norm	(1,5)	1.653749	1.672261	0.109694	**1.009871**
ETH-POLS	norm	(2,2)	0.083202	0.085767	norm	(2,2)	1.868452	1.920937	0.136953	**1.254584**
ETH-RLY	norm	(4,5)	0.071047	0.074052	norm	(4,5)	1.620583	1.682297	0.110910	**1.037966**
ETH-ROOK	norm	(3,5)	0.092230	0.094954	norm	(3,5)	2.044641	2.098956	0.098632	**0.910844**
ETH-SAND	norm	(5,4)	0.099074	0.102936	norm	(5,4)	2.190947	2.266993	0.155824	**1.419038**
ETH-SNC	norm	(1,4)	0.077447	0.079907	norm	(2,4)	1.747415	1.795169	0.120163	**1.139026**
ETH-STAKE	norm	(5,4)	0.081719	0.085864	norm	(5,4)	1.835702	1.919788	0.128814	**1.206233**
ETH-STRONG	sstd	(5,5)	0.058675	0.065804	sstd	(5,5)	1.469863	1.639668	0.094716	**0.945801**
ETH-SWAP	norm	(1,5)	0.088296	0.088973	norm	(1,5)	1.974655	1.987751	0.119387	**1.160948**
ETH-TEND	norm	(5,3)	0.266078	0.268341	norm	(5,3)	4.505484	4.620253	**0.133779**	**1.233053**
ETH-UNI	norm	(4,3)	0.077089	0.079164	norm	(5,3)	1.742396	1.787470	0.114209	**1.096037**
ETH-USDC	norm	(1,5)	0.035122	0.035471	norm	(1,5)	0.861190	0.868655	0.093053	0.918352
ETH-USDT	norm	(1,5)	0.034996	0.035344	norm	(1,5)	0.858108	0.865579	0.057307	**0.619695**
ETH-YFI	norm	(2,4)	0.074647	0.075337	norm	(2,4)	1.690194	1.705368	0.116505	**1.099954**
USDC-USDT	norm	(4,5)	0.000530	0.000546	norm	(4,5)	0.063721	0.064110	0.001304	0.064241

Note: *DeepAR* that overperfom GARCH are in **bold**, otherwise GARCH perform better.

pegged to the US dollar. However, the Wilcoxon test results indicate that only the USDC-USDT pair within the liquidity pool presents lower risk than simply holding the assets, confirmed by both GARCH and *DeepAR* forecasts. This underscores that liquidity pools, due to the absence of impermanent loss, offer higher returns owing to the UNISWAP-V2 protocol's 0.3% fee.

Score functions highlight that, contrary to typical GARCH(1,1) models prevalent in risk forecasting literature, our data suggests different lag values for the most suitable GARCH models for both VaR and ES (HANSEN *et al.*, 2022; MÜLLER *et al.*, 2022; TROSTER *et al.*, 2019). These higher lag values suggest a more complex and persistent volatility pattern in returns from Liquidity Pools and Portfolios. These emerging assets exhibit distinctive characteristics reflected in their properties (LIU *et al.*, 2020), showcasing greater inter-temporal autocorrelation in our data. Moreover, *DeepAR*, a probabilistic forecasting method, outperforms the best GARCH model in forecasting Value-at-Risk and Expected Shortfall for distinct portfolios—ETH-AMPL, ETH-BTC, ETH-ROOK, ETH-SWAP, ETH-STRONG at 1% significance level, and pairs ETH-BTC and ETH-TEND at 5% significance level.

Regarding the limitations of our study, our reliance on data from a specific DEX and particular liquidity pools represents only a fraction of the total within the DEX ecosystem. Variations in user behavior, token offerings, and trading dynamics across different DEX platforms within the Ethereum blockchain make generalization unwise. Similarly, extending our findings to other blockchains like Polygon or Binance Smart Chain would be unwarranted. In summary, our research provides valuable insights into specific DEX (UNISWAP-V2) and examined periods. Future research should widen its scope by encompassing a broader array of DEXs, liquidity pools, and models like GAS, extending observations to other relevant periods. This approach will facilitate the understanding of the decentralized exchange landscape and contribute to a more complete understanding of blockchain ecosystems as a whole.

Chapter II

Pricing efficiency in cryptocurrencies: the case of centralized and decentralized markets

1 Abstract

This article presents a comparative analysis of the Ethereum (ETH) weak form of market efficiency priced in Bitcoin (BTC), Dai (DAI), and Tether (USDT). The investigation encompasses data from Uniswap-V2, a decentralized app utilizing a Constant Product Market Maker (CFMM) for cryptocurrency pricing, and Binance, a centralized exchange. The study employs different rolling windows to apply the asymmetric MF-DFA. The efficiency of exchange pairs is ranked using the market deficiency measure (MDM). Besides aligning with the literature, revealing an efficiency increase with larger rolling window sizes across centralized and decentralized exchanges and overall, upward and downward trends, our findings reveal that the CFMM employed by Uniswap-V2 leads to a more efficient market for the ETH-BTC pair compared to Binance, making it among the first studies to compare efficiency across these exchanges types. To delve deeper into this phenomenon and explore the dynamics between distinct pricing mechanisms, the Thermal Optimal Path is employed. The analysis highlights a lead-lag relationship between ETH prices in centralized and decentralized exchanges. The results suggest that market efficiency emerges first in the decentralized exchange, particularly when ETH is priced in BTC. The asymmetric MF-DFA was also employed on the pairs datasets before and after the Ethereum 2.0 hard fork. The findings of this analysis revealed significant results indicating that following the fork, Uniswap-V2 exhibited superior market efficiency compared to Binance for the majority of overall and downward trends, a phenomenon that was not observed prior to the merge. These findings contribute

to the existing literature on cryptocurrency market efficiency by emphasizing the influence of network upgrades in trading platforms. Notably, this research reveals that, for the ETH-BTC pair, decentralized exchanges exhibit superior a level of weak form efficiency.

Keywords: Ether (ETH), market efficiency, centralized and decentralized exchanges, price dynamics.

Notes: This research was presented at the Annual Conference of the Banco Central do Brasil (2024), the Crypto Asset Lab Conference, and the Eurasia Business and Economics Society Conference. It is published in the Journal of Economics and Business, Volume 133, 2025 (2024 JCR Impact Factor: 3.4).

2 Introduction

In recent years, the efficiency of cryptocurrency markets has sparked considerable debate, particularly regarding BTC (NADARAJAH e CHU, 2017; NAN e KAIZOJI, 2019; URQUHART, 2016; VIDAL-TOMÁS e IBAÑEZ, 2018; ZARGAR e KUMAR, 2019) and Ethereum (ETH) (KAKINAKA e UMENO, 2022; NAEEM *et al.*, 2021). The outcomes of these debates hold significant implications for both market participants and governmental decision-makers. This is largely driven by the rise of cryptocurrencies, which are seen as alternatives to conventional government-backed currencies and as innovative digital assets for investment. Bitcoin leads in market capitalization and trading volume, with Ethereum following closely behind. These two cryptocurrencies attract significant interest from both researchers and investors.

Cryptocurrencies, by design, are often based on decentralized principles, aiming to eliminate the need for central intermediaries. Liquidity pools, which is the pricing mechanism employed by Uniswap-V2, rely on algorithms (smart contracts) to price two assets based on the ratio reserves, which can lead to inefficiencies during periods of high volatility or when large trades cause significant price slippage. This system operates with investors providing liquidity in exchange for a return based exclusively on the volume of tokens traded in that specific pool. Order books, which are the pricing mechanism of centralized exchanges, may suffer from liquidity imbalances; if there are not enough buy or sell orders at different price levels, it can lead to large spreads and price volatility.

While data from centralized sources—such as exchanges or price aggregators like CoinMarketCap (AL-YAHYAEE *et al.*, 2020; CHENG *et al.*, 2019) and CryptoDataDownload (NAEEM *et al.*, 2021)—provide valuable insights, it is crucial to also examine decentralized pricing mechanisms. Exploring these differences reveals

how liquidity pools, unlike order books, respond to fluctuations in supply and demand, offering insights into price discovery processes and the associated financial risks (MUSSOI ALMEIDA *et al.*, 2024; PANI, 2021). Relying solely on centralized data may lead to inaccuracies when assessing the impact of Ethereum blockchain modifications, such as forks and updates to smart contracts within DEX.

Furthermore, studying the dynamics of market efficiency in liquidity pools is crucial as it reveals the complex mechanisms that govern decentralized finance (DeFi) ecosystems. Understanding these dynamics helps in assessing risks related to impermanent loss and equips investors with tools for informed decision-making (HEIMBACH *et al.*, 2022b). This understanding also provides essential data for designing resilient DeFi protocols, detecting market manipulation, and promoting regulatory transparency (BELLARE e ROGAWAY, 1993; CHOHAN, 2021).

While the study of liquidity pools provides critical insights into the mechanisms governing decentralized finance, applying methods like MF-DFA allows us to quantitatively assess the weak form of market efficiency within these environments. Although MF-DFA is not directly associated with the Efficient Market Hypothesis (EMH), it can be employed to assess weak form market efficiency by detecting multifractal properties in price series. If a time series shows significant multifractality, it may indicate deviations from the weak form of EMH, suggesting that past prices or patterns could be used to predict future prices. However, MF-DFA is less suited for evaluating semi-strong and strong forms of efficiency, which involve the assimilation of public and private information, respectively. These forms of information are not directly analyzed by the scaling and correlation structures that MF-DFA assesses. Therefore, the findings of MF-DFA primarily pertain to the efficiency of price adjustments over time, rather than the market's reaction to new information. In this analysis, we employed the asymmetric version of MF-DFA, known as asymmetric MF-DFA (CAO *et al.*, 2013; NAEEM *et al.*, 2021; SHAHZAD *et al.*, 2020), which incorporates asymmetry into the multifractal analysis. This approach captures differences in scaling behavior between upward and downward movements, offering a deeper understanding of market dynamics and potential inefficiencies.

This research builds upon previous studies, such as AL-YAHYAEE *et al.* (2018) and ŞAHIN TELLI e CHEN (2020), which investigated the multifractality of both bitcoin and gold, noting that investors in these assets exhibit distinct investments and behavioral approaches (WEN *et al.*, 2022). Additionally, our research aligns with CORBET *et al.* (2020), NAEEM *et al.* (2021) and KAKINAKA e UMENO (2022), which examine the Covid-19 period providing analyses of data reflecting macroeconomic impacts and structural breaks. However, our dataset spans a much longer period following COVID-19 than the timeframe used in these studies, offering a broader perspective. By using daily data as in CHENG *et al.* (2019) and AL-

YAHYAEE *et al.* (2020), in contrast to the high-frequency, one-hour data used in MENSI *et al.* (2019) and NAEEM *et al.* (2021), we examine the weak form of market efficiency across our entire timeframe to capture long-term trends and minimize short-term noise. We also analyze market efficiency before and after the Ethereum 2.0 hard fork, extending the approach taken by AHN *et al.* (2024). Our research diverges in both data and theoretical frameworks from the aforementioned literature's.

In this research, we specifically examine how the pricing mechanisms of order books (Binance) and liquidity pools (Uniswap-V2 in the Ethereum blockchain) impact the levels of the weak form of market efficiency across three distinct cryptocurrency pairs: ETH-BTC, Ethereum-DAI (ETH-DAI) and ETH-USDT. Since ETH is the native currency of the Ethereum blockchain, BTC is a trusted asset. DAI and USDT are common stablecoins - with distinctive properties each - our research hypothesis posits that ETH on a decentralized exchange would demonstrate higher efficiency in the weak form of the efficient market hypothesis (EMH) during the same period when compared to a centralized exchange. Given the inherent complexity of cryptocurrency markets, which is reflected by previous evidence of non-linearity and asymmetric multifractality, the application of Multifractal Detrended Fluctuation Analysis (MF-DFA) is deemed an appropriate method for studying market efficiency in this context.

A hard fork in Ethereum is a significant update to the blockchain protocol, which can be used to implement new features, fix security vulnerabilities[1], or change the rules of the network[2]; thus, they are inherently relevant to the study of the weak form of market efficiency through the application of the asymmetric MF-DFA. Ethereum's blockchain was engineered to transition from a Proof of Work (PoW) (DWORK e NAOR, 1993; VUJIČIĆ *et al.*, 2018) to a Proof of Stake (PoS) (KING e NADAL, 2012) consensus mechanism to enhance sustainability. Under PoS, network participants, known as validators, validate transactions and create new blocks according to the amount of cryptocurrency they hold and are willing to "stake" as collateral. By staking a specific amount of coins, validators earn the right to authenticate transactions and secure the network, receiving rewards in the form of cryptocurrency.

In economics and finance, time series data often exhibits instability. Factors such as regime shifts and evolving expectations can alter lagged correlations and causality between series. The TOP (SORNETTE e ZHOU, 2005; ZHOU e SORNETTE, 2006) is a method used to analyze causal relationships and lagged dependencies between two time series. It seeks to identify the optimal path or direction of causality

[1]The Byzantium hard fork (2017) - improved smart contract security

[2]In some cases, a hard fork can lead to to the creation of a new, separate blockchain if there is a disagreement within the community about the change - which is the case of The DAO fork (2016) leading the split Ethereum and Ethereum Classic.

between the series by considering their dynamic interactions over time. Building on the findings from the MF-DFA analysis, we extended our contribution to market efficiency research by integrating TOP (SORNETTE e ZHOU, 2005), which helps establish the lead-lag relationship between Binance and Uniswap-V2 for each ETH pricing scenario. This approach allows us to determine whether market efficiency for ETH priced in BTC tends to manifest first, on average, in Binance or Uniswap-V2.

This research is organized into four distinct sections. The introduction, Section 2, sets the stage by outlining the significance of evaluating market efficiency in the context of ETH pricing across both centralized (Binance) and decentralized (Uniswap-V2) platforms. Section 3 delves into the data collection process, detailing the sources and types of data utilized for analysis and elucidates the implementation of the MF-DFA, asymmetric MF-DFA, and TOP technique, elaborating on its applications to assess market efficiency and compare the pricing mechanisms of order books and liquidity pools. Section 4, presents the findings derived from the analysis, shedding light on the weak form of EMH disparities between the two platforms and the performance of the distinct pricing mechanisms. Finally, Section 5, concludes the research by synthesizing the key findings, discussing their implications, offering insights into the broader implications for decentralized financial ecosystems and market efficiency enhancements, and discussing potential avenues for future research in the field.

3 Data and Methodology

In this section, the dataset from The Graph decentralized protocol and Binance are introduced, accompanied by the essential procedures for computing both MF-DFA and the TOP.

3.1 Data

Data was collected from The Graph (`https://thegraph.com/`) and Binance for ETH prices against BTC, DAI, and USDT. The data, extracted in May 2023, was obtained using specific queries for each currency pair address. Uniswap has three versions: the first launched on November 2, 2018, the second in May 2020, and the third on May 31, 2021. SushiSwap was launched on August 28, 2020, and Curve Finance was launched in January 2020, initially only exchanging stablecoins. Thus, the data was restricted to the launch date of Uniswap-V2, with additional considerations for delays in adoption, pool creation and Total Value Locked (TVL). Matching data from different DEXs would result in a smaller dataset timeframe. The

Uniswap-V2 [3] subgraph is accessible for queries at `https://api.thegraph.com/subgraphs/name/uniswap/uniswap-v2`. Accurate data extraction from Uniswap-V2 can be problematic due to several factors. The decentralized exchanges' reliance on smart contracts means data accuracy depends on the integrity of these contracts, which can sometimes be compromised by coding errors and vulnerabilities. Additionally, changes in the structure of the exchange can lead to discrepancies and gaps in historical data - we can cite the introduction of Uniswap-V3 on May 31, 2021.

Regarding both Binance and Uniswap-V2, the dataset encompasses 1014 daily observations spanning from August 11, 2020, to May 23, 2023. All the time series within our dataset exhibit stationarity according to ADF (DICKEY e FULLER, 1979b) and KPSS (KWIATKOWSKI *et al.*, 1992) tests. The analyzed time frame encompasses a challenging period marked by significant events, including peaks in Covid-19 pandemic infections, a United States presidential inauguration, disruptions in the global supply chain, BTC reaching an all-time high price, the crash and contagion of Terra-Luna, FTX's bankruptcy, and the Ethereum merge. This period offers a valuable context for assessing decentralized finance market efficiency, given its inclusion of major milestones. It allows for an examination of market responses to significant external shocks and systemic changes.

Analyzing the price efficiency of ETH across BTC, DAI, and USDT trading pairs is a robust parameter for gaining comprehensive insights into the broader cryptocurrency market dynamics. Each of these currency pairs represents distinct aspects of the cryptocurrency landscape: BTC signifies the relationship between two major cryptocurrencies, DAI[4] is a stablecoin from a decentralized autonomous organization, and USDT is a widely used stablecoin with ties to centralized finance - both tethered to the US dollar.

3.2 Methodology

We conduct a rolling window analysis to observe the local market efficiency trend. We propose an approach where the MF-DFA, see Section 3.3, window size varies among three different numbers of observations: 256, which is the explicit minimum requirement set by the Basel Committee on Banking Supervision (BASEL COMMITTEE ON BANKING SUPERVISION, 2013), we also consider 512 following the approach of ALOUI *et al.* (2018) and SHRESTHA (2021), while 384 denotes the

[3] Uniswap-V2's launch date is in May 2020, with transactions for some pools commencing in August 2020.

[4] DAI is a stablecoin that functions on the Ethereum blockchain and is governed by MakerDAO, a decentralized autonomous organization. Its primary objective is to maintain a stable value in relation to the US dollar, achieved through a system of collateralized debt positions (CDPs) and smart contracts. DAI's decentralized nature and reliance on blockchain technology set it apart from Tether, which has stronger ties to centralized, traditional finance.

average between the other two values. This permits us to compare and rank market efficiency between the Constant Function Market Maker (Uniswap-V2)[5] and order book (Binance) pricing mechanisms.

CFMM are fundamental in DeFi ecosystems. They are smart contract-based algorithms designed to provide liquidity to decentralized exchanges and trading platforms (HANSON, 2003; KRISHNAMACHARI *et al.*, 2021; SZABO, 1996). Unlike traditional market makers who adjust their prices based on external factors like supply and demand, CFMM operate with a fixed pricing function (ANGERIS e CHITRA, 2020). This function typically involves a linear relationship between the quantities of two assets in a trading pair. As users deposit assets into the LP, they receive LP tokens in return (ADAMS *et al.*, 2020), representing their share of the pool. These LP tokens can later be used to withdraw their portion of the liquidity and any accumulated trading fees. This innovative mechanism enables users to contribute to liquidity in a decentralized manner, facilitating smoother trading and minimizing slippage on decentralized exchanges. It is important to note that while CFMM offer liquidity, they also come with risks such as impermanent loss, where the value of deposited assets can change relative to holding them outside the pool due to price fluctuations (AIGNER e DHALIWAL, 2021; LOESCH *et al.*, 2021).

By WANG *et al.* (2017),ALOUI *et al.* (2018) and AL-YAHYAEE *et al.* (2020), we employ a market efficiency measure (D[6][7]), Equation II.1. This measure allows us to systematically assess and rank the inefficiency levels exhibited by the same trading pair on centralized and decentralized exchanges. In contrast to other market efficiency measures that indicate whether a period was efficient or not - such as the variance ratio test LO e MACKINLAY (1988) and the Wild Bootstrap Automatic Variance Ration (WBAVR) test KIM (2009) - the MF-DFA approach furnishes us with more comprehensive insights. This methodology is pivotal to our research, allowing for a comprehensive analysis of market efficiency for ETH against BTC, DAI, and USDT on both Binance and Uniswap-V2.

$$D = \frac{1}{2}(|h(-q) - 0.5| - |h(q) - 0.5|). \tag{II.1}$$

It is important to highlight that efficiency is indicated in a cryptocurrency market when all price dynamics, encompassing both large ($q = 4$) and small ($q = -4$) fluctuations, conform to a random walk behavior. Consequently, if the market is perfectly efficient, the calculated value of the market efficiency measure (Equation II.1) would be zero - where $h(q)$ is the generalized Hurst exponent, and q its order,

[5] Uniswap-V2 uses a constant product market maker structure.

[6] In AL-YAHYAEE *et al.* (2018),AL-YAHYAEE *et al.* (2020) and ALOUI *et al.* (2018) it is called Market Deficiency Measure (MDM), but in MNIF *et al.* (2020) and MNIF e JARBOUI (2021) it is magnitude of long memory (MLM).

[7] We have chosen to adopt the vocabulary presented in the study by WANG *et al.* (2009).

$q > 0$ represents large fluctuations and $q < 0$ small fluctuations. Otherwise, the market might exhibit inefficiency. The efficiency of cryptocurrency pairs in the period is assessed by the mean of Equation II.1 values. Subsequently, the thermal optimal path, see 3.4, is employed on the outcomes of the MF-DFA across the three window sizes in both Binance and Uniswap-V2 datasets. To the best of our knowledge, this is the first time this methodology has been applied in this specific context. However, it has been employed in other areas within the field of economics and finance (CHEN *et al.*, 2023; MENG *et al.*, 2017; YANG e SHAO, 2020).

We further explored the applicability of the asymmetric MF-DFA by dividing our data into two distinct periods: before and after Ethereum 2.0 hard fork (the Merge), which occurred on September 15, 2022. By splitting the data this way, the MDM (Equation II.1) can be employed to examine how the Ethereum update affected the market efficiency of ETH priced in terms of BTC, DAI, and USDT for both centralized and decentralized data. This analysis will also reveal whether, following the Ethereum update, the decentralized ETH price is more efficient than its centralized counterpart.

3.3 Asymmetric Multifractal Detrended Fluctuation Analysis

In this subsection, we present details about the parameter specifications utilized in the procedure. To perform the asymmetric MF-DFA (Multifractal Detrended Fluctuation Analysis), we adhere to the five-step approach introduced by KANTELHARDT *et al.* (2002), which has been widely replicated in the literature (ALOUI *et al.*, 2018; WANG *et al.*, 2009) and, extended in its asymmetric form (NAEEM *et al.*, 2021) . For a more comprehensive understanding of the procedure and its steps, we suggest KANTELHARDT *et al.* (2002).

Following the methodology proposed by PENG *et al.* (1994) and KANTELHARDT *et al.* (2002), let's us assume that $\{x(t),\ t = 1, \cdots, N\}$ is a time series with N observations. In the first step, it is necessary to generate a new series:

$$y(j) = \sum_{t=1}^{j} (x(t) - \overline{x}),\ \ t = 1,\ \cdots,N,$$

where $\overline{x}$ is the average of the entire time series, and the profile $y(j)$ is the cumulative sum of the deviations from the sample mean from period one up to period j - this procedure converts the time series $x(t)$ white noise into the random walk.

Then, in the second step, $y(j)$ is divided into $N_s \equiv int(N/s)$ of non-overlapping segments of equal length s, where the function $int(\cdot)$ denotes the integer part of a length of s. Since N/s may have a decimal part, disregarding them from the N_s

segments could lead to nontrivial sample attrition. Therefore, we divide the time series twice: once from period 1 to N, leaving out the $N - N_s \times s$ observations, and once from period N to 1, leaving out the first $N - N_s \times s$ observations. This procedure provides us with a total of $2N_s$ segments. As a result, the scales for segment length, denoted as s, fall within the range of $30 < s < N_s/5$, following WANG *et al.* (2009).

For the jth segment, let the kth element be $\upsilon_{j,k}$, with $k = 1, ..., N$; accordingly, the jth segment of the original time series $\{x(t)\}$ is denoted as $\Upsilon_j = \{\upsilon_{j,k}, k = 1, ..., s\}$, $j = 1, 2, ..., 2N_s$. Similarly, for the jth segment of length s, let the kth profile be $y_{j,k}$; accordingly, the jth segment of the profile is written as $Y_j = \{y_{j,k}, k = 1, ..., s\}$, $j = 1, 2, ..., 2N_s$. That is,

$$\upsilon_{j,k} = \begin{cases} x((j-1)s + k, \ j = 1, ..., N_s \\ x(N - (j - N_s)s + k), \ j = N_s + 1, ..., 2N_s, \end{cases} \tag{II.2}$$

$$y_{j,k} = \begin{cases} y((j-1)s + k, \ j = 1, ..., N_s \\ y(N - (j - N_s)s + k), \ j = N_s + 1, ..., 2N_s, \end{cases} \tag{II.3}$$

Following the procedure, we need to determine the local trend for each of the $2N_s$ segments, using a least square square approach[8] fit for each jth sub-interval of Υ_j and Y_j, respectively:

$$\widehat{\upsilon}_{j,k} = \alpha_j^{\upsilon} + \beta_j^{\upsilon} k, \tag{II.4a}$$

$$\widehat{y}_{j,k} = \alpha_j^{y} + \beta_j^{y} k, \tag{II.4b}$$

where $\widehat{\upsilon}_{j,k}$ is the fitted value for $\upsilon_{j,k}$, and $\widehat{y}_{j,k}$ is the fitted value for $y_{j,k}$, α_j^{υ} and α_j^{y} are the intercepts, while β_j^{υ} and β_j^{y} are the slopes.

We distinguish between positive and negative values of β_j^{υ} to capture asymmetric multifractality effectively. If $\beta_j^{\upsilon} > 0$, then over segment j, $x(t)$ is predominantly increasing, resulting in an upward trend in the profile. Conversely, if $\beta_j^{\upsilon} < 0$, then over segment j, $x(t)$ is predominantly decreasing, leading to a downward trend in the profile. Thus, the corresponding detrended time series for Υ_j and the corresponding profile Y_j is given by the difference between the actual value and its estimate (tendency). For the jth segment, the variance function is given as follows:

$$F_j(s) = \frac{1}{s} \sum_{k=1}^{s} (y_{j,k} - \widehat{y}_{j,k})^2. \tag{II.5}$$

If $x(t)$ exhibits trends that are either positive over certain segments, it might display the property of asymmetric cross-correlation scaling. The qth order fluctuations

[8]This approach is mandatory by the requirements of the asymmetric MF-DFA method (AL-YAHYAEE *et al.*, 2020; ALOUI *et al.*, 2018).

are obtained by averaging the variance over all sub-intervals,

$$F_q(s) = \begin{cases} \left(\frac{1}{N_s} \sum_{j=1}^{2N_s} \left(F_j(s) \right)^{q/2} \right)^{1/q} & q \neq 0, \\ \exp\left(\frac{1}{N_s} \sum_{j=1}^{2N_s} \ln(F_j(s))^{1/q} \right) & q = 0, \end{cases} \tag{II.6}$$

when $q = 2$, it corresponds to the classic Detrended Fluctuation Analysis (DFA). To assess the degree of asymmetry, we employ two directional variance function (or average fluctuation function)

$$F_+^q = \left(\frac{1}{M^+} \sum_{j=1}^{2N_s} \frac{\text{sign}(\beta_j^v) + 1}{2} (F_j(s))^{q/2} \right)^{1/q}, \tag{II.7a}$$

$$F_-^q = \left(\frac{1}{M^-} \sum_{j=1}^{2N_s} \frac{-\text{sign}(\beta_j^v) + 1}{2} (F_j(s))^{q/2} \right)^{1/q}, \tag{II.7b}$$

we opted to omit the case when $q = 0$. M^+ and M^- are the number of segments with positive or negative trends:

$$M^+ = \sum_{j=1}^{2N_s} \frac{\text{sign}(\beta_j^v) + 1}{2}, \tag{II.8a}$$

$$M^- = \sum_{j=1}^{2N_s} \frac{-\text{sign}(\beta_j^v) + 1}{2}. \tag{II.8b}$$

Thus, the scaling behavior of the two-directional fluctuation functions, Equations II.7a and II.7b is determined by analyzing their log-log plots against s for each value of q. If the series exhibits long-range power-law correlation, $F_q(s)$ increases as a power-law for large values of s,

$$F_q(s) \approx s^{h(q)}. \tag{II.9}$$

The asymmetric MF-DFA technique provides a spectrum of generalized Hurst exponents, which play a crucial role in determining the nature of the time series being analyzed, whether it exhibits random walk behavior or stationarity. In the literature, various suggested ranges for the order of fluctuation (q) are suggested. For instance, WANG *et al.* (2009) and LAIB *et al.* (2018) propose an interval of -10 to 10. CAJUEIRO e TABAK (2007) and SHRESTHA (2021) suggest -6 to 6, while KHUNTIA e PATTANAYAK (2020) use a range of -5 to 5. On the other

hand, ALI *et al.* (2018), ALOUI *et al.* (2018) and NAEEM *et al.* (2021) utilize -4 to 4, small and large fluctuations respectively. For our analysis, we will use the interval [-4, 4] as the range for the order of fluctuations. This choice is motivated by the "inverse-cubic" power law, which describes the thickness of the tails of financial fluctuations ALOUI *et al.* (2018); GOPIKRISHNAN *et al.* (1998); KWAPIEŃ e DROŻDŻ (2012).

The exponent $h(q)$, in Equation II.9, represents the generalized Hurst exponent, which may vary with different values of q. For stationary time series, $h(2)$ corresponds to the well-known Hurst exponent H. The family of generalized exponents $h(q)$ can be obtained by observing the slope of the log-log plot of $F_q(s)$ versus s using the least squares method.

In the context of the analysis, if the Hurst exponent $h(s)$ falls within the range $0.5 < H < 1$, it indicates that the series exhibits long-range dependence or the property of long memory. If the Hurst exponent $h(s)$ is not related to the moment of order q, then the process can be characterized as monofractal; otherwise, if related, it is called multifractal. According to the literature present in section 2, the market portrays efficiency if and only if all of its fluctuations follow a random walk behavior. This is equal to saying that all $h(q)$ related to different q should be equal to 0.5.

Additionally, the MF-DFA method facilitates the ranking of markets based on their efficiency levels. By employing the MF-DFA approach, the stationarity or random walk characteristics of financial time series can be determined by examining a spectrum of generalized Hurst exponents. This technique, which explores multifractal properties in non-stationary time series, offers greater to Detrended Fluctuation Analysis (DFA) PENG *et al.* (1994, 1995).

3.4 Thermal Optimal Path

The TOP method takes into account the evolving structure of causality and is particularly responsive to regime shifts and changing agent expectations. It has demonstrated its versatility across a range of applications within the finance literature, encompassing tasks such as testing dependencies between pairs of economic time series ((GUO *et al.*, 2011; JIA *et al.*, 2016), examining lead-lag relationships between stock indices and their futures (GONG *et al.*, 2016), and investigating lead-lag connections between economic variables and stock markets (GUO *et al.*, 2017; TRICHILLI *et al.*, 2020; YAO e LI, 2020). While its application to cryptocurrencies remains relatively limited, a handful of studies have employed this methodology (TRICHILLI e BOUJELBÉNE, 2023; TRICHILLI e BOUJELBÈNE ABBES, 2023). Utilizing the TOP method for analyzing data from both Binance and Uniswap-V2 across diverse ETH price pairs (BTC, DAI, and USDT) assists in establishing the

precedence of market efficiency in centralized versus decentralized finance. This lead-lag validation method contributes to a deeper comprehension of the intrinsic pricing mechanisms unique to these approaches.

Consider two time series denoted as $\{x(t_1),;t_1 = 1,..,N_1\}$ and $\{y(t_2),;t_2 = 1,..,N_2\}$, where N_1 and N_2 represent the number of observations, which may vary between the two series. While the thermal optimal path is not limited to time series with an equal number of observations, in the context of economic and financial data, it is common for N_1 to be equal to N_2. However, it is important to note that the two time series can have distinct characteristics, such as varying scales and meanings. To address this, both time series are normalized by their respective standard deviations. From this point forward, $X(t_1)$ and $Y(t_2)$ will refer to the normalized versions of the original time series.

A distance matrix, denoted as $E_{X,Y}$, is constructed using the normalized series $X(t_1)$ and $Y(t_2)$. The elements of this matrix are defined as follows:

$$\varepsilon(t_1, t_2) = |X(t_1) - Y(t_2)|^q. \tag{II.10}$$

Although the TOP method can be applied with any appropriate distance measure (Equation II.10), it is important to consider the nature of the time series under analysis when selecting the most suitable choice. For instance, using a value of $q > 1$ would place greater emphasis on larger discrepancies in the data. Therefore, the choice of the distance measure can be tailored to the specific characteristics and requirements of the time series being studied. In this research, however, we have specifically set $q = 1$ (SORNETTE e ZHOU, 2005; XU *et al.*, 2017a; YAO e LI, 2020; ZHOU e SORNETTE, 2006).

Moving forward, there are two situations concerning the minimization of the path in the thermal optimal path method. The first situation involves searching for the absolute minimum, aiming to identify the most precise and accurate path between the time series (HALPIN-HEALY e ZHANG, 1995). However, in the second situation, the path is relaxed, taking into consideration that the distance matrix $E_{X,Y}$ may contain noise or irrelevant patterns. In this case, the focus is on finding a path that captures the essential patterns while allowing for some level of tolerance to noise. This path is determined by minimizing the energy or cost function associated with the TOP method across the entire range of starting and ending points.

In the studies conducted by SORNETTE e ZHOU (2005) and ZHOU e SORNETTE (2006), they introduced the concept of "thermal" excitations or fluctuations around the optimal path. This means that path configurations with slightly higher global energies are permitted, but their probabilities decrease as their energy increases. This approach allows for a more flexible exploration of path configurations

and considers the influence of thermal-like fluctuations in the analysis.

The temperature, often referred to as the "thermal" factor, plays a significant role in the TOP method and has been subject to exploration in various research studies. In the literature, the temperature value ranges from T=2 (as found in studies by WANG *et al.* (2017); YAO e LI (2020); YUAN *et al.* (2021)) to T=0.05 (as observed in the study by (YAN e LAI, 2019)). The temperature, represented by T, is an element of the Boltzmann weight factor used to reduce noise in the analysis.

If two time series exhibit a perfect causal relationship, the optimal path in the TOP method would correspond to the diagonal of the distance matrix. This is because the diagonal represents the points where $X(t_1)$ and $Y(t_2)$ are equal, indicating a direct mapping from one time point to the corresponding time point in the other series. If the optimal path deviates from the diagonal, it indicates a lead-lag relationship between the two time series. The extent and direction of the deviation reveal the lead or lag between the two series, providing insights into the temporal relationship and potential causal interactions.

Considering the number of observations in our data, as mentioned in section 3.1, and the computational resources required by the thermal optimal path method, we have decided to use a temperature value of $T = 0.05$. This choice allows us to maintain the full set of observations without compromising the inclusion of relevant periods that could be lost if the number of observations was reduced.

4 Results

This section begins by examining the results of the asymmetric MF-DFA across upward, overall, and downward trends for the three cryptocurrency pairs. The findings are then merged with existing literature trying to provide insights on the understanding of why the ETH-BTC pair exhibits a higher level of weak form efficiency in Uniswap-V2 (DEX) compared to Binance (CEX), with emphasis on transparency and arbitrage opportunities. Following this, the results of the asymmetric MF-DFA for subsets before and after the Ethereum 2.0 hard fork are analyzed. Finally, the outcomes of the TOP method are explored, considering the entire data set.

Table II.1 presents the rankings of ETH values as assigned by three different cryptocurrencies using Equation II.1, considering the upward, downward trends as well as overall. For all three pairs, the efficiency is influenced by the rolling window length - as the rolling window sizes increase, there is a decrease in the mean values obtained by Equation II.1, suggesting an improvement in efficiency. When observing the pair ETH-BTC, it appears that Uniswap-V2 demonstrates enhanced efficiency in its price compared to Binance. However, it is worth noting that there is one exception to this trend, which occurs during the upward trend at $n = 256$.

Among the three pairs, the ETH-BTC pair exhibits the lowest overall efficiency (as determined by MF-DFA with a linear polynomial), while the ETH-USDT pair demonstrates the highest efficiency in both CEX and DEX. At a rolling window size of 256, the ETH-BTC pair displayed the highest efficiency at the upward trend, while the highest inefficiency at the downtrend is observed across all three rolling window sizes.

The findings presented in Table II.1 align with observations in existing literature (KAKINAKA e UMENO, 2022; MNIF *et al.*, 2020; NAEEM *et al.*, 2021), indicating that over the long term, the level of multifractality, as determined by Equation II.1, diminishes. This phenomenon is not limited to centralized exchanges; it is also evident in the daily data of Uniswap-V2 DEX. We delve into two complementary perspectives that are inherent to the structure of decentralized exchanges within public blockchains like Ethereum. The first viewpoint asserts that an increase in market transparency - which is one of the pillars of decentralized finance (QIN *et al.*, 2021) - enhances price efficiency (MADHAVAN, 1996). The second perspective contends that arbitrage opportunities reduce the profitability of market anomalies, thereby improving price efficiency (AKBAS *et al.*, 2016; SHLEIFER e VISHNY, 1997).

An explanatory framework for the ETH priced in BTC being more efficient in Uniswap-V2 may have its foundation placed in the argument that arbitrage drives more informed trading activity in Uniswap-V2 thus, corroborating with the literature finds IBIKUNLE *et al.* (2020). The notion that arbitrage plays a significant role in enhancing market efficiency is heightened by the attributes of the Ethereum blockchain and the pricing mechanisms within decentralized exchanges, particularly Uniswap-V2. Given the multitude of decentralized exchanges on the Ethereum blockchain, price disparities naturally increase as an inherent aspect of the ecosystem. This, in turn, facilitates the establishment of cross-exchange arbitrage within the market (VAKHMYANIN e VOLKOVICH, 2023; WANG *et al.*, 2022c). Overall, DEXs - such as Uniswap-V2 - offer global accessibility, enabling users from anywhere in the world to access and trade digital assets. This unrestricted access may foster a more diverse market, which, in turn, contributes to improved price discovery and market efficiency.

Building on the insights obtained from the application of asymmetric MF-DFA across the entire dataset - August 11, 2023, to May 23, 2023 - we further refine our analysis by applying the same method to data subsets corresponding to periods before and after the Ethereum 2.0 hard fork, allowing for a nuanced comparison of market efficiency across these distinct phases. The results from Table II.2 revealed improved ETH-BTC pair efficiency after the hard fork. For example, this can be seen in the overall trend of rolling window size of 256, where the Uniswap-V2 efficiency

score improved from 0.2868117 before the Merge to 0.2455755 after the Merge. The pair also consistently improved its weak form of market efficiency in both CEX and DEX across all rolling window sizes for overall and downward trends, except the rolling window size 512, where efficiency also improved in the upward trends. Consistent efficiency improvements in DEX after the Merge are also observed in ETH-DAI- and ETH-USDT pairs across all rolling window sizes for the downward trends. The exception occurs in the rolling window size 512, where improvements are also seen in the overall trends.

What is particularly noteworthy in the Table II.2 displayed results is that, when comparing the efficiency between Binance (CEX) and Uniswap-V2 (DEX) in each subsample (before and after the Merge), there is a marked improvement in the efficiency of DEX compared to CEX in the post-Merge period. This enhancement is especially evident in the ETH-DAI and ETH-USDT pairs. Specifically, for rolling window sizes of 256 and 384, there is a noticeable improvement in market efficiency in both overall and downward trends after the hard fork, indicating that DEX became more efficient than CEX. Additionally, at a rolling window of size 512, this improvement is observed exclusively in the downward trends. These findings are consistent with the literature (AHN *et al.*, 2024). However, this study is the first to report a transition in market efficiency from CEX to DEX following a major Ethereum blockchain fork.

The outcomes derived from employing the TOP approach to assess and contrast the lead-lag relationship between market efficiencies in Binance and Uniswap-V2 are presented in Table II.3. When lag values, l, are negative, it indicates that Uniswap-V2 is taking the lead over Binance regarding market efficiency. Among the cryptocurrency pairs, the ETH price in BTC exhibited market efficiency across the majority of all three rolling window sizes while indicating a marginal lead of Uniswap-V2 at the rolling window size 256 - as it is observed in the *Average* lag value II.3. Average observed lags are shorter than a 24-hour period.

Decentralized exchanges, exemplified by Uniswap-V2, may demonstrate early market efficiency through a synergy of influential factors. Users employing algorithmic trading strategies adeptly capitalize on market inefficiencies, responding swiftly to variations in price. These platforms lead the way in figuring out fair prices, attracting traders who skillfully make the most of the differences between decentralized exchanges. Uniswap-V2's decentralized nature, characterized by fewer regulatory hurdles, enables the expeditious implementation of changes and innovations, contributing to a nimble adaptation to evolving market conditions. Within the dynamic decentralized finance (DeFi) ecosystem linked to these exchanges, a culture of financial innovation and rapid adoption of novel concepts further accelerate responses to challenges in market efficiency.

Table II.1: Results of market efficiency analysis using the A-MFDFA method for various cryptocurrency pairs (ETH/BTC, ETH/DAI, ETH/USDT) on decentralized (UNISWAP-V2) and centralized (Binance) exchanges for three distinct rolling window sizes. Daily observations ranges 08-11-2020 to 05-21-2023.

		256		384		512	
Pair	Trend	CEX	DEX	CEX	DEX	CEX	DEX
ETH-BTC	Upward	0.3355879	0.3361385	0.1897869	**0.1882941**	0.1750358	**0.1736835**
	Overall	0.2741586	**0.2736823**	0.1967518	**0.1937898**	0.1906434	**0.1884947**
	Downward	0.4084979	**0.4071882**	0.2773122	**0.2744801**	0.2515778	**0.2502286**
ETH-DAI	Upward	0.3813555	0.3841368	0.2056301	0.2090857	0.1443068	0.1469087
	Overall	0.2597662	0.2624997	0.1906225	0.1927645	0.1609086	0.1631811
	Downward	0.3182727	0.3209481	0.2164476	0.2173746	0.2008711	0.2017603
ETH-USDT	Upward	0.3797283	0.3832554	0.2047452	0.2071532	0.1434919	0.1451900
	Overall	0.2594787	0.2608073	0.1901602	0.1910223	0.1606802	0.1613630
	Upward	0.3182516	0.3198945	0.2169442	**0.2166703**	0.2009969	0.2011437

Notes: Market efficiency is assessed using the asymmetric MFDFA (Multifractal Detrended Fluctuation Analysis) method. Lower values indicate higher market efficiency, while higher values suggest lower efficiency. Bolded values indicates if the pair is more efficient in the decentralized exchange.

Table II.2: Results of market efficiency analysis using the A-MFDFA method for various cryptocurrency pairs (ETH/BTC, ETH/DAI, ETH/USDT) on decentralized (Uniswap-V2) and centralized (Binance) exchanges for three distinct rolling window sizes. Daily observations ranges 08-11-2020 to 09-15-2022 (before the Merge) and 09-16-2022 to 05-21-2023 (after the Merge).

		256				384				512			
		Before the Merge		After the Merge		Before the Merge		After the Merge		Before the Merge		After the Merge	
Pair	Trend	CEX	DEX	CEX	DEX	CEX	DEX	CEX	DEX	CEX	DEX	CEX	DEX
ETH-BTC	Upward	0.2673869	**0.2671899**	0.4758433	0.4780005	0.1519333	**0.1513563**	0.2484992	**0.2456316**	0.1780118	**0.1770681**	0.1722758†	**0.1705065**†
	Overall	0.2867183	0.2868117	0.2471670†	**0.2455755**†	0.1980617	**0.1967305**	0.1945855†	**0.1891159**†	0.2103739	**0.2086666**	0.1704593†	**0.1678585**†
	Downward	0..4444098	**0.4426663**	0.3340384†	**0.3336764**†	0.3079454	0.3082158	0.2294892†	**0.2219131**†	0.3157609	0.3160392	0.1854040†	**0.1823765**†
ETH-DAI	Upward	0.3490265	0.3493023	0.4478602	0.4558697	0.1664528	0.1691117	0.2664489	0.271113	0.1345670	0.1377171	0.1543177	0.1563471
	Overall	0.2289317	0.2317619	0.320800	0.3256248	0.1845311	0.1871954	0.2003757	0.2017031	0.1702656	0.1716994	0.1510242†	0.1528176 †
	Downward	0.3213415	0.3493023	0.3128095†	**0.3089358**†	0.2130336	0.2156767	0.2220877	**0.2203263**†	0.2264871	0.227783	0.1738246†	0.1742973†
ETH-USDT	Upward	0.3462789	0.3485693	0.4485348	0.4546923	0.1645624	0.1662605	0.2671159	0.2706251	0.1334970	0.1352865	0.1537506	0.1553586
	Overall	0.2275495	0.2297373	0.3250553	**0.3246258**	0.1829965	0.1845122	0.2015785	**0.2014293**†	0.1695506	0.1706950	0.1512964†	0.1515043†
	Downward	0.3215003	0.3264051	0.3124260†	**0.3073997**†	0.2136359	0.2154392	0.2224280	**0.2189496**†	0.2263231	0.2272935	0.1742425†	**0.1735518**†

Notes: Market efficiency is assessed using the asymmetric MF-DFA (Multifractal Detrended Fluctuation Analysis) method. Lower values indicate higher market efficiency, while higher values suggest lower efficiency. Bolded values indicate if the pair trend in the decentralized exchange is more efficient in either the subset before or after the Merge. † indicates that the pair trend displayed an improvement in market efficiency after the Merge when compared to the before subset.

Table II.3: This table presents the TOP method results across time lags from -3 to +1 days, highlighting temporal relationships between decentralized and centralized exchange pairs. It includes the percentage of lags under 1 day, indicating instances where decentralized pairs lead, and the average lags/leads per day, offering insights into temporal dynamics and synchronization patterns.

Lag (l)	ETH-DAI			ETH-USDT			ETH-BTC		
	256	384	512	256	384	512	256	384	512
-3< l ≤-2	0.264	0.000	0.199	0.000	0.000	0.000	0.000	0.000	0.000
-2< l ≤-1	1.717	2.384	2.395	1.321	0.317	0.000	1.056	0.000	0.000
-1< l <0	44.385	38.951	48.902	56.671	49.920	45.508	57.727	51.351	51.497
0< l ≤1	51.915	55.166	42.914	41.479	49.602	54.291	41.083	48.648	48.303
1< l ≤2	1.717	3.497	4.591	0.528	.158	0.199	0.132	0.000	0.000
Average	−0.051	0.008	0.018	−0.063	−0.0006	−0.006	−0.008	0.041	0.028

5 Conclusion

This research presents a comprehensive comparative analysis of the weak form of market efficiency, focusing on ETH pricing in BTC, DAI, and USDT. The investigation incorporates data from Uniswap-V2, a decentralized application utilizing liquidity pools for cryptocurrency pricing, and Binance, a centralized exchange. Employing a rolling window procedure with window sizes of 256, 384, and 512 observations, the study applies the asymmetric MF-DFA methodology to rank the efficiency of exchange pairs using the market deficiency measure (MDM) and to analyze changes in market efficiency before and after the Ethereum 2.0 hard fork. Moreover, for a more profound exploration of this phenomenon and to delve into the dynamics inherent to distinct pricing mechanisms, we employed the Thermal Optimal Path method to derive the lead-lag relationship of the investigated ETH prices.

The asymmetric MF-DFA results indicate that with an increase in the number of rolling window observations, there is a consistent increase in the market efficiency of all ETH prices for both CEX (Binance) and DEX (Uniswap-V2). This observed pattern gains additional weight because this is also acknowledged in existing literature. The results also indicate that the pair ETH-BTC exhibits a greater market efficiency in Uniswap-V2 than Binance. When data is divided into periods before and after the Ethereum 2.0 hard fork (The Merge), the ETH-BTC pair shows an improvement in market efficiency across all three rolling window sizes and in both overall and downward trends. For the ETH-DAI and ETH-USDT pairs, the improvement in market efficiency is more pronounced in downward trends and overall in the long-term window sizes. Notably, following The Merge, market efficiency on DEX surpassed that on CEX for ETH-DAI downward trends at rolling window sizes 256 and 384, and for ETH-USDT downward and overall trends. A behavior that is

not observed in the data prior to The Merge.

Concerning the ETH price in BTC, the data highlights a lead favoring Uniswap-V2. This trend is noticeable through the average lag value. Upon analyzing 256 data points, it becomes evident that there is no substantial lead-lag relationship between Binance and Uniswap-V2; observed lags are within a 24-hour timeframe. However, when examining a longer-term investment horizon with 512 data points, it becomes clear that ETH-DAI and ETH-USDT display similar lag durations. Importantly, in both of these cryptocurrencies, Uniswap-V2 consistently maintains a one-day lead over Binance in terms of the ETH price.

The nuanced factors contributing to these dynamics were explored, drawing from market transparency and arbitrage opportunities. Gaining a more in-depth comprehension of digital assets holds the advantage of guiding investors toward making well-founded choices when buying or selling. This enhanced understanding also empowers institutions and developers to devise superior products and solutions contributing to the industry's growth. Opportunities for future research lie in exploring the weak form of market efficiency across different trading pairs, automated market makers, exchanges, and blockchains. This analysis would deepen our understanding of the decentralized financial ecosystem.

Chapter III

Bitcoin's halving events and the fractal nature of mining energy consumption

1 Introduction

Cryptocurrencies are increasingly central to discussions of financial decentralization and energy consumption. Among them, Bitcoin operates as the pioneering decentralized currency using a PoW consensus mechanism that requires substantial computational power to secure its network (KÜFEOĞLU e ÖZKURAN, 2019; LI *et al.*, 2019; O'DWYER e MALONE, 2014; QIN *et al.*, 2023; VRANKEN, 2017). Since its inception, energy consumption has been a topic of intense debate, often criticized for its environmental impact (KABAKLARLI, 2022; VRANKEN, 2017). The periodic halving events of Bitcoin, preprogrammed reductions in block rewards, have long been studied for their impact on price (M'BAKOB, 2024; MEYNKHARD, 2019) and mining behavior (LI *et al.*, 2019, 2023); however, their long-term implications for the network's energy consumption patterns remain insufficiently understood.

Bitcoin and Ethereum dominate the cryptocurrency ecosystem but serve distinct purposes. Bitcoin is a secure, decentralized currency with limited programmability that operates on energy-intensive PoW consensus (GERVAIS *et al.*, 2016b). Ethereum, by contrast, originally operated under PoW but transitioned to PoS in 2022 (KING e NADAL, 2012), a shift that drastically reduced its energy consumption (SALEH, 2021b; ZHANG e CHAN, 2020). Moreover, Ethereum's smart contract capability enables DeFi, liquidity pools, and Decentralized Applications (DApps), making it a programmable financial platform. While Bitcoin is becoming a digital safe heaven (JIN e TIAN, 2024; UMAR *et al.*, 2021) and an inflation hedge (CHOI e SHIN, 2022), Ethereum functions as a global settlement layer for

decentralized finance.

The PoW consensus mechanism remains fundamental to Bitcoin's design, as it provides a distinct decentralization advantage (GENCER *et al.*, 2018). PoW delivers robust security because the computational work required to attack the network makes such attempts prohibitively expensive, thus ensuring economic infeasibility for malicious actors (GERVAIS *et al.*, 2016b; JOHN *et al.*, 2025). Although alternative mechanisms like PoS have been proposed for the Bitcoin blockchain, the community strongly resists such a fundamental change. This commitment to PoW reflects Bitcoin's core philosophy as immutable, a monetary asset with a fixed algorithmically enforced scarcity.

As the literature delves deeper into the operational costs of mining, energy consumption emerges as the most critical and contentious factor. It is the crucial input that keeps the bitcoin blockchain secure and functional. A substantial body of work is dedicated to estimating the scale of this consumption, with methodologies evolving in complexity (CAMBRIDGE CENTRE FOR ALTERNATIVE FINANCE, 2022; DE VRIES, 2018; KÖHLER e PIZZOL, 2019; KRAUSE e TOLAYMAT, 2018; MORA *et al.*, 2018; STOLL *et al.*, 2019; VRANKEN, 2017). Studies like VRANKEN (2017) and KÜFEOĞLU e ÖZKURAN (2019) established foundational models, often based on network hashrate and average hardware efficiency. This was followed by more dynamic approaches, such as those from DE VRIES (2020), who argued that many models underestimate consumption by failing to adequately account for market dynamics, economic incentives, and the rapid turnover of mining hardware.

Beyond the challenge of estimation, research must also address the significant economic implications of such a substantial energy draw. The discourse on Bitcoin's energy consumption remains nascent (RASOOL MALIK *et al.*, 2024), with recent studies highlighting an escalating energy crisis linked to mining operations (CHARI *et al.*, 2019; DAS e DUTTA, 2020; DE VRIES, 2018; HUYNH *et al.*, 2022; KÜFEOĞLU e ÖZKURAN, 2019). This has sparked intense debate regarding its long-term sustainability (DE VRIES e STOLL, 2021). Research indicates that mining expenses are a crucial determinant of profitability (BADEA e MUNGIU-PUPAZAN, 2021; VRANKEN, 2017), with profits inversely related to energy usage (DAS e DUTTA, 2020). Future energy consumption remains difficult to predict due to Bitcoin prices' immediate impact on mining activity (KÜFEOĞLU e ÖZKURAN, 2019). Studies also document relationships between energy consumption and Bitcoin returns, with trading volumes exhibiting a directional impact on consumption (HUYNH *et al.*, 2022).Furthermore, empirical results confirm that the energy consumption required for cryptocurrency mining exerts a direct, sustained, and statistically significant influence on the financial performance of utility and energy sector companies (CORBET *et al.*, 2021). This impact is not uniform but varies consid-

erably based on a company's geographic jurisdiction and the regulatory landscape governing its operations.

Scarcity in Bitcoin is programmatically enforced through halving events, which reduce the block reward by 50% every 210,000 blocks according to a predetermined schedule that ends at 21 million units (TAYEBI e AMINI, 2024). These predictable supply shocks trigger immediate adjustments in computational resource allocation, creating distinct phases in energy consumption and cryptographic security (MEINHOLD *et al.*, 2025; TAYEBI e AMINI, 2024). As block rewards diminish, the relationship between computational effort, electricity inputs, and network security undergoes a fundamental transformation, an equilibrium influenced by hardware efficiency, energy markets, and the global distribution of mining operations (KRISTOUFEK, 2020). Research by SOMPOLINSKY e ZOHAR (2018) and MEYNKHARD (2019) demonstrates that Bitcoin halvings systematically enforce digital scarcity and substantially influence its market valuation. The macroeconomic implications are profound, with M'BAKOB (2024) identifying these events as catalysts for the formation of economic bubbles in Bitcoin and other cryptocurrencies.

Employing data from the Cambridge Centre for Alternative Finance (CAMBRIDGE CENTRE FOR ALTERNATIVE FINANCE, 2022), this research conceptualizes Bitcoin's programmed halving events as structural supply shocks that systematically reconfigure the incentives, infrastructure, and energy intensity of cryptocurrency mining. While previous work has examined market reactions to exogenous crises (KHAN *et al.*, 2022; NAEEM *et al.*, 2023), insufficient attention has been given to the impact of these predetermined halvings on mining energy consumption. To address this gap, we employ asymmetric MF-DFA (CAO *et al.*, 2013; NAEEM *et al.*, 2021; SHAHZAD *et al.*, 2020) to detect hidden persistence and directional biases in consumption trends. This method identifies whether shifts stem from long-term structural changes (AHN *et al.*, 2024; KAKINAKA e UMENO, 2022; MUSSOI ALMEIDA *et al.*, 2024) or short-term adaptations. Our analysis examines multifractal spectrum width to indicate response complexity in Bitcoin's energy consumption (ALMEIDA *et al.*, 2025; CAO *et al.*, 2013), while asymmetry reveals if consumption spikes exhibit different persistence properties than consumption drops. The Chow test (CHOW, 1960) is then employed on these multifractal outputs to statistically verify significant structural breakpoints following each halving and exogenous shocks like China's mining ban (JIANG *et al.*, 2021). This methodology identifies whether complex shifts stem from long-term structural changes (AHN *et al.*, 2024; KAKINAKA e UMENO, 2022; MUSSOI ALMEIDA *et al.*, 2024).

Multifractal analysis decodes the trajectory of Bitcoin mining's energy footprint, fundamentally advancing our comprehension of its consumption patterns. The

findings reveal a remarkable transition from the persistent, heterogeneous patterns characteristic of Bitcoin's early expansion toward increasingly efficient and random consumption behavior following the fourth halving event. This structural break is quantitatively confirmed by Chow tests, which demonstrate that the differences in the upward and downward Hurst exponents are statistically significant for the 90-day periods before and after each halving event. The proposed multiscale approach further uncovers the precise scale dependence of miner responsiveness, showing how different temporal horizons capture unique aspects of energy adaptation dynamics

Building on the evidence of these structural shifts, this study crucially also provides empirical evidence of cross-chain energy contagion. It reveals how Ethereum's transition to PoS consensus materially altered Bitcoin's energy consumption persistence. Together, these insights establish a transformative analytical framework for evaluating cryptocurrency sustainability, providing powerful new methodologies for modeling environmental, social, and governance risks in complex adaptive systems where discontinuous technological innovations and dynamic market forces reshape energy consumption patterns.

This article is systematically organized into four principal sections. It begins with an Introduction that establishes the conceptual and environmental framework for Bitcoin energy consumption indices. The Data and Methodology section subsequently delineates the selected index, the Cambridge Bitcoin Electricity Consumption Index (CBECI), and details the application of the asymmetric MF-DFA. The Results segment then presents the empirical findings, elucidating the presence of on-chain and off-chain shocks and revealing a significant cross-chain influence from Ethereum to Bitcoin mining energy dynamics post-Merge. Finally, the Conclusion synthesizes the core findings, discusses their broader implications, and proposes trajectories for future scholarly inquiry.

2 Data and Methodology

2.1 Data

We analyze daily estimates from the Cambridge Bitcoin Electricity Consumption Index (CBECI) (CAMBRIDGE CENTRE FOR ALTERNATIVE FINANCE, 2022) from August 2010 to December 2024 (5.266 daily observations), Figure III.1. This chosen period provides a comprehensive temporal scope, beginning just 18 months after Bitcoin's launch and first transaction, thereby capturing the network's complete developmental trajectory from its nascent stages to institutional maturity. The timeframe encompasses all major Bitcoin halving events, significant regulatory interventions including China's mining ban, and substantial market cycles, as com-

prehensively documented in Table III.3. By December 2024, the estimated annual consumption reached approximately 183 TWh - comparable to the output of the Zaporizhzhia Nuclear Power Plant (42 TWh)[1] and more than double the annual output of the Itaipu Hydroelectric Power Plant (75 TWh)[2].

Comparing the two series, Table III.1, implies that differencing removes the dominant trend, corroborated by the ADF and KPSS stationarity tests. Also from Table III.1, the extreme kurtosis in the growth rate series points to a potential for fat-tailed distributions, meaning extreme events might occur more frequently than would be expected under a normal distribution.

Figure III.1: Visualization of the Bitcoin network's energy consumption dynamics. Panel A displays the historical annualised electricity consumption in terawatt-hours (TWh), derived from the Cambridge Bitcoin Electricity Consumption Index (CBECI). Panel B presents the transformed series using the first difference of natural logarithms (Δlog).

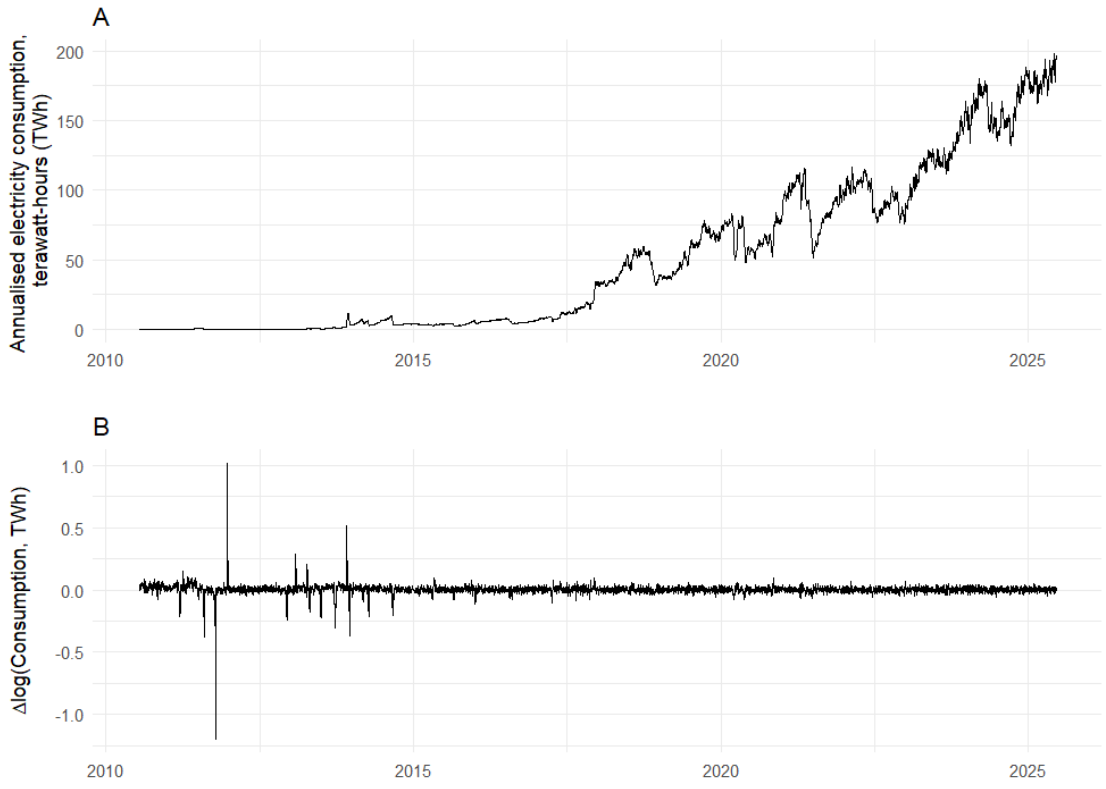

Bitcoin annual energy consumption data is obtained by hybrid top-down approach methodology that combines economic principles with hardware efficiency analysis. The model assumes miners operate as rational economic agents, deploy-

[1] `https://energoatom.com.ua/en/branch/zaporizka-aes` accessed: 13 June 2025

[2] `https://turismoitaipu.com.br/en/the-itaipu-plant/technical-data-of-the-itaipu-hydroelectric-pl` accessed: 13 June 2025

Table III.1: Descriptive statistics for the annualized electricity consumption time series. Statistics are shown for the raw data in levels (Annualised Consumption, TWh) and its first log-difference ($\Delta \log(y_t) = \log(y_t) - \log(y_{t-1})$).

Series	N	Mean	Median	Min	Max	Range	Std	Variance	Skewness	Kurtosis
Consumption, TWh	5447	49.5762	31.6832	0.0002	198.1535	198.1533	55.3350	3061.9653	0.8909	2.6136
$\Delta log(Consumption, TWh)$	5446	0.0025	0.0034	-1.1996	1.0115	2.2111	0.0408	0.0017	-2.3121	232.3252

ing only profitable hardware from a comprehensive basket of over 100 Application-Specific Integrated Circuit (ASIC) miners models, each with distinct energy efficiency ratings (measured in joules per terahash, J/TH). The CBECI evaluates Bitcoin's energy use through three distinct estimates. First, it considers Power Usage Effectiveness (PUE), which measures how efficiently mining facilities use energy accounting for cooling and other overhead. The lower-bound estimate assumes optimal operations with just 1% energy overhead[3] (PUE 1.01). The upper-bound reflects less efficient but still economically viable configurations with 20% overhead (PUE 1.20). The primary estimate weights all active hardware proportionally, assuming 10% overhead (PUE 1.10). This three-tiered approach captures the realistic range of Bitcoin's energy consumption.

The model also incorporates dynamic inputs such as Bitcoin's network hashrate, block rewards, transaction fees, and hardware efficiency trends - defaulting to a global average electricity cost of \$0.05/kWh. To enhance accuracy, a seven-day moving average is used to smooth short-term volatility in mining activity, and a depreciation-based weighting system prioritizes newer hardware over older models within a five-year economic lifespan. The annualized consumption figure is derived by extrapolating the daily power demand at the computed rate over a full year.

2.2 Methodology

Employing an asymmetric MFDFA rolling window method (NAEEM *et al.*, 2021), this analysis examines multifractality in Bitcoin energy consumption from the CBECI dataset. Three window sizes are utilized, including 256 observations per the Basel Committee (BASEL COMMITTEE ON BANKING SUPERVISION, 2013), as well as two sizes from prior research, 512 (ALOUI *et al.*, 2018; SHRESTHA, 2021) and 384 observations (ALMEIDA *et al.*, 2025). The research specifically assesses the influence of Bitcoin halving events on mining energy patterns before and after their occurrence, while controlling for external factors like energy price shifts and regulatory changes.

Although the motivation to capture asymmetric responses to on-chain and off-

[3]Energy overhead refers to additional power consumed by mining infrastructure beyond the actual mining hardware, including cooling, ventilation, and facility operations. PUE quantifies this as the ratio of total facility energy to mining hardware energy.

chain shocks shares a conceptual similarity with Difference-in-Differences (DiD) goal of measuring treatment effects, the DiD framework remains unsuitable. This is because these shocks are system-wide, affecting the entire Bitcoin mining ecosystem simultaneously rather than creating a treated group and a control group. Consequently, without a control group to establish a counterfactual trend, isolating the pure causal effect of a shock from broader market movements is not methodologically viable.

The implementation of asymmetric MF-DFA follows the MF-DFA five-step procedure originally developed by PENG *et al.* (1994) and subsequently implemented in numerous studies (ALOUI *et al.*, 2018; KANTELHARDT *et al.*, 2002; WANG *et al.*, 2009), with asymmetric extensions from NAEEM *et al.* (2021). The framework of PENG *et al.* (1994) and KANTELHARDT *et al.* (2002), considers a time series $\{x(t),\ t = 1, \cdots, N\}$ with N observations. The initial transformation step constructs the profile series:

$$y(j) = \sum_{t=1}^{j} (x(t) - \overline{x}),\quad t = 1,\ \cdots\ , N,$$

where $\overline{x} \equiv \frac{1}{N}\sum_{t=1}^{N} x(t)$ represents the sample mean of the time series, and $y(j)$ denotes the accumulated sum of deviations from this mean up to time j. This integration procedure transforms the original series $x(t)$, which may exhibit white noise characteristics, into a corresponding random walk profile.

In the second step, we partition the profile $y(j)$ into $N_s \equiv \text{int}(N/s)$ disjoint segments of equal length s, where $\text{int}(\cdot)$ denotes the integer part function. To address potential data loss from discarding the residual $N \mod s$ observations, we implement a two-way division: first from $t = 1$ to $t = N$ (discarding the last $N - N_s \times s$ points), then from $t = N$ to $t = 1$ (discarding the first $N - N_s \times s$ points). This bidirectional approach yields $2N_s$ total segments. Following WANG *et al.* (2009), we constrain the segment length s to the range $30 < s < N/5$ to ensure a robust estimation of the scaling behavior.

For the jth segment, we define $\upsilon_{j,k}$ as the kth element $(k = 1, \ldots, s)$ of the original time series $\{x(t)\}$, forming the segment $\Upsilon_j = \{\upsilon_{j,k}\}_{k=1}^{s}$ where $j = 1, \ldots, 2N_s$. Similarly, $y_{j,k}$ represents the kth profile point in segment $Y_j = \{y_{j,k}\}_{k=1}^{s}$. The forward $(j = 1, \ldots, N_s)$ and backward $(j = N_s + 1, \ldots, 2N_s)$ segments are constructed as:

$$\upsilon_{j,k} = \begin{cases} x((j-1)s + k), & j = 1, \ldots, N_s \\ x(N - (j - N_s)s + k), & j = N_s + 1, \ldots, 2N_s, \end{cases} \tag{III.1}$$

$$y_{j,k} = \begin{cases} y((j-1)s + k), & j = 1, \ldots, N_s \\ y(N - (j - N_s)s + k), & j = N_s + 1, \ldots, 2N_s. \end{cases} \tag{III.2}$$

This step is crucial for the asymmetric MF-DFA methodology, as it enables the separate analysis of upward and downward trends. For each of the $2N_s$ segments, we compute the local trend using ordinary least squares (OLS) fits to both Υ_j and Y_j:

$$\widehat{\upsilon}_{j,k} = \alpha_j^{\upsilon} + \beta_j^{\upsilon} k, \tag{III.3a}$$

$$\widehat{y}_{j,k} = \alpha_j^{y} + \beta_j^{y} k, \tag{III.3b}$$

where $\widehat{\upsilon}j, k$ and $\widehat{y}j, k$ are fitted values for $\upsilon_{j,k}$ and $y_{j,k}$; α_j^{υ} and α_j^{y} are intercepts; β_j^{υ} and β_j^{y} are slopes determining trend direction.

At the third stage of the MF-DFA procedure, we implement the key asymmetric component by categorizing segments according to their trend direction. The slope coefficient β_j^{υ} serves as our discriminator: when $\beta_j^{\upsilon} > 0$, the segment Υ_j reflects an upward trend in $x(t)$, while $\beta_j^{\upsilon} < 0$ indicates a downward trend. This directional separation allows us to compute detrended residuals through $y_{j,k} - \widehat{y}j, k$, where the fitted values $\widehat{y}j, k = \alpha_j^{y} + \beta_j^{y} k$ capture local trends. The resulting segment variance:

$$F_j(s) = \frac{1}{s} \sum^{s} k = 1(yj, k - \widehat{y}_{j,k})^2 \tag{III.4}$$

measures fluctuation intensity within each directional group. Progressing to the fourth calculation step, we derive the qth-order fluctuation function by aggregating variances across all $2N_s$ segments:

$$F_q(s) = \begin{cases} \left(\dfrac{1}{N_s} \displaystyle\sum_{j=1}^{2N_s} \left(F_j(s)\right)^{q/2} \right)^{1/q} & q \neq 0, \\ \exp\left(\dfrac{1}{N_s} \displaystyle\sum_{j=1}^{2N_s} \ln(F_j(s))^{1/q} \right) & q = 0, \end{cases} \tag{III.5}$$

the case where $q = 2$ reduces to the standard Detrended Fluctuation Analysis (DFA) method. To quantify directional asymmetry, we calculate separate fluctuation functions for positive and negative trends:

$$F_+^q = \left(\frac{1}{M^+} \sum_{j=1}^{2N_s} \frac{\text{sign}(\beta_j^{\upsilon}) + 1}{2} (F_j(s))^{q/2} \right)^{1/q}, \tag{III.6a}$$

$$F_-^q = \left(\frac{1}{M^-} \sum_{j=1}^{2N_s} \frac{-\text{sign}(\beta_j^{\upsilon}) + 1}{2} (F_j(s))^{q/2} \right)^{1/q}, \tag{III.6b}$$

where we exclude the $q = 0$ case for simplicity. The counts M^+ and M^- represent the number of segments exhibiting positive and negative trends respectively:

$$M^{+} = \sum_{j=1}^{2N_s} \frac{\text{sign}(\beta_j^v) + 1}{2}, \tag{III.7a}$$

$$M^{-} = \sum_{j=1}^{2N_s} \frac{-\text{sign}(\beta_j^v) + 1}{2}. \tag{III.7b}$$

As the concluding phase, fifth, of the MF-DFA framework developed by KANTELHARDT *et al.* (2002), we examine the scaling properties of the directional fluctuation functions (Equations III.6a and III.6b). By analyzing their log-log relationships with segment size s across different q orders, we identify power-law scaling behavior when long-range correlations exist:

$$F_q(s) \approx s^{h(q)} \tag{III.8}$$

The generalized Hurst exponent $h(q)$ emerging from this final step characterizes the scaling dynamics, with potential differences between F_+^q (positive trends) and F_-^q (negative trends) revealing directional asymmetries in the multifractal structure.

Existing research has proposed varying ranges for the fluctuation order q, predominantly in financial and cryptocurrency price analyzes. Studies of traditional markets by WANG *et al.* (2009) and LAIB *et al.* (2018) employ $[-10, 10]$, while cryptocurrency price studies by CAJUEIRO e TABAK (2007) and SHRESTHA (2021) use $[-6, 6]$, and KHUNTIA e PATTANAYAK (2020) adopt $[-5, 5]$. For energy consumption studies, different ranges have been used. Research on household energy consumption by KNOWLES *et al.* (2018) adopts $[-5, 5]$. Similarly, Bitcoin energy studies using Multifractal Detrended Cross Correlation Analysis (MFDCCA) such as (RASOOL MALIK *et al.*, 2024) also use $[-5, 5]$. However, while GHOSH e BOURI (2022) analyzes Bitcoin Energy Consumption Index in the same range $[-5, 5]$, these studies contains no systematic comparison of halving periods and offers limited analytical depth regarding these fundamental events.

For our analysis of Bitcoin mining energy consumption, we select the range [-4, 4] as implemented in prior studies ALI *et al.* (2018); ALOUI *et al.* (2018); NAEEM *et al.* (2021). This range effectively captures the scaling properties of energy time series and aligns with observed power-law behaviors in complex energy systems GOPIKRISHNAN *et al.* (1998); KWAPIEŃ e DROŻDŻ (2012).

The MFDFA (KANTELHARDT *et al.*, 2002) method analyzes the multifractal properties of a time series, revealing complex scaling behaviors and correlations at different time scales. By detecting multifractality, MF-DFA can provide insight into the presence of long-range correlations and varying volatility within a time series.

Our analysis employs the well-established five-step Multifractal Detrended Fluc-

tuation Analysis (MF-DFA) procedure (CAO *et al.*, 2013; NAEEM *et al.*, 2021; SHAHZAD *et al.*, 2020) to systematically investigate the scaling properties of Bitcoin's energy consumption. Following the standard methodology, we first construct the profile series $y(j) = \sum_{k=1}^{j}[E_k - \langle E \rangle]$ for $i = 1, ..., N$, where E_k represents the values of daily energy consumption and $\langle E \rangle$ denotes the mean of the series. We then divide the profile into N_s non-overlapping segments of equal length s and perform local detrending using second-order polynomial fits to eliminate trends while preserving intrinsic fluctuations. The variance $F^2(s)$ within each segment ν is calculated after removing these local trends.

$$F_j(s) = \frac{1}{s}\sum_{k=1}^{s}(y_{j,k} - \widehat{y}_{j,k})^2$$

allowing us to examine scale-dependent behavior through the $q-th$ order fluctuation function:

$$F_q(s) = \left\{ \frac{1}{2N_s} \sum_{\nu=1}^{2N_s} [F^2(s)]^{q/2} \right\}^{1/q}$$

for $q \in [-4, 4]$ (ALOUI *et al.*, 2018; GOPIKRISHNAN *et al.*, 1998; KWAPIEŃ e DROŻDŻ, 2012). The scaling behavior $F_q(s) \sim s^{h(q)}$ reveals the generalized Hurst exponents $h(q)$, where $q > 0$ emphasizes large fluctuations and $q < 0$ accentuates small fluctuations. From these exponents, we derive the multifractal spectrum $f(\alpha)$ via Legendre transformation, where represents the Hölder exponents and $f(\alpha)$ describes their fractal dimensions

3 Results

In this section we begin by analysing Table III.2. The conducted analysis on the logarithmic returns of the energy series, employed multiple rolling window lengths (256, 384, and 512 observations) (MUSSOI ALMEIDA *et al.*, 2024) to ensure robustness across different time scales. The table reports the mean values of key multifractal metrics (OŚWIĘCIMKA *et al.*, 2006) - including the overall (H), upward (H_+), and downward (H_-) Hurst exponents, the multifractal strength (ΔH) (CASTRO *et al.*, 2023), its shuffled-data counterpart (ΔH_{shuff}) (CAO *et al.*, 2013), and the fractal spectrum width ($\Delta\alpha$) - for the periods before the first halving, during the halving events, and after the fourth halving. The temporal evolution of the Hurst exponent is visualized in Figures III.2 to III.4. By focusing on the most prominent data points, Table III.3, across the three rolling windows, these figures complement Table 1 by highlighting specific periods where significant deviations in

miner behavior and energy consumption dynamics occurred.

In multifractal analysis, the Hurst exponent (H) quantifies long-range correlation, with H_+ and H_- specifically capturing the scaling of large upward and downward fluctuations, respectively. The multifractal strength (ΔH and $\Delta\alpha$) measures the overall heterogeneity in these scaling behaviors, while the source of multifractality is discerned by comparing ΔH and ΔH_{shuff}, if $\Delta H_{shuff} < \Delta H$ multifractality predominantly attributed to fat-tailed probability distributions rather than long-range correlations. When examining these dynamics through asymmetric MFDFA, we can observe distinct patterns in upward and downward movements. A downward anti-persistent Hurst exponent ($H_- < 0.5$) negative logarithmic returns in Bitcoin mining energy consumption tend to be followed by opposing movements, creating a choppy, fragmented pattern in the time series. Similarly, an upward persistent exponent ($H_+ > 0.5$) would suggest that increases display some degree of momentum.

Analysis of the pre-halving era data from Table III.2 reveals strong persistent behavior in Bitcoin mining energy consumption, indicating demand followed long-term patterns. The asymmetric MFDFA Hurst exponent results display this persistence while demonstrating multifractality in the time series. Notably, downward trends show the strongest persistence ($H = 0.7291$ at 384 window size) and widest multifractal spectrum ($\Delta\alpha = 2.3835$ - suggesting extreme intermittency during energy consumption declines), while upward trends in smaller windows (256 window size) exhibit near-random behavior ($H = 0.5237$). This multifractal structure aligns with the period's characteristics and the literature (M'BAKOB, 2024; MEYNKHARD, 2019; WILSON, 2022), where miners operated without major energy constraints amid rapid hardware and software advancements (CONG *et al.*, 2021), creating complex but generally persistent demand patterns across different market conditions.

Between Bitcoin's first and second halving, short term energy trends analyzed using 256 day windows showed near random scaling with Hurst exponents around 0.5. Longer term analysis using 384 and 512 day windows showed persistent upward trends with mean Hurst exponents reaching 0.7641, driven by technological advances and competitive pressures (PRAT e WALTER, 2021). These contrasted with anti-persistent downward movements showing Hurst exponents as low as 0.3184, suggesting temporary reductions rather than sustained cuts.

For the period between the second and third halving, a convergence in scaling behavior is observed. The Hurst exponents exhibit reduced asymmetry between upward and downward trends, with values ranging from 0.5073 to 0.54 for upward trends and 0.5459 to 0.5796 for downward trends across all window sizes, contrasting sharply with the previous period. This indicates that miners may have adopted more balanced adjustment mechanisms. The downward movements also show a reduced

$\Delta\alpha$ and ΔH compared to previous periods, reflecting a shift from abrupt crashes to gradual reductions, likely due to improved risk management and an increase in operational maturity (CONG *et al.*, 2021).

Regarding the results in the period between the third and fourth halving our results revealed the network's response to China's June 2021 mining ban effect in which is more visible on Figures III.2 to III.4, is consistent with literature findings (CHEN e LIU, 2022). The anti-persistent upward trends with Hurst exponents ranging from 0.2795 to 0.3186, may be reflecting the logistical challenges of redeploying nearly half of global hashrate[4], as miners faced bottlenecks, resulting in necessary but temporary capacity decreases (CONG *et al.*, 2021; JIANG *et al.*, 2021). Meanwhile, downward trends exhibited persistence, with Hurst exponents between 0.4849 and 0.5697, may demonstrate how physical infrastructure limitations slowed the drawdown of Chinese operations (NIAZ *et al.*, 2022). The observed patterns for the period, III.2 may highlight how Bitcoin mining's industrial scale physical requirements fundamentally constrained its adjustment speeds during this transition (LIU e TSYVINSKI, 2021).

Based on the results in Table III.2, the behavior of ΔH and $\Delta H_{\text{shuffled}}$ is observed. Until the post fourth halving period, the condition $\Delta H_{\text{shuffled}} < \Delta H$ holds, indicating that the multifractality originates from a fat tailed distribution. However, a different pattern, in which $\Delta H_{\text{shuffled}} > \Delta H$, appears in the post fourth halving which is observed exclusively in the upward trend across all window sizes. To the best of our knowledge, this study is the first to document this result, which indicates that the innate potential for volatile large scale expansion is possible being suppressed by the system's internal memory and long range dependencies. The critical role of passive miners[5] stems from their ability to enforce such stability through structured long term planning (HALABURDA e YERMACK, 2023) and power purchase contracts (BASTIAN-PINTO *et al.*, 2021; YAP *et al.*, 2023), which collectively introduce strong autocorrelations that mitigate the energy consumption logarithmic return volatility.

[4] `https://ccaf.io/cbnsi/cbeci/mining_map`

[5] Terminology follow SORIA *et al.* (2023).

Table III.2: Mean values of asymmetric MFDFA metrics for the logarithmic returns of Bitcoin mining energy consumption across different halving eras. Metrics include the upward (H_+), downward (H_-), and overall (H) Hurst exponents, the multifractal strength (ΔH), its shuffled counterpart (ΔH_{shuff}), and the fractal spectrum width ($\Delta\alpha$). Results were calculated using rolling window lengths of 256, 384, and 512 observations. The table also includes the mean (μ) and standard deviation (σ) of the raw energy consumption (TWh) for each period.

		Pre-halving				1st halving				2nd halving				3rd halving				4th halving			
	μ	0.0077				0.0029				0.0017				0.0005				0.0003			
	σ	0.0746				0.0474				0.0215				0.0189				0.0171			
Size		H	ΔH	ΔH_{shuff}	$\Delta\alpha$	H	ΔH	ΔH_{shuff}	$\Delta\alpha$	H	ΔH	ΔH_{shuff}	$\Delta\alpha$	H	ΔH	ΔH_{shuff}	$\Delta\alpha$	H	ΔH	ΔH_{shuff}	$\Delta\alpha$
	Upward	0.5237	0.8744	0.7235†	0.8734	0.4492***	1.0935	0.5480†	0.8212	0.5073	0.4320	0.2934†	0.2980	0.3186***	0.4039	0.2993†	0.3682	0.3995***	0.2466†	0.2592	0.2366
256	Overall	0.6847	0.9949	0.6437†	0.8431	0.6324***	0.8063	0.4538†	0.6149	0.6185***	0.4482	0.2479†	0.1043	0.4550	0.3833	0.2440†	0.3597	0.3975	0.2589	0.2208†	0.3241
	Downward	0.5871	1.3037	0.6657†	1.14356	0.5056***	1.1552	0.4001†	1.2395	0.5459***	0.5808	0.2868†	0.5596	0.5697***	0.6289	0.2760†	0.4372	0.4372	0.3201	0.2572†	0.4006
	Upward	0.6331	0.9748	0.7118†	1.1319	0.6356***	0.9189	0.4109†	1.0285	0.5400***	0.2661	0.1868†	0.1398	0.2942***	0.2621	0.1836†	0.3496	0.28771***	0.1273†	0.1547	0.2121
384	Overall	0.6766	1.3403	0.6261†	1.2178	0.5648	0.8526	0.3413†	0.9108	0.5916	0.2734	0.1537†	0.1450	0.4367***	0.2328	0.1460†	0.2530	0.3145***	0.1830	0.1326†	0.3268
	Downward	0.7291	2.1067	0.6671†	2.3835	0.4005***	1.0297	0.3001†	1.1355	0.5796	0.5453	0.1908†	0.7183	0.4849**	0.5043	0.1790†	0.6957	0.3461***	0.3040	0.1695†	0.5071
	Upward	0.5750	1.3681	0.6777†	1.7650	0.7641***	0.8967	0.4303†	1.0471	0.5324***	0.2700	0.1615†	0.1641	0.2795***	0.2865	0.1554†	0.4331	0.2535***	0.1191†	0.1435	0.2013
512	Overall	0.7138	0.8936	0.5739†	0.8697	0.5580***	0.8071	0.3578†	0.9526	0.5779***	0.1955	0.1295†	0.1350	0.4574***	0.1583	0.1226†	0.1771	0.6920***	0.1669	0.1143†	0.2810
	Downward	0.7139	1.3608	0.6467†	1.5559	0.3184***	0.8609	0.3090†	1.1180	0.5654	0.4393	0.1640†	0.6078	0.5559***	0.3719	0.1516†	0.5203	0.2866***	0.2427	0.1429†	0.3928

Note:

† *indicates the smaller value between* ΔH *and* ΔH_{shuff} *for a given period.*

$***p < 0.01$, $**p < 0.05$, *p-values of the Chow test for a structural break around each halving, estimated using a 90-day window before and after the event.*

Empirical results from the Chow test, Table III.4, indicate that the long-memory properties of Bitcoin's energy consumption, as captured by the Hurst exponent, are considerably disrupted by both on-chain and off-chain shocks. Statistically significant breaks are precipitated not only by endogenous protocol events but also by severe external crises, with the magnitude of disruption varying dramatically across the components of the series. The data, Table III.4, reveals that structural rupture occurred not only courred during a halving, but in the aftermath of a market collapse, as is indicated by literature (MAITI, 2022; SAPRA *et al.*, 2024).

The data reveals a distinct structural shift in the upward trending component of Bitcoin's energy consumption around the conclusion of its first major market cycle in late 2011. This transition period reflects a fundamental transformation in how the network's energy consumption maintained persistent behavior patterns. The observed change coincides with the mining ecosystem's adaptation to substantially reduced profitability conditions, representing a complete recalibration of operational dynamics following the market contraction. Conversely, the most severe break in the Overall, at 384-day sizeobservations, series occurs in March 2020, signaling a comprehensive structural reconstitution following the global market crash. For the Downward component, the most pronounced break is found in mid 2021 during China's mining ban (512-day size), highlighting a fundamental shift in the mean-reverting dynamics of the network. As observed in the data, these extreme shock values are most consistently significant in the 384 and 512-day window sizes due to their capacity to encapsulate the entire duration of a prolonged market transition, thereby filtering out short-term noise and providing a more robust statistical signal of a true structural break in the long-memory properties of the energy series.

The statistical identification of structural breaks requires large observation windows to separate permanent regime changes from temporary volatility. Against this analytical backdrop, Ethereum's Merge on September 15, 2022 stands out as an unequivocal structural shock to Bitcoin's energy consumption patterns. The breakpoint significance is firmly established through results in Table III.4. The simultaneous significance in both Upward (13.0345) and Downward (5.7138) components for the 384-day window indicates a comprehensive transformation of Bitcoin's energy dynamics. The Upward break reveals fundamental disruption in persistent growth patterns, while the Downward break demonstrates altered mean-reversion behavior during corrective phases. This dual transformation indicates The Merge precipitated not merely a temporary disturbance but a permanent recalibration of the statistical processes governing Bitcoin's energy consumption.

Table III.3: Timeline of exogenous shocks and protocol-defined events considered in this study for their potential influence on the multifractal properties of Bitcoin's energy consumption.

Events	**Description**	
19/07/2010	By October 2010, the release of GPU mining software. November 27 launch of Slush Pool, Bitcoin's first mining pool.	(LIU e TSYVINSKI, 2021)
28/06/2011	Bitcoin reached its first major price peak at US33.00 on June 10, 2010.	SAPRA *et al.* (2024)
17/12/2011	Bitcoin's first bubble burst on 18/11/2011, bottoming at US2.00.	(SAPRA *et al.*, 2024; TASKINSOY, 2022)
28/11/2012	First Halving.	(FABUS *et al.*, 2024; KÜFEOĞLU e ÖZKURAN, 2019)
08/10/2013	Silk Road shutting down. Goverment crypto oversight.	
12/12/2013	Bitcoin peaked on 30/11/2013 after an 800% surge since October 2013. The People's Bank of China (PBOC) and four agencies emitted in December the Circular on Bitcoin Risk Prevention, imposing the first major restrictions on cryptocurrency trading.	(KAISER *et al.*, 2018; MACAIRE e NAEF, 2022)
09/07/2016	Second Halving.	(FABUS *et al.*, 2024; KÜFEOĞLU e ÖZKURAN, 2019)
30/01/2020	COVID-19 Outbreak.	(YUAN *et al.*, 2022)
26/03/2020	The COVID-19 market crash; FED quantitative easing.	(YUAN *et al.*, 2022)
11/05/2020	Third Halving.	FABUS *et al.* (2024)
23/07/2021	Final 2021 bull run to $69K.	SAPRA *et al.* (2024)
15/09/2022	Ethereum Merge to PoS	(ALMEIDA *et al.*, 2025)
16/04/2024	ETFs cement Bitcoin's $60K floor.	
24/09/2021	Chinas PBOC Ban[6]	(MACAIRE e NAEF, 2022)
20/04/2024	Fourth Halving.	

Table III.4: F-statistics from Chow tests assessing structural breaks in the Hurst exponent time series computed from Cambridge Bitcoin Electricity Consumption Index (CEBCI) data. Breakpoints represent major on-chain events and off-chain shocks, Table III.3, impacting Bitcoin mining energy patterns. The test employed a 90-day window before and after each shock to detect structural changes.

		Pre-halving				1st halving			2nd halving			3rd halving				4th halving
Size		2010-07-19	2011-06-28	2011-12-17	**2012-11-28**	2013-10-08	2013-12-12	**2016-07-09**	2020-01-30	2020-03-26	**2020-05-11**	2021-07-23	2021-09-24	2022-09-15	2024-04-16	**2024-04-20**
	Upwardv	-	2.5^{*}	3.0423^{*}	77.2236^{***}	0.7785	1.9696	2.0901	34.3227^{***}	1.3984	5.1175^{***}	0.1093	2.1197	1.465	10.9883^{***}	15.8531^{***}
256	Overall	-	11.873^{***}	0.1259	10.2233^{***}	7.8146^{***}	12.3941^{***}	7.6155^{***}	8.5093^{***}	14.6507^{***}	1.1358	4.9892^{***}	7.569^{***}	4.0554^{**}	2.6746^{*}	2.0551
	Downward	-	5.0968^{***}	15.9062^{***}	28.8402^{***}	0.6657	2.3225	14.3791^{***}	10.0323^{***}	0.3277	16.667^{***}	15.4049^{***}	0.8014	1.2805	1.7253	0.9162
	Upward	-	-	292.5477^{***}	17.364^{***}	71.5714^{***}	29.7896^{***}	6.3667^{***}	20.5896^{***}	5.904^{***}	11.5091^{***}	3.2362^{**}	4.655^{**}	13.0345^{***}	17.4541^{***}	7.6934^{***}
384	Overall	-	-	0.7602	0.7474	17.6203^{***}	55.6862^{***}	2.401^{*}	18.4664^{***}	160.7016^{***}	191.6055^{***}	60.9489^{***}	15.5137^{***}	24.514^{***}	18.6421^{***}	19.4633^{***}
	Downward	-	-	39.6303^{***}	119.8959^{***}	39.168^{***}	1.2084	1.0379	42.5591^{***}	4.8799^{***}	3.1469^{**}	1.1049	17.0442^{***}	5.7138^{***}	17.3154^{***}	16.9944^{***}
	Upward	-	-	12.6354^{***}	41.5175^{***}	31.361^{***}	25.8443^{***}	29.5243^{***}	33.4412^{***}	69.7138^{***}	41.1657^{***}	20.5867^{***}	12.6419^{***}	3.4397^{**}	11.2103^{***}	11.7902^{***}
512	Overall	-	-	1.6149	110.4415^{***}	116.0672^{***}	105.3705^{***}	38.9008^{***}	17.5206^{***}	39.642^{***}	71.8719^{***}	9.8683^{***}	19.2437^{***}	29.9828^{***}	68.407^{***}	46.3932^{***}
	Downward	-	-	0.2718	51.8687^{***}	42.2912^{***}	4.4176^{**}	1.6816	6.1075^{***}	48.0144^{***}	30.1236^{***}	58.4364^{***}	26.4628^{***}	14.64^{***}	8.8771^{***}	11.1273^{***}

Notes: Significance levels are indicated as follows: $^{***}p < 0.01$, $^{**}p < 0.05$, $^{*}p < 0.1$. Dates in **bold** indicate Bitcoin halving events.

The results presented in Figures 1, 2, and 3 provide a complementary analysis, demonstrating that varying the rolling window size reveals distinct aspects of mining energy dynamics influenced by both halving events and other significant market events. The 256 day window captures immediate miner responses to market shocks with high sensitivity. The 512 day window identifies long term structural patterns in energy consumption and the intermediate 384 day window balances responsiveness. Together these window sizes provide a multiscale understanding of mining behavior across various time horizons.

In Figure III.2 A, rolling window with 256 observations, shows that Bitcoin's first halving event triggered an considerable antipersistent behavior in mining energy consumption, aligning with the literature in which Halvings triggers descontinuity on miners revenues SEDLMEIR *et al.* (2024); ZHENG *et al.* (2023). This period marked Bitcoin mining's "Cambrian explosion", a fundamental industry shift from CPU to GPU mining that completely transformed the ecosystem, corroborating with the literature by displaying a price-responsive capital allocation of miners to efficient hardware (LIU e TSYVINSKI, 2021; WILSON, 2022). The simultaneous emergence of mining pools and delayed GPU adoption created perfect conditions for network instability, causing inefficient miners to collapse (SEDLMEIR *et al.*, 2024). These energy dynamics demonstrate persistent energy drawdowns and weak recoveries that reflect both forced miner exits and the broader industry's challenging adaptation to new technological requirements. The first halving essentially stress tested the mining infrastructure during this evolutionary stage.

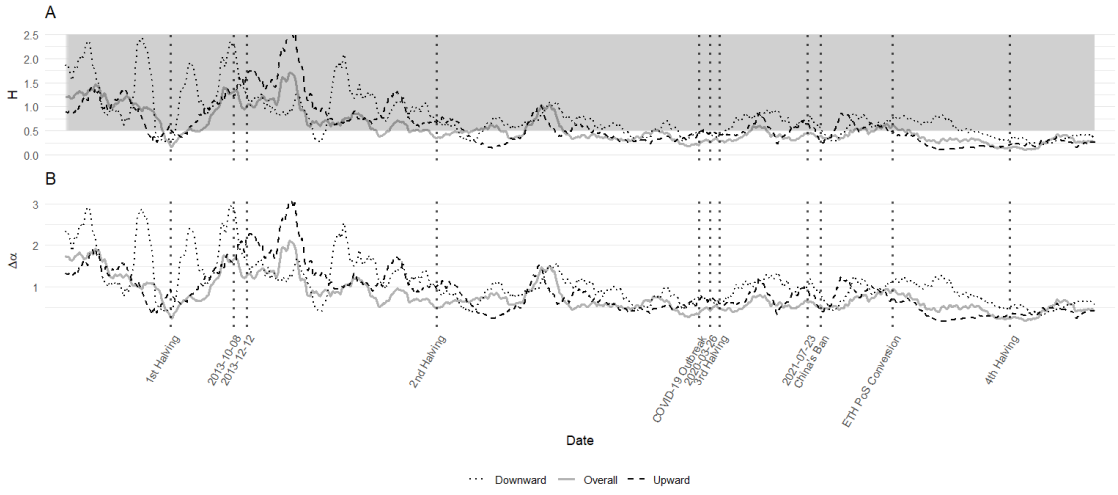

Figure III.2: Time-varying asymmetric multifractality in Bitcoin mining energy consumption. The rolling upward (H_+), downward (H_-), and overall Hurst exponent (H), along with the delta alpha ($\Delta\alpha$) are shown, calculated from the logarithmic returns using asymmetric MFDFA with a window size of 256 observations. To clarify the short-term trend without losing critical information, the results are smoothed using a 90 days moving average. Horizontal shaded band indicates values over 0.5.

Following the first halving,a persistent growth in energy use is observed as miners expanded operations. However, during 2013, downward trends became more persistent than upward, signaling growing operational pressures. The system shifted dramatically after China's 12/12/2013 PBOC intervention, entering a new phase where H_- became anti-persistent while H_+ showed unusual volatility. Thus, demonstrating a possible altering state on energy consumption behavior caused by policy shocks.

Between the second and third halvings period, the immediate responses captured by the 256 size windown demonstrate a profit-driven operation by the miners as Bitcoin approached $USD20.000,00$ due to the behavior in which $H_+ > 0.5 > H_-$. This finding supports KRISTOUFEK (2020), HUYNH *et al.* (2022) and LIU e TSYVINSKI (2021), which posits that Bitcoin's price is a considerable driver of mining costs. When the value of Bitcoin increases, the revenue from mining increases, which discourages miners from shutting off their equipment (BRUNO *et al.*, 2023). Between the third and fourth halving a inversion in the dynamics of upward and downward Hurst exponent, in which $H_- > 0.5 > H_+$, is more prominently this happens simultaneously to the China mining ban in later september 2021[7] and to the 2022 crash ($USD70.000$ to $USD16.000$), yet saw an overall energy consumption growth. Localized collapses, such as China's ban, may be causing lasting declines in log returns, while relocations show only a transient growth in log returns. This anti-persistent behavior ($H_+ < 0.5$) is likely due to the adaptation process in new regions. The analysis of Figure III.2 indicates that the aggregation of numerous short-lived expansions outweighs the effect of persistent contractions.

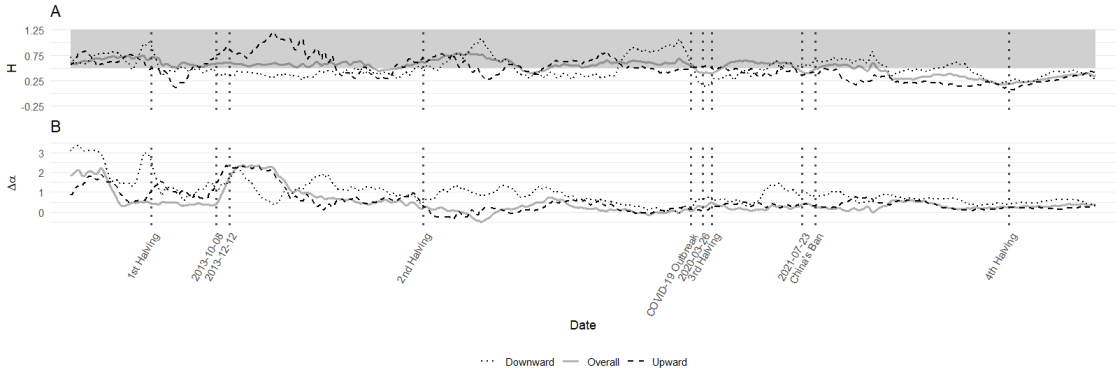

Figure III.3: Time-varying asymmetric multifractality in Bitcoin mining energy consumption. The rolling upward (H_+), downward (H_-), and overall Hurst exponent (H), along with the delta alpha ($\Delta\alpha$) are shown, calculated from the logarithmic returns using asymmetric MFDFA with a window size of 384 observations. To clarify the short-term trend without losing critical information, the results are smoothed using a 90 days moving average. Horizontal shaded band indicates values over 0.5.

[7]http://www.pbc.gov.cn/goutongjiaoliu/113456/113469/4348556/index.html

Figure III.3 A displays a pattern similar to that in Figure III.2 A. However, a prevalence of persistency in H_+ is observed until the second halving, revealing that the analysis is scale-dependent (ALMEIDA *et al.*, 2025; ALVAREZ-RAMIREZ e RODRIGUEZ, 2021; MUSSOI ALMEIDA *et al.*, 2024) and indicating a shift from reactive to strategic energy management, a transition that coincides with the documented growth of the phase in mining users (CORBET *et al.*, 2021) and the beginning of institutionalization (BEJAN *et al.*, 2023) noted in the literature. The larger window more effectively filters out short-term noise, providing a clearer measure of long-term persistence. This reveals the sustained momentum and structural impact of shocks with greater prominence than the 256 window. Between the third and fourth halvings, the 384 observations rolling window analysis showed $H_- > 0.5 > H_+$ prevailing through most of the period, possible reflecting the intermediate-term response to Bitcoin price crashes and China's mining ban.

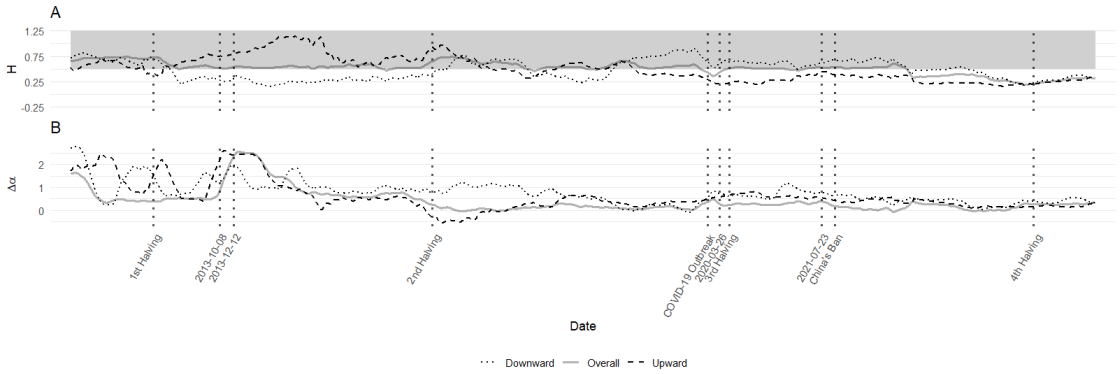

Figure III.4: Time-varying asymmetric multifractality in Bitcoin mining energy consumption. The rolling upward (H_+), downward (H_-), and overall Hurst exponent (H), along with the delta alpha ($\Delta\alpha$) are shown, calculated from the logarithmic returns using asymmetric MFDFA with a window size of 512 observations. To clarify the short-term trend without losing critical information, the results are smoothed using a 90 days moving average. Horizontal shaded band indicates values over 0.5.

For the long-term perspective of the 512 observation window, Figure III.4 A, the upward and downward Hurst exponents pre and during the first to second halving displayed similar behavior to the smaller windows, Figures III.2 A and III.3 A. This can be partly explained by the lack of a established long-term perspective on Bitcoin mining as a profitable operation. A distinct peak in persistent upward trends (H_+) emerged around the second halving in this long-term view; while the 256 and 384 windows also show persistence here, the 512 window's peak is unique, likely capturing the amplified, sustained bullish momentum solidifying minings profitability for a broader audience (CORBET *et al.*, 2021; KRISTOUFEK, 2020). Unlike the shorter windows where H_- shifted to anti-persistence, the 512 window displayed a maintained persistent downward trends, though they weakened significantly, approaching

the 0.5 threshold during the COVID-19 outbreak and third halving anticipation, indicating a loss of strong negative momentum.

Ultimately, across all window sizes, the post-fourth halving period displays a pronounced convergence of H_+, H_-, and the overall H towards efficiency, representing a market maturation where persistent trends have dissolved into more random, efficient-like behavior. This is in agreement with the findings shown in Table III.2, in which $\Delta H_{shuffled} > \Delta H$. In III.4 the narrowing gap between H_+ and H_- indicates that upward trends now tend to break and reverse with a statistical similarity to how downward trends recover. The results show that the observation is not of moves of the same size, but rather of a convergence in how rallies and declines lose momentum and reverse, explaining the decrease of multifractal strength measured by ΔH.

To the best of our knowledge, this study is also the first in the literature to identify the effects of Ethereum's transition to PoS on Bitcoin's energy behavior. As depicted in Figure III.4 A, which utilizes a long-term 512 observations rolling window, a considerable decrease is observed at the time of Ethereum's conversion from PoW to PoS. Specifically, the values for H_-, H_+, and the overall Hurst exponent (H) all fell significantly, remaining below the 0.5 threshold thereafter. The effect can be seen in Figures III.2 as well but is indistinguishable in Figure III.2, reaffirming its scale dependency. Our results indicate that The Merge precipitated a regime shift, characterized by a sharp transition to anti-persistence in H_- alongside a decrease in H_+ within the log-returns of Bitcoin's energy consumption. This shift is attributed to the effective displacement of Ethereum's Proof-of-Work mechanism, which alleviated competitive pressures and uncertainties in energy and hardware markets. This may suggest that cross-chain technological events could potentially influence the energy consumption behavior of otherwise independent blockchain networks.

Our results reveals that The Merge catalyzed a regime shift, marked by a sharp transition to anti-persistence of H_- in the log-returns of Bitcoin's energy use, accompanied by a decreasse in H_+ as well. We attribute this change to the removal of Ethereum's Proof-of-Work operations, which reduced competitive pressure and uncertainty in energy and hardware markets. The pre-event decline in multifractality—captured by our 512-day window—reflects anticipated miner wind-downs. This provides compelling evidence that cross-chain technological events can have profound, measurable effects on the energy consumption behavior of seemingly independent blockchain networks."

4 Conclusions

This research presents a comprehensive multifractal analysis of the scaling properties and efficiency dynamics in Bitcoin mining energy consumption. Employing asymmetric MFDFA with rolling window sizes of 256, 384, and 512 observations on the logarithmic returns of the annualized energy consumption time series, the study investigates the evolution of miner behavior across halving epochs and major exogenous shocks.

Employing asymmetric MFDFA across multiple temporal scales, the analysis of Bitcoin mining energy consumption logarithmic returns a distinct evolutionary trajectory. Initial periods were characterized by strong persistence ($H > 0.5$) and significant multifractal strength (ΔH), which transitioned through epochs of highly asymmetric behavior following regulatory shocks. The system ultimately seems to converge toward efficiency in the post-fourth halving period with Hurst exponents approaching 0.5, showing a notable inversion where $\Delta H_{shuff} > \Delta H$ that indicates long-range correlations now suppress volatility. Crucially, the analysis provides the first documented evidence of a significant cross-chain effect, identifying Ethereum's transition to Proof-of-Stake (The Merge) as a catalyst for a pronounced and lasting regime shift towards anti-persistence, demonstrating that the energy consumption behavior of the Bitcoin network is not isolated but can be profoundly influenced by external technological events in the broader blockchain ecosystem.

The findings also suggest that Bitcoin's market price acts as a primary mechanism influencing mining energy consumption patterns. Following the network's experimental beginnings, anti-persistent Hurst exponents during price declines reveal miners actively calibrating their energy use to preserve margins. Although external shocks occurred, their influence on consumption was channelled through subsequent price movements, stating that Bitcoin's value may acts as a signal for operational adjustment and resource allocation within the mining ecosystem.

Employing a multifractal framework, this study intends to decipher the evolution of Bitcoin mining energy consumption, tracing its progression from probability-driven volatility to efficiency governed by long-range correlations. The research reveals a maturation in Bitcoin's energy consumption, marked by a efficiency transition and a susceptibility to cross-chain shocks, providing a new framework for analyzing the environmental impact of proof-of-work systems. Opportunities for future research lie in exploring the multifractal properties of core blockchain metrics, such as block time intervals and block size distributions, and their relationship to energy consumption patterns. This analysis would deepen our understanding of how protocol-level mechanics influence the economic and environmental performance of decentralized systems.

References

ACEREDA, B., LEON, A., MORA, J., 2020, "Estimating the expected shortfall of cryptocurrencies: An evaluation based on backtesting", *Finance Research Letters*, v. 33, pp. 101181.

ADACHI, M., COMINETTA, M., KAUFMANN, C., et al., 2020, "A regulatory and financial stability perspective on global stablecoins", *Macroprudential Bulletin*, v. 10.

ADAMS, H., ZINSMEISTER, N., ROBINSON, D., 2020, "Uniswap v2 Core. 2020", *URL: https://uniswap. org/whitepaper. pdf.*

ADAMS, H., ZINSMEISTER, N., SALEM, M., et al., 2021. "Uniswap v3 core". .

AHN, J., YI, E., KIM, M., 2024, "Ethereum 2.0 Hard Fork: Consensus Change and Market Efficiency", *The Journal of The British Blockchain Association.*

AIGNER, A. A., DHALIWAL, G., 2021, "Uniswap: Impermanent loss and risk profile of a liquidity provider", *arXiv preprint arXiv:2106.14404*.

AKBAS, F., ARMSTRONG, W. J., SORESCU, S., et al., 2016, "Capital market efficiency and arbitrage efficacy", *Journal of Financial and Quantitative Analysis*, v. 51, n. 2, pp. 387–413.

AL-YAHYAEE, K. H., MENSI, W., YOON, S.-M., 2018, "Efficiency, multifractality, and the long-memory property of the Bitcoin market: A comparative analysis with stock, currency, and gold markets", *Finance Research Letters*, v. 27, pp. 228–234.

AL-YAHYAEE, K. H., MENSI, W., KO, H.-U., et al., 2020, "Why cryptocurrency markets are inefficient: The impact of liquidity and volatility", *The North American Journal of Economics and Finance*, v. 52, pp. 101168.

ALI, S., SHAHZAD, S. J. H., RAZA, N., et al., 2018, "Stock market efficiency: A comparative analysis of Islamic and conventional stock markets", *Physica A: Statistical Mechanics and Its Applications*, v. 503, pp. 139–153.

ALMEIDA, L. M., PERLIN, M. S., MÜLLER, F. M., 2025, "Pricing efficiency in cryptocurrencies: The case of centralized and decentralized markets", *Journal of Economics and Business*, v. 133, pp. 106224. ISSN: 0148-6195. doi: https://doi.org/10.1016/j.jeconbus.2024.106224. Disponível em: <https://www.sciencedirect.com/science/article/pii/S0148619524000663>. Digital Finance - Transforming Financial Landscapes for Companies and Households.

ALOUI, C., SHAHZAD, S. J. H., JAMMAZI, R., 2018, "Dynamic efficiency of European credit sectors: A rolling-window multifractal detrended fluctuation analysis", *Physica A: Statistical Mechanics and Its Applications*, v. 506, pp. 337–349.

ALQASSEM, I., RAHWAN, I., SVETINOVIC, D., 2018, "The Anti-Social System Properties: Bitcoin Network Data Analysis", *IEEE Transactions on Systems, Man, and Cybernetics: Systems*, v. 50, n. 1, pp. 21–31.

ALVAREZ-RAMIREZ, J., RODRIGUEZ, E., 2021, "A singular value decomposition approach for testing the efficiency of Bitcoin and Ethereum markets", *Economics Letters*, v. 206, pp. 109997.

ANGERIS, G., CHITRA, T., 2020, "Improved Price Oracles: Constant Function Market Makers". In: *Proceedings of the 2nd ACM Conference on Advances in Financial Technologies*, AFT '20, p. 80–91, New York, NY, USA, 6. Association for Computing Machinery. ISBN: 9781450381390.

ANGERIS, G., AGRAWAL, A., EVANS, A., et al., 2022a, "Constant Function Market Makers: Multi-asset Trades via Convex Optimization". In: *Handbook on Blockchain*, p. 415–444, New York, NY, USA, Springer International Publishing, a. ISBN: 9783031075353. doi: 10.1007/978-3-031-07535-3_13. Disponível em: <http://dx.doi.org/10.1007/978-3-031-07535-3_13>.

ANGERIS, G., EVANS, A., CHITRA, T., et al., 2022b, "Optimal routing for constant function market makers". In: *Proceedings of the 23rd ACM Conference on Economics and Computation*, pp. 115–128, b.

ARDIA, D., BLUTEAU, K., RÜEDE, M., 2019, "Regime changes in Bitcoin GARCH volatility dynamics", *Finance Research Letters*, v. 29, pp. 266–271.

BADEA, L., MUNGIU-PUPAZAN, M. C., 2021, "The Economic and Environmental Impact of Bitcoin", *IEEE Access*, v. 9, pp. 48091–48104. ISSN:

2169-3536. doi: 10.1109/access.2021.3068636. Disponível em: <http://dx.doi.org/10.1109/ACCESS.2021.3068636>.

BASEL COMMITTEE ON BANKING SUPERVISION, 2013, "Fundamental review of the trading book: A revised market risk framework", *Consultative Document, October*.

BASTIAN-PINTO, C. L., ARAUJO, F. V. D. S., BRANDÃO, L. E., et al., 2021, "Hedging renewable energy investments with Bitcoin mining", *Renewable and Sustainable Energy Reviews*, v. 138, pp. 110520.

BECK, R., MÜLLER-BLOCH, C., 2017, "Blockchain as Radical Innovation: A Framework for Engaging with Distributed Ledgers as Incumbent Organization". In: *Proceedings of the 50th Hawaii International Conference on System Sciences (2017)*, HICSS. Hawaii International Conference on System Sciences, 01. doi: 10.24251/hicss.2017.653. Disponível em: <http://dx.doi.org/10.24251/HICSS.2017.653>.

BECK, R., MÜLLER-BLOCH, C., KING, J. L., 2018, "Governance in the blockchain economy: A framework and research agenda", *Journal of the Association for Information Systems*, v. 19, n. 10, pp. 1.

BEJAN, C. A., BUCERZAN, D., CRĂCIUN, M. D., 2023, "Bitcoin price evolution versus energy consumption; trend analysis", *Applied Economics*, v. 55, n. 13, pp. 1497–1511.

BELLARE, M., ROGAWAY, P., 1993, "Random oracles are practical: a paradigm for designing efficient protocols". In: *Proceedings of the 1st ACM conference on Computer and communications security - CCS '93*, CCS '93, p. 62–73. ACM Press, 12. doi: 10.1145/168588.168596. Disponível em: <http://dx.doi.org/10.1145/168588.168596>.

BERG, J. A., FRITSCH, R., HEIMBACH, L., et al., 2022, "An empirical study of market inefficiencies in Uniswap and SushiSwap", *arXiv preprint arXiv:2203.07774*.

BRUNO, A., WEBER, P., YATES, A. J., 2023, "Can Bitcoin mining increase renewable electricity capacity?" *Resource and Energy Economics*, v. 74, pp. 101376.

BUTERIN, V., OTHERS, 2014. "A next-generation smart contract and decentralized application platform". .

BÖHME, R., CHRISTIN, N., EDELMAN, B., et al., 2015, "Bitcoin: Economics, Technology, and Governance", *Journal of Economic Perspectives*, v. 29, n. 2 (5), pp. 213–38.

CAJUEIRO, D. O., TABAK, B. M., 2007, "Long-range dependence and multifractality in the term structure of LIBOR interest rates", *Physica A: Statistical Mechanics and its Applications*, v. 373, pp. 603–614.

CALDARELLI, G., ELLUL, J., 2021, "The blockchain oracle problem in decentralized finance—a multivocal approach", *Applied Sciences*, v. 11, n. 16, pp. 7572.

CAMBRIDGE CENTRE FOR ALTERNATIVE FINANCE, 2022. "Cambridge Bitcoin Electricity Consumption Index". Disponível em: <`https://ccaf.io/cbnsi/cbeci`>. Accessed: 11 June 2025. Licensed under CC BY-NC-SA 4.0.

CAO, G., CAO, J., XU, L., 2013, "Asymmetric multifractal scaling behavior in the Chinese stock market: Based on asymmetric MF-DFA", *Physica A: statistical mechanics and its applications*, v. 392, n. 4, pp. 797–807.

CASTRO, A. L., MARCATO, A. L. M., DE AGUIAR, E. P., 2023, "Multifractal Analysis of the Brazilian Electricity Market", *IEEE Access*, v. 11, pp. 98939–98957.

CHARI, M. D., DAVID, P., DURU, A., et al., 2019, "Bowman's risk-return paradox: An agency theory perspective", *Journal of Business Research*, v. 95 (fev.), pp. 357–375. ISSN: 0148-2963. doi: 10.1016/j.jbusres.2018.08.010. Disponível em: <`http://dx.doi.org/10.1016/j.jbusres.2018.08.010`>.

CHAUHAN, A., MALVIYA, O. P., VERMA, M., et al., 2018, "Blockchain and Scalability". In: *2018 IEEE International Conference on Software Quality, Reliability and Security Companion (QRS-C)*. IEEE, jul. doi: 10.1109/qrs-c.2018.00034. Disponível em: <`http://dx.doi.org/10.1109/QRS-C.2018.00034`>.

CHEN, C., LIU, L., 2022, "How effective is China's cryptocurrency trading ban?" *Finance Research Letters*, v. 46, pp. 102429.

CHEN, Z.-H., REN, F., YANG, M.-Y., et al., 2023, "Dynamic lead–lag relationship between Chinese carbon emission trading and stock markets under exogenous shocks", *International Review of Economics & Finance*, v. 85, pp. 295–305.

CHENG, Q., LIU, X., ZHU, X., 2019, "Cryptocurrency momentum effect: DFA and MF-DFA analysis", *Physica A: Statistical Mechanics and its Applications*, v. 526, pp. 120847.

CHOHAN, U. W., 2021, "Decentralized finance (DeFi): an emergent alternative financial architecture", *Critical Blockchain Research Initiative (CBRI) Working Papers*.

CHOI, S., SHIN, J., 2022, "Bitcoin: An inflation hedge but not a safe haven", *Finance Research Letters*, v. 46, pp. 102379.

CHOW, G. C., 1960, "Tests of Equality Between Sets of Coefficients in Two Linear Regressions", *Econometrica*, v. 28, n. 3, pp. 591–605. ISSN: 00129682, 14680262. Disponível em: <http://www.jstor.org/stable/1910133>.

COMMITTEE, B., OTHERS, 2013, "Fundamental review of the trading book: A revised market risk framework", *Consultative Document, October*.

CONG, L. W., HE, Z., LI, J., 2021, "Decentralized mining in centralized pools", *The Review of Financial Studies*, v. 34, n. 3, pp. 1191–1235.

CONSENSYS, 2021. "MetaMask surpasses 10 million Maus, making it the world's leading non-custodial crypto wallet". Aug. Disponível em: <https://consensys.net/blog/press-release/metamask-surpasses-10-million-maus-making-it-the-worlds-leading-non-custod

CONSENSYS, 2022. "METAMASK integrates with Brazilian payment provider PIX for instant crypto purchases". Sep. Disponível em: <https://consensys.net/blog/metamask/metamask-integrates-with-brazilian-payment-provider-pix-for-instant-crypto

CORBET, S., LARKIN, C., LUCEY, B., 2020, "The contagion effects of the COVID-19 pandemic: Evidence from gold and cryptocurrencies", *Finance Research Letters*, v. 35, pp. 101554.

CORBET, S., LUCEY, B., YAROVAYA, L., 2021, "Bitcoin-energy markets interrelationships-New evidence", *Resources Policy*, v. 70, pp. 101916.

DAIAN, P., GOLDFEDER, S., KELL, T., et al., 2019, "Flash boys 2.0: Frontrunning, transaction reordering, and consensus instability in decentralized exchanges", *arXiv preprint arXiv:1904.05234*.

DAS, D., DUTTA, A., 2020, "Bitcoin's energy consumption: Is it the Achilles heel to miner's revenue?" *Economics Letters*, v. 186 (jan.), pp. 108530. ISSN:

0165-1765. doi: 10.1016/j.econlet.2019.108530. Disponível em: <http://dx.doi.org/10.1016/j.econlet.2019.108530>.

DE LIMA SILVA, P. C., SADAEI, H. J., BALLINI, R., et al., 2019, "Probabilistic forecasting with fuzzy time series", *IEEE Transactions on Fuzzy Systems*, v. 28, n. 8, pp. 1771–1784.

DE VRIES, A., 2018, "Bitcoin's Growing Energy Problem", *Joule*, v. 2, n. 5 (May), pp. 801–805. ISSN: 2542-4785. doi: 10.1016/j.joule.2018.04.016. Disponível em: <https://doi.org/10.1016/j.joule.2018.04.016>.

DE VRIES, A., 2020, "Bitcoin's energy consumption is underestimated: A market dynamics approach", *Energy Research amp; Social Science*, v. 70 (dez.), pp. 101721. ISSN: 2214-6296. doi: 10.1016/j.erss.2020.101721. Disponível em: <http://dx.doi.org/10.1016/j.erss.2020.101721>.

DE VRIES, A., STOLL, C., 2021, "Bitcoin's growing e-waste problem", *Resources, Conservation and Recycling*, v. 175 (dez.), pp. 105901. ISSN: 0921-3449. doi: 10.1016/j.resconrec.2021.105901. Disponível em: <http://dx.doi.org/10.1016/j.resconrec.2021.105901>.

DIAZ, A., GARCIA-DONATO, G., MORA-VALENCIA, A., 2017, "Risk quantification in turmoil markets", *Risk Management*, v. 19, pp. 202–224.

DICKEY, D. A., FULLER, W. A., 1979a, "Distribution of the estimators for autoregressive time series with a unit root", *Journal of the American statistical association*, v. 74, n. 366a, pp. 427–431.

DICKEY, D. A., FULLER, W. A., 1979b, "Distribution of the estimators for autoregressive time series with a unit root", *Journal of the American statistical association*, v. 74, n. 366a, pp. 427–431.

DÜDDER, B., ROSS, O., 2017, "Timber tracking: reducing complexity of due diligence by using blockchain technology", *Available at SSRN 3015219*.

DWORK, C., NAOR, M., 1993, "Pricing via Processing or Combatting Junk Mail". In: Brickell, E. F. (Ed.), *Advances in Cryptology — CRYPTO' 92*, pp. 139–147, Berlin, Heidelberg, 05. Springer Berlin Heidelberg. ISBN: 978-3-540-48071-6.

EARLE, T. C., 2009, "Trust, Confidence, and the 2008 Global Financial Crisis", *Risk Analysis*, v. 29, n. 6, pp. 785–792.

FABUS, J., KREMENOVA, I., STALMASEKOVA, N., et al., 2024, "An Empirical Examination of Bitcoin's Halving Effects: Assessing Cryptocurrency Sustainability within the Landscape of Financial Technologies", *Journal of Risk and Financial Management*, v. 17, n. 6 (maio), pp. 229. ISSN: 1911-8074. doi: 10.3390/jrfm17060229. Disponível em: <http://dx.doi.org/10.3390/jrfm17060229>.

FATOUROS, G., MAKRIDIS, G., KOTIOS, D., et al., 2022, "DeepVaR: a framework for portfolio risk assessment leveraging probabilistic deep neural networks", *Digital finance*, pp. 1–28.

FISSLER, T., ZIEGEL, J. F., 2016, "HIGHER ORDER ELICITABILITY AND OSBAND'S PRINCIPLE", *The Annals of Statistics*, v. 44, n. 4, pp. 1680–1707. ISSN: 00905364. Disponível em: <http://www.jstor.org/stable/43974729>.

FISSLER, T., ZIEGEL, J. F., GNEITING, T., 2016, "Expected Shortfall is jointly elicitable with Value at Risk-Implications for backtesting", *Risk Magazine*.

FRONGILLO, R., PAPIREDDYGARI, M., WAGGONER, B., 2023, "An Axiomatic Characterization of CFMMs and Equivalence to Prediction Markets", *arXiv preprint arXiv:2302.00196*.

GASTHAUS, J., BENIDIS, K., WANG, Y., et al., 2019, "Probabilistic forecasting with spline quantile function RNNs". In: *The 22nd international conference on artificial intelligence and statistics*, pp. 1901–1910. PMLR, 04.

GENCER, A. E., BASU, S., EYAL, I., et al., 2018, "Decentralization in Bitcoin and Ethereum Networks", *arXiv*, (03). doi: 10.48550/ARXIV.1801.03998. Disponível em: <https://arxiv.org/abs/1801.03998>.

GERLACH, R., WALPOLE, D., WANG, C., 2017, "Semi-parametric Bayesian tail risk forecasting incorporating realized measures of volatility", *Quantitative Finance*, v. 17, n. 2, pp. 199–215.

GERVAIS, A., KARAME, G. O., WÜST, K., et al., 2016a, "On the security and performance of proof of work blockchains". In: *Proceedings of the 2016 ACM SIGSAC conference on computer and communications security*, pp. 3–16, a.

GERVAIS, A., KARAME, G. O., WÜST, K., et al., 2016b, "On the security and performance of proof of work blockchains". In: *Proceedings of the 2016 ACM SIGSAC conference on computer and communications security*, pp. 3–16, b.

GHOSH, B., BOURI, E., 2022, "Is Bitcoin's carbon footprint persistent? Multifractal evidence and policy implications", *Entropy*, v. 24, n. 5, pp. 647.

GNEITING, T., 2011, "Making and evaluating point forecasts", *Journal of the American Statistical Association*, v. 106, n. 494, pp. 746–762.

GNEITING, T., RAFTERY, A. E., 2007, "Strictly proper scoring rules, prediction, and estimation", *Journal of the American statistical Association*, v. 102, n. 477, pp. 359–378.

GONG, C.-C., JI, S.-D., SU, L.-L., et al., 2016, "The lead–lag relationship between stock index and stock index futures: A thermal optimal path method", *Physica A: Statistical Mechanics and its Applications*, v. 444, pp. 63–72.

GOPIKRISHNAN, P., MEYER, M., AMARAL, L. N., et al., 1998, "Inverse cubic law for the distribution of stock price variations", *The European Physical Journal B-Condensed Matter and Complex Systems*, v. 3, n. 2, pp. 139–140.

GÖRGEN, K., MEIRER, J., SCHIENLE, M., 2022, "Predicting Value at Risk for Cryptocurrencies Using Generalized Random Forests", *arXiv preprint arXiv:2203.08224*.

GOYAL, M., RAMSEYER, G., GOEL, A., et al., 2022, "Finding the Right Curve: Optimal Design of Constant Function Market Makers", *arXiv preprint arXiv:2212.03340*.

GUO, K., ZHOU, W.-X., CHENG, S.-W., et al., 2011, "The US stock market leads the Federal funds rate and Treasury bond yields", *PLoS One*, v. 6, n. 8, pp. e22794.

GUO, K., SUN, Y., QIAN, X., 2017, "Can investor sentiment be used to predict the stock price? Dynamic analysis based on China stock market", *Physica A: Statistical Mechanics and its Applications*, v. 469, pp. 390–396.

GUO, Z.-Y., 2022, "Risk management of Bitcoin futures with GARCH models", *Finance Research Letters*, v. 45, pp. 102197.

HALABURDA, H., YERMACK, D., 2023, *Bitcoin mining meets Wall Street: A study of publicly traded crypto mining companies*. Relatório técnico, National Bureau of Economic Research.

HALPIN-HEALY, T., ZHANG, Y.-C., 1995, "Kinetic roughening phenomena, stochastic growth, directed polymers and all that. Aspects of multidisciplinary statistical mechanics", *Physics Reports*, v. 254, n. 4, pp. 215–414. ISSN: 0370-1573.

HANSEN, P. R., KIM, C., KIMBROUGH, W., 2022, "Periodicity in Cryptocurrency Volatility and Liquidity*", *Journal of Financial Econometrics*, (10). ISSN: 1479-8409. nbac034.

HANSON, R., 2003, "Combinatorial information market design", *Information Systems Frontiers*, v. 5, pp. 107–119.

HEIMBACH, L., WANG, Y., WATTENHOFER, R., 2021, "Behavior of liquidity providers in decentralized exchanges", *arXiv preprint arXiv:2105.13822*.

HEIMBACH, L., SCHERTENLEIB, E., WATTENHOFER, R., 2022a, "Risks and Returns of Uniswap V3 Liquidity Providers". In: *4th ACM Conference on Advances in Financial Technologies (AFT), Cambridge, Massachusetts, USA*, Septembera.

HEIMBACH, L., SCHERTENLEIB, E., WATTENHOFER, R., 2022b, "Risks and returns of uniswap v3 liquidity providers", *arXiv preprint arXiv:2205.08904*.

HERSBACH, H., 2000, "Decomposition of the continuous ranked probability score for ensemble prediction systems", *Weather and Forecasting*, v. 15, n. 5, pp. 559–570.

HUYNH, A. N. Q., DUONG, D., BURGGRAF, T., et al., 2022, "Energy consumption and Bitcoin market", *Asia-Pacific Financial Markets*, v. 29, n. 1, pp. 79–93.

IBIKUNLE, G., MCGROARTY, F., RZAYEV, K., 2020, "More heat than light: Investor attention and bitcoin price discovery", *International Review of Financial Analysis*, v. 69, pp. 101459.

JIA, R.-L., WANG, D.-H., TU, J.-Q., et al., 2016, "Correlation between agricultural markets in dynamic perspective—Evidence from China and the US futures markets", *Physica A: Statistical Mechanics and its Applications*, v. 464, pp. 83–92.

JIANG, S., LI, Y., LU, Q., et al., 2021, "Policy assessments for the carbon emission flows and sustainability of Bitcoin blockchain operation in China", *Nature communications*, v. 12, n. 1, pp. 1938.

JIMÉNEZ, I., MORA-VALENCIA, A., PEROTE, J., 2020, "Risk quantification and validation for Bitcoin", *Operations Research Letters*, v. 48, n. 4, pp. 534–541.

JIN, C., TIAN, X., 2024, "Enhanced safe-haven status of Bitcoin: Evidence from the Silicon Valley Bank collapse", *Finance Research Letters*, v. 59, pp. 104689.

JOHN, K., RIVERA, T. J., SALEH, F., 2025, "Proof-of-Work versus Proof-of-Stake: A Comparative Economic Analysis", *The Review of Financial Studies*, v. 38, n. 7 (03), pp. 1955–2004.

KABAKLARLI, E., 2022, "Green FinTech: sustainability of bitcoin", *Digital finance*, v. 4, n. 4, pp. 265–273.

KAISER, B., JURADO, M., LEDGER, A., 2018. "The Looming Threat of China: An Analysis of Chinese Influence on Bitcoin". Disponível em: <`https://arxiv.org/abs/1810.02466`>.

KAJTAZI, A., MORO, A., 2019, "The role of bitcoin in well diversified portfolios: A comparative global study", *International Review of Financial Analysis*, v. 61, pp. 143–157.

KAKINAKA, S., UMENO, K., 2022, "Cryptocurrency market efficiency in short- and long-term horizons during COVID-19: An asymmetric multifractal analysis approach", *Finance Research Letters*, v. 46, pp. 102319.

KANTELHARDT, J. W., ZSCHIEGNER, S. A., KOSCIELNY-BUNDE, E., et al., 2002, "Multifractal detrended fluctuation analysis of nonstationary time series", *Physica A: Statistical Mechanics and its Applications*, v. 316, n. 1-4, pp. 87–114.

KHAN, K., SU, C.-W., KHURSHID, A., et al., 2022, "COVID-19 impact on multifractality of energy prices: Asymmetric multifractality analysis", *Energy*, v. 256, pp. 124607.

KHAN, M. A., SAQIB, S., ALYAS, T., et al., 2020, "Effective demand forecasting model using business intelligence empowered with machine learning", *IEEE Access*, v. 8, pp. 116013–116023.

KHUNTIA, S., PATTANAYAK, J., 2020, "Adaptive long memory in volatility of intra-day bitcoin returns and the impact of trading volume", *Finance Research Letters*, v. 32, pp. 101077.

KILIMCI, H., YILDIRIM, M., KILIMCI, Z. H., 2021, "The Prediction of Short-Term Bitcoin Dollar Rate (BTC/USDT) using Deep and Hybrid Deep Learning Techniques". In: *2021 5th International Symposium on Multidisciplinary Studies and Innovative Technologies (ISMSIT)*, p. 633–637. IEEE, out. doi: 10.1109/ismsit52890.2021.9604741. Disponível em: <http://dx.doi.org/10.1109/ISMSIT52890.2021.9604741>.

KIM, J. H., 2009, "Automatic variance ratio test under conditional heteroskedasticity", *Finance Research Letters*, v. 6, n. 3, pp. 179–185.

KING, S., NADAL, S., 2012, "Ppcoin: Peer-to-peer crypto-currency with proof-of-stake", *self-published paper, August*, v. 19, n. 1.

KLAGES-MUNDT, A., HARZ, D., GUDGEON, L., et al., 2020, "Stablecoins 2.0: Economic Foundations and Risk-Based Models". In: *Proceedings of the 2nd ACM Conference on Advances in Financial Technologies*, AFT '20, p. 59–79, New York, NY, USA, 10. Association for Computing Machinery. ISBN: 9781450381390.

KNOWLES, H. S., HOSTETLER, M. E., LIEBOVITCH, L. S., 2018, "Describing the dynamics, distributions, and multiscale relationships in the time evolution of residential building energy consumption", *Energy and Buildings*, v. 158, pp. 310–325. ISSN: 0378-7788.

KÖHLER, S., PIZZOL, M., 2019, "Life Cycle Assessment of Bitcoin Mining", *Environmental Science & Technology*, v. 53, n. 23 (Dec), pp. 13598–13606. ISSN: 0013-936X. doi: 10.1021/acs.est.9b05687. Disponível em: <https://doi.org/10.1021/acs.est.9b05687>.

KOSBA, A., MILLER, A., SHI, E., et al., 2016, "Hawk: The Blockchain Model of Cryptography and Privacy-Preserving Smart Contracts". In: *2016 IEEE Symposium on Security and Privacy (SP)*, pp. 839–858, 05.

KRAUSE, M. J., TOLAYMAT, T., 2018, "Quantification of energy and carbon costs for mining cryptocurrencies", *Nature Sustainability*, v. 1, n. 11 (nov.), pp. 711–718. ISSN: 2398-9629. doi: 10.1038/s41893-018-0152-7. Disponível em: <http://dx.doi.org/10.1038/s41893-018-0152-7>.

KRISHNAMACHARI, B., FENG, Q., GRIPPO, E., 2021, "Dynamic curves for decentralized autonomous cryptocurrency exchanges", *arXiv preprint arXiv:2101.02778*.

KRISTOUFEK, L., 2020, "Bitcoin and its mining on the equilibrium path", *Energy Economics*, v. 85, pp. 104588.

KWAPIEŃ, J., DROŻDŻ, S., 2012, "Physical approach to complex systems", *Physics Reports*, v. 515, n. 3-4, pp. 115–226.

KWIATKOWSKI, D., PHILLIPS, P. C., SCHMIDT, P., et al., 1992, "Testing the null hypothesis of stationarity against the alternative of a unit root: How sure are we that economic time series have a unit root?" *Journal of econometrics*, v. 54, n. 1-3, pp. 159–178.

KÜFEOĞLU, S., ÖZKURAN, M., 2019, "Bitcoin mining: A global review of energy and power demand", *Energy Research & Social Science*, v. 58, pp. 101273. ISSN: 2214-6296. doi: https://doi.org/10.1016/j.erss.2019.101273. Disponível em: <`https://www.sciencedirect.com/science/article/pii/S2214629619305948`>.

LABAZOVA, O., 2019, "Towards a Framework for Evaluation of Blockchain Implementations." In: *ICIS*, 12.

LAIB, M., GOLAY, J., TELESCA, L., et al., 2018, "Multifractal analysis of the time series of daily means of wind speed in complex regions", *Chaos, Solitons & Fractals*, v. 109, pp. 118–127.

LI, J., LI, N., PENG, J., et al., 2019, "Energy consumption of cryptocurrency mining: A study of electricity consumption in mining cryptocurrencies", *Energy*, v. 168, pp. 160–168.

LI, Y., YU, R., SHAHABI, C., et al., 2017, "Diffusion convolutional recurrent neural network: Data-driven traffic forecasting", *arXiv preprint arXiv:1707.01926*.

LI, Z., LI, J., ZHOU, K., 2023, "Bitcoin transaction fees and the decentralization of Bitcoin mining pools", *Finance Research Letters*, v. 58, pp. 104347.

LIKITRATCHAROEN, D., RANONG, T. N., CHUENGSUKSOMBOON, R., et al., 2018, "Value at risk performance in cryptocurrencies", *The Journal of Risk Management and Insurance*, v. 22, n. 1, pp. 11–28.

LIU, W., SEMEYUTIN, A., LAU, C. K. M., et al., 2020, "Forecasting value-at-risk of cryptocurrencies with riskmetrics type models", *Research in International Business and Finance*, v. 54, pp. 101259.

LIU, Y., TSYVINSKI, A., 2021, "Risks and returns of cryptocurrency", *The Review of Financial Studies*, v. 34, n. 6, pp. 2689–2727.

LO, A. W., MACKINLAY, A. C., 1988, "Stock market prices do not follow random walks: Evidence from a simple specification test", *The review of financial studies*, v. 1, n. 1, pp. 41–66.

LO, Y. C., MEDDA, F., 2022, "Do DEXs work? Using Uniswap V2 to explore the effectiveness of decentralized exchanges", *Journal of Financial Market Infrastructures*.

LOESCH, S., HINDMAN, N., RICHARDSON, M. B., et al., 2021, "Impermanent loss in uniswap v3", *arXiv preprint arXiv:2111.09192*.

MACAIRE, C., NAEF, A., 2022, "Greening monetary policy: evidence from the People's Bank of China", *Climate Policy*, v. 23, n. 1 (jan.), pp. 138–149. ISSN: 1752-7457. doi: 10.1080/14693062.2021.2013153. Disponível em: <http://dx.doi.org/10.1080/14693062.2021.2013153>.

MADHAVAN, A., 1996, "Security prices and market transparency", *Journal of Financial Intermediation*, v. 5, n. 3, pp. 255–283.

MAESA, D., MARINO, A., RICCI, L., 2019, "The bow tie structure of the Bitcoin users graph", *Applied Network Science*, v. 4, n. 56, pp. 21–31.

MAITI, M., 2022, "Dynamics of bitcoin prices and energy consumption", *Chaos, Solitons Fractals: X*, v. 9, pp. 100086. ISSN: 2590-0544. Disponível em: <https://www.sciencedirect.com/science/article/pii/S259005442200015X>.

MATHONSI, T., VAN ZYL, T. L., 2021, "A statistics and deep learning hybrid method for multivariate time series forecasting and mortality modeling", *Forecasting*, v. 4, n. 1, pp. 1–25.

M'BAKOB, G. B., 2024, "Bubbles in Bitcoin and Ethereum: The role of halving in the formation of super cycles", *Sustainable Futures*, v. 7, pp. 100178.

MEINHOLD, R., WAGNER, C., DHAR, B. K., 2025, "Digital sustainability and eco-environmental sustainability: A review of emerging technologies, resource challenges, and policy implications", *Sustainable Development*, v. 33, n. 2, pp. 2323–2338.

MENG, H., XU, H.-C., ZHOU, W.-X., et al., 2017, "Symmetric thermal optimal path and time-dependent lead-lag relationship: novel statistical tests and application to UK and US real-estate and monetary policies", *Quantitative Finance*, v. 17, n. 6, pp. 959–977.

MENG, X., TAYLOR, J. W., 2020, "Estimating Value-at-Risk and Expected Shortfall using the intraday low and range data", *European Journal of Operational Research*, v. 280, n. 1, pp. 191–202. ISSN: 0377-2217.

MENSI, W., LEE, Y.-J., AL-YAHYAEE, K. H., et al., 2019, "Intraday downward/upward multifractality and long memory in Bitcoin and Ethereum markets: An asymmetric multifractal detrended fluctuation analysis", *Finance Research Letters*, v. 31, pp. 19–25.

MEYNKHARD, A., 2019, "Fair market value of bitcoin: Halving effect", *Investment Management & Financial Innovations*, v. 16, n. 4, pp. 72.

MNIF, E., JARBOUI, A., 2021, "COVID-19, bitcoin market efficiency, herd behaviour", *Review of Behavioral Finance*, v. 13, n. 1, pp. 69–84.

MNIF, E., JARBOUI, A., MOUAKHAR, K., 2020, "How the cryptocurrency market has performed during COVID 19? A multifractal analysis", *Finance research letters*, v. 36, pp. 101647.

MORA, C., ROLLINS, R. L., TALADAY, K., et al., 2018, "Bitcoin emissions alone could push global warming above 2°C", *Nature Climate Change*, v. 8, n. 11 (out.), pp. 931–933. ISSN: 1758-6798. doi: 10.1038/s41558-018-0321-8. Disponível em: <http://dx.doi.org/10.1038/s41558-018-0321-8>.

MÜLLER, F. M., RIGHI, M. B., 2018, "Numerical comparison of multivariate models to forecasting risk measures", *Risk Management*, v. 20, n. 1 (out.), pp. 29–50.

MÜLLER, F. M., RIGHI, M. B., 2022, "Comparison of Value at Risk (VaR) Multivariate Forecast Models", *Computational Economics*, pp. 1–36.

MUSSOI ALMEIDA, L., MÜLLER, F. M., PERLIN, M. S., 2024, "Risk Forecasting Comparisons in Decentralized Finance: An Approach in Constant Product Market Makers", *Computational Economics*, (abr.). ISSN: 1572-9974. Disponível em: <http://dx.doi.org/10.1007/s10614-024-10585-6>.

MÜLLER, F. M., SANTOS, S. S., GÖSSLING, T. W., et al., 2022, "Comparison of risk forecasts for cryptocurrencies: A focus on Range Value at Risk", *Finance Research Letters*, v. 48, pp. 102916. ISSN: 1544-6123.

NADARAJAH, S., CHU, J., 2017, "On the inefficiency of Bitcoin", *Economics Letters*, v. 150, pp. 6–9.

NAEEM, M. A., BOURI, E., PENG, Z., et al., 2021, "Asymmetric efficiency of cryptocurrencies during COVID19", *Physica A: Statistical Mechanics and its Applications*, v. 565, pp. 125562.

NAEEM, M. A., YOUSAF, I., KARIM, S., et al., 2023, "Comparing asymmetric price efficiency in regional ESG markets before and during COVID-19", *Economic Modelling*, v. 118, pp. 106095.

NAKAMOTO, S., 2008, "Bitcoin: A peer-to-peer electronic cash system", *Decentralized Business Review*, p. 21260.

NAN, Z., KAIZOJI, T., 2019, "Market efficiency of the bitcoin exchange rate: Weak and semi-strong form tests with the spot, futures and forward foreign exchange rates", *International Review of Financial Analysis*, v. 64, pp. 273–281.

NARAYANAN, A., BONNEAU, J., FELTEN, E., et al., 2016, *Bitcoin and Cryptocurrency Technologies: A Comprehensive Introduction*. USA, Princeton University Press. ISBN: 0691171696.

NIAZ, H., SHAMS, M. H., LIU, J. J., et al., 2022, "Mining bitcoins with carbon capture and renewable energy for carbon neutrality across states in the USA", *Energy & Environmental Science*, v. 15, n. 9, pp. 3551–3570.

NOLDE, N., ZIEGEL, J. F., 2017, "Elicitability and backtesting: Perspectives for banking regulation", *The annals of applied statistics*, v. 11, n. 4, pp. 1833–1874.

O'DWYER, K. J., MALONE, D., 2014, "Bitcoin mining and its energy footprint". In: *25th IET Irish Signals & Systems Conference 2014 and 2014 China-Ireland International Conference on Information and Communications Technologies (ISSC 2014/CIICT 2014)*, pp. 280–285. IET, 06.

OŚWIĘCIMKA, P., KWAPIEŃ, J., DROŻDŻ, S., 2006, "Wavelet versus detrended fluctuation analysis of multifractal structures", *Physical Review E—Statistical, Nonlinear, and Soft Matter Physics*, v. 74, n. 1, pp. 016103.

OTHMAN, A., SANDHOLM, T., 2010, "Automated market-making in the large: the Gates Hillman prediction market". In: *Proceedings of the 11th ACM conference on Electronic commerce*, pp. 367–376, 06.

PANI, S., 2021, "Liquidity in high resolution in limit order markets", *International Journal of Financial Markets and Derivatives*, v. 8, n. 1, pp. 23–49.

PENG, C.-K., BULDYREV, S. V., HAVLIN, S., et al., 1994, "Mosaic organization of DNA nucleotides", *Physical review e*, v. 49, n. 2, pp. 1685.

PENG, C.-K., HAVLIN, S., STANLEY, H. E., et al., 1995, "Quantification of scaling exponents and crossover phenomena in nonstationary heartbeat time series", *Chaos: an interdisciplinary journal of nonlinear science*, v. 5, n. 1, pp. 82–87.

PHILLIPS, P. C., PERRON, P., 1988, "Testing for a unit root in time series regression", *Biometrika*, v. 75, n. 2, pp. 335–346.

PRAT, J., WALTER, B., 2021, "An equilibrium model of the market for bitcoin mining", *Journal of Political Economy*, v. 129, n. 8, pp. 2415–2452.

QIN, K., ZHOU, L., AFONIN, Y., et al., 2021, "CeFi vs. DeFi–Comparing Centralized to Decentralized Finance", *arXiv preprint arXiv:2106.08157*.

QIN, M., WU, T., MA, X., et al., 2023, "Are energy consumption and carbon emission caused by Bitcoin? A novel time-varying technique", *Economic Analysis and Policy*, v. 80, pp. 109–120.

RASOOL MALIK, A., ASLAM, F., FERREIRA, P., 2024, "Bitcoin's multifractal influence: deciphering the relationship with conventional and renewable energy markets", *Cogent Economics & Finance*, v. 12, n. 1, pp. 2395413.

REBANE, J., KARLSSON, I., PAPAPETROU, P., et al., 2018, "Seq2Seq RNNs and ARIMA models for cryptocurrency prediction: A comparative study". In: *SIGKDD Fintech'18, London, UK, 2018*, 08.

REYES-MACEDO, V. G., SALINAS-ROSALES, M., GALLEGOS GARCIA, G., 2019, "A Method for Blockchain Transactions Analysis", *IEEE Latin America Transactions*, v. 17, n. 07, pp. 1080–1087.

RIGHI, M., MÜLLER, F., 2022, "Range Based Risk Measures and Their Applications", *Available at SSRN 4051687*.

RIGHI, M. B., CERETTA, P. S., 2015, "A comparison of expected shortfall estimation models", *Journal of Economics and Business*, v. 78, pp. 14–47.

SALEH, F., 2021a, "Blockchain without waste: Proof-of-stake", *The Review of financial studies*, v. 34, n. 3, pp. 1156–1190.

SALEH, F., 2021b, "Blockchain without waste: Proof-of-stake", *The Review of financial studies*, v. 34, n. 3, pp. 1156–1190.

SALINAS, D., FLUNKERT, V., GASTHAUS, J., et al., 2020, "DeepAR: Probabilistic forecasting with autoregressive recurrent networks", *International Journal of Forecasting*, v. 36, n. 3, pp. 1181–1191.

SAPRA, N., SHAIKH, I., ROUBAUD, D., et al., 2024, "Uncovering Bitcoin's electricity consumption relationships with volatility and price: Environmental Repercussions", *Journal of Environmental Management*, v. 356 (abr.), pp. 120528. ISSN: 0301-4797. doi: 10.1016/j.jenvman.2024.120528. Disponível em: <http://dx.doi.org/10.1016/j.jenvman.2024.120528>.

SEDLMEIR, J., ZHOU, Y., PAPAGEORGIOU, O., et al., 2024, "The Imminent (and Avoidable) Security Risk of Bitcoin Halving", *SSRN Electronic Journal*. ISSN: 1556-5068. doi: 10.2139/ssrn.4801113. Disponível em: <http://dx.doi.org/10.2139/ssrn.4801113>.

SEN, R., YU, H.-F., DHILLON, I. S., 2019, "Think globally, act locally: A deep neural network approach to high-dimensional time series forecasting", *Advances in neural information processing systems*, v. 32.

SHAHZAD, S. J. H., BOURI, E., KAYANI, G. M., et al., 2020, "Are clean energy stocks efficient? Asymmetric multifractal scaling behaviour", *Physica A: Statistical Mechanics and its Applications*, v. 550, pp. 124519.

SHAN, F., HE, X., ARMAGHANI, D. J., et al., 2022, "Success and challenges in predicting TBM penetration rate using recurrent neural networks", *Tunnelling and Underground Space Technology*, v. 130, pp. 104728.

SHEN, Z., WAN, Q., LEATHAM, D. J., 2021, "Bitcoin return volatility forecasting: A comparative study between GARCH and RNN", *Journal of Risk and Financial Management*, v. 14, n. 7, pp. 337.

SHLEIFER, A., VISHNY, R. W., 1997, "The limits of arbitrage", *The Journal of finance*, v. 52, n. 1, pp. 35–55.

SHRESTHA, K., 2021, "Multifractal detrended fluctuation analysis of return on Bitcoin", *International Review of Finance*, v. 21, n. 1, pp. 312–323.

SIHANANTO, A. N., SARI, A. P., PRASETYO, M. E., et al., 2022, "Reinforcement Learning for Automatic Cryptocurrency Trading". In: *2022 IEEE 8th Information Technology International Seminar (ITIS)*, pp. 345–349, 10.

SLAMKA, C., SKIERA, B., SPANN, M., 2012, "Prediction market performance and market liquidity: A comparison of automated market makers", *IEEE Transactions on Engineering Management*, v. 60, n. 1, pp. 169–185.

SOMPOLINSKY, Y., ZOHAR, A., 2018, "Bitcoin's underlying incentives", *Communications of the ACM*, v. 61, n. 3 (fev.), pp. 46–53. ISSN: 1557-7317. doi: 10.1145/3152481. Disponível em: <http://dx.doi.org/10.1145/3152481>.

SORIA, J., MOYA, J., MOHAZAB, A., 2023, "Optimal mining in proof-of-work blockchain protocols", *Finance research letters*, v. 53, pp. 103610.

SORNETTE, D., ZHOU, W.-X., 2005, "Non-parametric determination of real-time lag structure between two time series: the 'optimal thermal causal path'method", *Quantitative Finance*, v. 5, n. 6, pp. 577–591.

STOLL, C., KLAASSEN, L., GALLERSDÖRFER, U., 2019, "The Carbon Footprint of Bitcoin", *Joule*, v. 3, n. 7 (Jul), pp. 1647–1661. ISSN: 2542-4785. doi: 10.1016/j.joule.2019.05.012. Disponível em: <https://doi.org/10.1016/j.joule.2019.05.012>.

SZABO, N., 1996, "Smart contracts: building blocks for digital markets", *EXTROPY: The Journal of Transhumanist Thought,(16)*, v. 18, n. 2, pp. 28.

TASCA, P., HAYES, A., LIU, S., 2018, "The evolution of the bitcoin economy: Extracting and analyzing the network of payment relationships", *The Journal of Risk Finance*, v. 19, n. 2, pp. 94–126.

TASKINSOY, J., 2022, "The great silent crash of the 21st century", *Available at SSRN 4274584*.

TAYEBI, S., AMINI, H., 2024, "The flip side of the coin: Exploring the environmental and health impacts of proof-of-work cryptocurrency mining", *Environmental Research*, v. 252, pp. 118798. ISSN: 0013-9351. doi: https://doi.org/10.1016/j.envres.2024.118798. Disponível em: <https://www.sciencedirect.com/science/article/pii/S0013935124007023>.

TOYODA, K., TAKIS MATHIOPOULOS, P., OHTSUKI, T., 2019, "A Novel Methodology for HYIP Operators' Bitcoin Addresses Identification", *IEEE Access*, v. 7, pp. 74835–74848.

TRICHILLI, Y., BOUJELBÉNE, M., 2023, "Regime specific spillover between Dow Jones Islamic Market World Index, Islamic gold-backed crypto currencies

and the blockchain halal index", *International Journal of Islamic and Middle Eastern Finance and Management*, v. 16, n. 3, pp. 464–481.

TRICHILLI, Y., BOUJELBÈNE ABBES, M., 2023, "The impact of COVID-19 on the portfolio optimization", *EuroMed Journal of Business*, v. 18, n. 2, pp. 207–228.

TRICHILLI, Y., ABDELHÉDI, M., BOUJELBÈNE ABBES, M., 2020, "The thermal optimal path model: does Google search queries help to predict dynamic relationship between investor's sentiment and indexes returns?" *Journal of asset management*, v. 21, pp. 261–279.

TROSTER, V., TIWARI, A. K., SHAHBAZ, M., et al., 2019, "Bitcoin returns and risk: A general GARCH and GAS analysis", *Finance Research Letters*, v. 30, pp. 187–193.

TRUCÍOS, C., TAYLOR, J. W., 2022, "A comparison of methods for forecasting value at risk and expected shortfall of cryptocurrencies", *Journal of Forecasting*.

TRUCÍOS, C., 2019, "Forecasting Bitcoin risk measures: A robust approach", *International Journal of Forecasting*, v. 35, n. 3, pp. 836–847. ISSN: 0169-2070. Forecasting issues in developing economies.

UMAR, M., SU, C.-W., RIZVI, S. K. A., et al., 2021, "Bitcoin: A safe haven asset and a winner amid political and economic uncertainties in the US?" *Technological Forecasting and Social Change*, v. 167, pp. 120680.

UNISWAP, 2023, 04. Disponível em: <`https://docs.uniswap.org/contracts/v2/concepts/advanced-topics/understanding-returns`>.

URQUHART, A., 2016, "The inefficiency of Bitcoin", *Economics Letters*, v. 148, pp. 80–82.

VAKHMYANIN, I., VOLKOVICH, Y., 2023, "Price Arbitrage for DeFi Derivatives". In: *2023 IEEE International Conference on Blockchain and Cryptocurrency (ICBC)*, pp. 1–4, 05. doi: 10.1109/ICBC56567.2023.10174884.

VIDAL-TOMÁS, D., IBAÑEZ, A., 2018. "Semi-strong efficiency of bitcoin. Finance Res Lett 27: 259–265". .

VRANKEN, H., 2017, "Sustainability of bitcoin and blockchains", *Current Opinion in Environmental Sustainability*, v. 28, pp. 1–9. ISSN: 1877-3435. doi: https://doi.org/10.1016/j.cosust.2017.04.011.

Disponível em: <https://www.sciencedirect.com/science/article/pii/S1877343517300015>. Sustainability governance.

VUJIČIĆ, D., JAGODIĆ, D., RANDIĆ, S., 2018, "Blockchain technology, bitcoin, and Ethereum: A brief overview". In: *2018 17th international symposium infoteh-jahorina (infoteh)*, pp. 1–6. IEEE, 03.

WALSH, C., O'REILLY, P., GLEASURE, R., et al., 2016, "New kid on the block: a strategic archetypes approach to understanding the Blockchain". In: *2016 International Conference on Information Systems, ICIS 2016*, p. 6. Association for Information Systems. AIS Electronic Library (AISeL), 12.

WANG, D., TU, J., CHANG, X., et al., 2017, "The lead–lag relationship between the spot and futures markets in China", *Quantitative Finance*, v. 17, n. 9, pp. 1447–1456.

WANG, H., HE, D., JI, Y., 2020, "Designated-verifier proof of assets for bitcoin exchange using elliptic curve cryptography", *Future Generation Computer Systems*, v. 107, pp. 854–862.

WANG, J., WANG, S., ZENG, B., et al., 2022a, "A novel ensemble probabilistic forecasting system for uncertainty in wind speed", *Applied Energy*, v. 313, pp. 118796.

WANG, Y., CHEN, Y., WU, H., et al., 2022b, "Cyclic Arbitrage in Decentralized Exchanges". In: *Report on the 12th International Workshop on Location and the Web (LocWeb 2022) at WWW 2022*, WWW '22, p. 12–19, New York, NY, USA, b. Association for Computing Machinery. ISBN: 9781450391306.

WANG, Y., CHEN, Y., WU, H., et al., 2022c, "Cyclic arbitrage in decentralized exchanges". In: *Companion Proceedings of the Web Conference 2022*, pp. 12–19, c.

WANG, Y., LIU, L., GU, R., 2009, "Analysis of efficiency for Shenzhen stock market based on multifractal detrended fluctuation analysis", *International Review of Financial Analysis*, v. 18, n. 5, pp. 271–276.

WEN, F., TONG, X., REN, X., 2022, "Gold or Bitcoin, which is the safe haven during the COVID-19 pandemic?" *International Review of Financial Analysis*, v. 81, pp. 102121.

WILSON, L., 2022, "GPU prices and cryptocurrency returns", *Applied Finance Letters*, v. 11, pp. 2–8.

XIA, P., WANG, H., GAO, B., et al., 2021, "Trade or Trick?" *Proceedings of the ACM on Measurement and Analysis of Computing Systems*, v. 5, n. 3 (dez.), pp. 1–26.

XU, H.-C., ZHOU, W.-X., SORNETTE, D., 2017a, "Time-dependent lead-lag relationship between the onshore and offshore Renminbi exchange rates", *Journal of International Financial Markets, Institutions and Money*, v. 49, pp. 173–183.

XU, X., WEBER, I., STAPLES, M., et al., 2017b, "A taxonomy of blockchain-based systems for architecture design". In: *2017 IEEE international conference on software architecture (ICSA)*, pp. 243–252. IEEE, b.

YAN, D., LAI, K. K., 2019, "An Analysis of China's Onshore and Offshore Exchange Rates—Adjusted Thermal Optimal Path Approach Based on Pruning and Path Segmentation", *Entropy*, v. 21, n. 5, pp. 499.

YANG, Y.-H., SHAO, Y.-H., 2020, "Time-dependent lead-lag relationships between the VIX and VIX futures markets", *The North American Journal of Economics and Finance*, v. 53, pp. 101196.

YAO, C.-Z., LI, H.-Y., 2020, "Time-varying lead–lag structure between investor sentiment and stock market", *The North American Journal of Economics and Finance*, v. 52, pp. 101148.

YAP, K. Y., CHIN, H. H., KLEMEŠ, J. J., 2023, "Blockchain technology for distributed generation: A review of current development, challenges and future prospect", *Renewable and Sustainable Energy Reviews*, v. 175, pp. 113170.

YOUSAF, I., YAROVAYA, L., 2022, "Static and dynamic connectedness between NFTs, Defi and other assets: Portfolio implication", *Global Finance Journal*, v. 53, pp. 100719. ISSN: 1044-0283.

YUAN, X., SU, C.-W., PECULEA, A. D., 2022, "Dynamic linkage of the bitcoin market and energy consumption:An analysis across time", *Energy Strategy Reviews*, v. 44 (nov.), pp. 100976. ISSN: 2211-467X. doi: 10.1016/j.esr.2022.100976. Disponível em: <http://dx.doi.org/10.1016/j.esr.2022.100976>.

YUAN, X., JIN, L., LIAN, F., 2021, "The lead–lag relationship between Chinese mainland and Hong Kong stock markets", *Physica A: Statistical Mechanics and its Applications*, v. 574, pp. 125999.

ZARGAR, F. N., KUMAR, D., 2019, "Informational inefficiency of Bitcoin: A study based on high-frequency data", *Research in International Business and Finance*, v. 47, pp. 344–353.

ZHANG, R., CHAN, W. K. V., 2020, "Evaluation of energy consumption in blockchains with proof of work and proof of stake". In: *Journal of Physics: Conference Series*, v. 1584, p. 012023. IOP Publishing, 07.

ZHENG, M., FENG, G.-F., ZHAO, X., et al., 2023, "The transaction behavior of cryptocurrency and electricity consumption", *Financial Innovation*, v. 9, n. 1, pp. 44.

ZHOU, W.-X., SORNETTE, D., 2006, "Non-parametric determination of real-time lag structure between two time series: The "optimal thermal causal path" method with applications to economic data", *Journal of Macroeconomics*, v. 28, n. 1, pp. 195–224.

ZIEGEL, J. F., 2016, "Coherence and elicitability", *Mathematical Finance*, v. 26, n. 4, pp. 901–918.

ŞAHIN TELLI, CHEN, H., 2020, "Multifractal behavior in return and volatility series of Bitcoin and gold in comparison", *Chaos, Solitons & Fractals*, v. 139, pp. 109994. ISSN: 0960-0779. doi: https://doi.org/10.1016/j.chaos.2020.109994. Disponível em: <`https://www.sciencedirect.com/science/article/pii/S0960077920303933`>.